SCATTERING BY A STRIP IN A HOMOGENEOUS MEDIUM

Jan Thorbecke

18 January 1991

Delft University of Technology
Faculty of Mining and Petroleum Engineering
Section Applied Geophysics
Delft
The Netherlands

Title	:	Scattering by a strip in a homogeneous medium.
Author	:	Jan Thorbecke
Date	:	18 January 1991
Laboratory	:	Applied Geophysics
Report number	:	1991-2
Abstract code	:	PA 91.90
Address	:	Delft University of Technology Dept. of Mining and Petroleum Engineering Section of Applied Geophysics P.o. Box 5028 2600 GA Delft The Netherlands

[122]

Ik ben altijd ontsteld wanneer ik iets voltooi. Ik schrik en wordt door verdriet overmand. Mijn volmaaktheidsinstinct zou me moeten beletten iets te voltooien; het zou me zelfs moeten beletten ergens aan te beginnen. Maar ik ben verstrooid en doe het toch, met als resultaat een produkt dat bij mij niet voortkomt uit de wil,maar uit de afwezigheid ervan. Ik begin omdat ik geen kracht heb om te denken; ik voltooi omdat mijn ziel de kracht mist om eerder op te houden. Dit boek is mijn lafheid.

Fernando Pessoa, *Het Boek Der Rusteloosheid*

Preface

Two years ago, in December 1988, I was ready to start with the last few steps of my study, but I couldn't find any motivation to start with it. I was looking for something I would never find; I was asking questions which I couldn't answer. I considered stoping to study, but I couldn't find any reason why I should stop, neither could I find any reason to finish it. For some reasons, of which I don't care anymore of not knowing them, my last steps of the study came to an end.

This thesis represents the results of my final project at the Department of Mining and Petroleum Engineering, section Applied Geophysics, at the Delft University of Technology. The accompany of this project was done by J.T. Fokkema and P.M. van den Berg , which I would like to thank for their support and understanding. I also would like to thank prof. A.M. Ziolkowski for reading this report and making many helpful comments and suggestions and, everybody who was at the 'Geophysics room', to whom I could ask everything, for helping me with all aspects of my final project and for trying to make me feel at home.

The program I have written, which is based on this report, will be used to produce a reference data set for a new theory about the removal of surface related wave phenomena in the marine case which is develloped by J.T. Fokkema and P.M. van den Berg.

Contents

Chapter 3 Source and receiver

Chapter 4 Iterative schemes based on minimization of a uniform error criterion

Chapter 5 Numerical implementation

Abstract

The theory described in this thesis is part of a project at the applied Geophysics section of the faculty of Mining and Petroleum Engineering. The project started with a new theoretical approach which describes the removal of surface related wave phenomena in the marine case (Fokkema and van den Berg, 1990). In order to test this new theory a well defined test problem is needed. This report gives the theoretical description of the test problem.

Starting with Rayleigh's reciprocity theorem and the method of Green's functions, the integral equation for the scattered field is derived. The scattered field is calculated in detail for a rigid and compliant strip both in an unbounded and a bounded medium. The unknown function in these integral equations is the field on the strip. All equations are derived for a 2-dimensional medium. The Hankel function of the first kind plays an important role in these 2-dimensional scattering problems. In this report the Hankel function is calculated in the wavenumber domain. The integral equations, which are a spatial convolution of the Hankel function (or the second derivative of the Hankel function) with the unknown function, can therefore be reduced to a product in the wavenumber domain. However the unknown function cannot be solved by direct deconvolution because the field outside the strip is not known. The integral equations can be solved only by using numerical schemes.

The numerical scheme used is the preconditioned conjugate gradient scheme (Berg, van den, 1989). This scheme uses a preconditioning operator which is an appropriate inverse of the integral operator on the strip. This scheme converges in a few iterations to the estimated field on the strip within a certain grade of precision.

After numerically solving the integral equation, the field on the strip is known and, by using Rayleigh's reciprocity theorem, the scattered field can be calculated everywhere in the medium of interest. The scattered field is calculated for different source positions in an unbounded and a bounded medium.

Notations and conventions

In general, Italic, Roman and Greek symbols are used for scalar quantities. The subscript notation for Cartesian vectors and tensors is used. Lower case Latin subscripts are used for three dimensions, Greek's subscripts are used for two dimensions. The summation convention applies to repeated subscripts. Occasionally bold-face Roman and Greek type letters are used for vectors.

To locate a point in space, orthogonal Cartesian coordinates x_1, x_2 and x_3 are employed with respect to a given orthogonal Cartesian reference frame with origin O and the three mutually perpendicular unit vectors i_1, i_2 and i_3 ; in the given order, i_1, i_2 and i_3 form a right-handed system. The unit vector i_2 points downwards. The vector $\mathbf{x} = x_1 i_1 + x_2 i_2$ denotes the two-dimensional position vector in the x_1, x_2 space.

Use is made of the temporal and spatial Fourier transform pairs. The circumflex $\widehat{\mathrm{F}}$ denotes the Fourier transform of F with respect to the time coordinate; the tilde $\widetilde{\mathrm{F}}$ denotes the Fourier transform of F with respect to the spatial and time coordinate. Further an asterisk $(*)$ denotes convolution. The scattering problem is treated in only two dimensions to keep the notation of the problem simple. The definition of the temporal Fourier transform is given by

$$\widehat{\mathrm{X}}(\omega) = \int_{-\infty}^{+\infty} \mathrm{X}(t) \exp(j\omega t)\, dt \,, \tag{1.1-1}$$

$$\mathrm{X}(t) = \frac{1}{2\pi} \int_{-\infty}^{+\infty} \widehat{\mathrm{X}}(\omega) \exp(-j\omega t)\, d\omega \,. \tag{1.1-2}$$

The explicit functional dependence on ω is omitted if it is not confusing.
The following definition of the forward and backward spatial Fourier transform is used:

$$\widetilde{\mathrm{X}}(\mathbf{k}) = \int_{-\infty}^{+\infty} \widehat{\mathrm{X}}(\mathbf{x}) \exp(-jk_\beta x_\beta)\, dx_\beta \,, \tag{1.1-3}$$

$$\widehat{\mathrm{X}}(\mathbf{x}) = \left(\frac{1}{2\pi}\right)^2 \int_{-\infty}^{+\infty} \widetilde{\mathrm{X}}(\mathbf{k}) \exp(jk_\beta x_\beta)\, dk_\beta \,. \tag{1.1-4}$$

A list of major symbols is given below.

SYMBOL	DESCRIPTION	DIMENSION
P	acoustic pressure	[Nm^{-2}] = [Pa]
P^{in}	incident pressure field	[Nm^{-2}]
P^{sc}	scattered pressure field	[Nm^{-2}]
V_α	particle velocity vector	[ms^{-1}]
V_α^{in}	incident particle velocity field	[ms^{-1}]
V_α^{sc}	scattered particle velocity field	[ms^{-1}]
F_α	volume force density	[Nm^{-3}]
Q	volume injection rate density	[s^{-1}]
∂f_α	equivalent surface force source of the strip	[Nm^{-2}]
∂q	equivalent surface injection source of the strip	[ms^{-1}]
ρ	volume density of mass	[kgm^{-3}]
κ	compressibility	[N^{-1}m^{2}]
$c = \left(\kappa\rho\right)^{-\frac{1}{2}}$	acoustic wave speed	[ms^{-1}]
$j = \sqrt{-1}$	the imaginary number	
ω	angular frequency	[s^{-1}]
$k = \frac{\omega}{c}$	wavenumber	[m^{-1}]
$\mathbf{k} = k_1 i_1 + k_2 i_2$	wave vector	[m^{-1}]
k_β	spatial wavenumber	[m^{-1}]
k_1	horizontal wavenumber	[m^{-1}]
$k_2 = \left(k^2 - k_1^{2}\right)^{\frac{1}{2}}$	vertical wavenumber	[m^{-1}]
$\mathbf{x} = x_1 i_1 + x_2 i_2$	vectorial position	[m]
x_β	spatial coordinates	[m]
$\{i_1, i_2\}$	base unit vectors that are mutually perpendicularly oriented	
∂_α	partial derivative with respect to x_α	[m^{-1}]
$\nabla^2 = \partial_\alpha \partial_\alpha = \partial_1^2 + \partial_2^2$	Laplace operator	[m^{-2}]
$-k_\alpha k_\alpha = -\left(k_1^2 + k_2^2\right)$	Laplace operator in wavenumber domain	[m^{-2}]
D	domain in space	
∂D	boundary of domain D	
dA_m	vectorial elemtary area on ∂D oriented away from D	[m^{2}]
V	volume of domain D	[m^{3}]

SYMBOL	DESCRIPTION	DIMENSION
$\hat{G}(\mathbf{x} \mid \mathbf{x}')$	Green's function with source position $\mathbf{x}'$	
$\hat{G}^{q}(\mathbf{x} \mid \mathbf{x}')$	pressure tensor of the injection source Green's state	$[Nm^{-4}s]$
$\hat{\Gamma}_{\alpha}^{q}(\mathbf{x} \mid \mathbf{x}')$	particle velocity tensor of the injection source Green's state	$[m^{-1}]$
$\hat{G}_{\beta}^{f}(\mathbf{x} \mid \mathbf{x}')$	pressure tensor of the force source Green's state	$[m^{-1}]$
$\hat{\Gamma}_{\alpha,\beta}^{f}(\mathbf{x} \mid \mathbf{x}')$	particle velocity tensor of the force source Green's state	$[N^{-1}m^{2}s^{-1}]$
$\hat{s}$	source signature of the injection source	$[m^{2}]$
$\hat{s}_{\alpha}$	source signature of the force source	$[Nsm^{-1}]$
$\mathbf{x}'$	position of the point source in the Green's function	[m]
$\delta_{m,k}$	Kronecker delta $= 0$ if $m \neq k$ $= 1$ if $m = k$	
$\delta(x_{\beta} - x'_{\beta})$	Dirac function	$[m^{-2}]$
$H_{0}^{(1)}(\mathbf{x} \mid \mathbf{x}')$	zero order Hankel function of the first kind	
Δ^{s}	bounded domain representing the disk area	
$D^{s,-}$	surface around the disk with the normal oriented in the $-x_2$ direction	
$D^{s,+}$	surface around the disk with the normal oriented in the $+x_2$ direction	
Lu	linear operator L acting on a function $u \in D$	
L^{*}	Hilbert adjoint operator of L	
T	bounded linear operator on D	
ϕ_N	linearly independent expansion function for the unknown function u	
$\alpha_n^{(N)}$	expansion coefficients for ϕ_N	
ψ_N	linearly orthogonal expansion function for the unknown function u	
$\beta_n^{(N)}$	expansion coefficients for ψ_N	
r_N	residual at the N-th step of iteration	
ERR_N	global root-mean-square error	
$\widehat{ERR}_N$	normalized root-mean-square error	

INTRODUCTION

The theory described in this thesis is part of a project at the applied Geophysics section of the faculty of Mining and Petroleum Engineering. The project started with a new theoretical approach which describes the removal of surface related wave phenomena in the marine case developed by Fokkema and van den Berg (1990). In order to test this new theory, a well defined test problem is needed. This thesis gives the theoretical description of the test problem. According to this theory a program has been written which produces a reference data set. As test problem the scattering by a strip is chosen because of the clear theoretical description of this problem. Another advantage of this problem is that the new theory of surface effects removal and the scattering theory are using Rayleigh's reciprocity theorem to derive the fundamental integral equations.

The aim of my project is to make a data set in which the situation is given in an unbounded medium and with the same configuration in a bounded medium. In the bounded medium multiples distort the original data which is given by the unbouded medium. In geophysics the distortion introduced by the multiples must be removed, or at least suppressed, in order to make a reliable picture of the earth by further data processing.

In Chapter 1 a brief introduction is given of the tools needed to describe the scattering problem. The tools which lead to the description of the scattering problem are Rayleigh's reciprocity theorem and the method of Green's functions. The description of scattering by a compliant strip and by a rigid strip, in an unbounded medium, are given in the last two sections of Chapter 1. The solutions are given as integral equations which can only be solved numerically. In Chapter 2 the Green's function is adapted to the scattering situation in a halfspace. In this chapter the strength of the Green's function method becomes clear. The effect of the halfspace is that ghosts (reflected sources and receivers) and surface multiples are introduced in the scattering picture. All these effects can be described with the Green's function. Chapter 3 summarizes some results and incorporates the effect of source and receiver. At the end of Chapter 3 an example is worked out to show how the different parts of the theory can be used to solve the scattering problem.

Chapter 4 gives a description of the numerical scheme which can solve the integral equations derived in earlier chapters. These schemes and the computer program which implements these schemes are developed by P.M. van den Berg (1989). Chapter 5 gives the operator expressions which the numerical scheme, adapted to the strip problem, needs in order to solve the integral equation. In solving the problem Fourier transforms are intensively used. Therefore in the remaining part of Chapter 5 a short description is given of Fourier transforms, branch points, and causality. Finally in Chapter 6 some pictures are given. The configuration is chosen such that it can be 'compared' with a marine shot gather. The pictures are made for different source positions for a compliant and a rigid strip both in a bounded and an unbouded medium.

Chapter 1

SCATTERING BY A STRIP IN AN UNBOUNDED MEDIUM

1.0 INTRODUCTION

When a sound wave encounters an obstacle, some of the wave is deflected from it is original course. The difference between the actual wave field and the undisturbed wave field, which would be present if the obstacle were not there, is defined as the scattered wave field. In the present sections the scattering of an incident acoustic wave by an impenetrable strip of vanishing thickness and of bounded extent is investigated. The strip is embedded in a homogeneous, isotropic fluid of infinite extent. The object is impenetrable, and hence explicit boundary conditions have to be prescribed upon approaching either side of the strip.

To set up the scattering theory Rayleigh's reciprocity theorem and the method of Green's functions is used. A brief introduction of these tools is given in section 1.1 and section 1.2. In section 1.3 a general setup is made for the scattering problem by a strip. Sections 1.4 and 1.5 deal with two types of boundary conditions, one where the pressure on the disk is zero and another where the particle velocity perpendicular to the surface of the disk is zero.

The scattering problem is treated in only two dimensions to keep the notation simple. The integral-equation formulation of these scattering problems is presented in the frequency-space domain.

The definition of the temporal Fourier transform is given by

$$\hat{X}(\omega) = \int_{-\infty}^{+\infty} X(t) \exp(j\omega t)\, dt \,, \tag{1.1-1}$$

$$X(t) = \frac{1}{2\pi} \int_{-\infty}^{+\infty} \hat{X}(\omega) \exp(-j\omega t)\, d\omega \,. \tag{1.1-2}$$

The explicit functional dependence on ω is omitted if it is not confusing.
The following definition of the forward and backward spatial Fourier transform is used:

$$\tilde{X}(\mathbf{k}) = \int_{-\infty}^{+\infty} \hat{X}(\mathbf{x}) \exp(-jk_\beta x_\beta)\, dx_\beta \,, \tag{1.1-3}$$

$$\hat{X}(\mathbf{x}) = \left(\frac{1}{2\pi}\right)^2 \int_{-\infty}^{+\infty} \tilde{X}(\mathbf{k}) \exp(jk_\beta x_\beta)\, dk_\beta \,. \tag{1.1-4}$$

1.1 RAYLEIGH'S RECIPROCITY THEOREM

The reciprocity theorem interrelates the field quantities associated with two non-identical physical states that occur in one and the same, time invariant, domain in space (de Hoop, 1988). The two states will be distinguished by the superscripts a and b.

The acoustic wave field equations in the frequency domain are for state A and B:

$$\partial_k \hat{P}^{a,b} + \hat{\zeta}\hat{V}_k^{a,b} = \hat{F}_k^{a,b} \quad , \tag{1.1-5}$$

$$\partial_r \hat{V}_r^{a,b} + \hat{\eta}\hat{P}^{a,b} = \hat{Q}^{a,b} \quad , \tag{1.1-6}$$

where the following notation is used:

$$\begin{aligned} \hat{\zeta} &= -j\omega\rho \\ \hat{\eta} &= -j\omega\kappa \quad . \end{aligned} \tag{1.1-7}$$

$\hat{P}(\mathbf{x},\omega)$ is the acoustic pressure, $\hat{V}_k(\mathbf{x},\omega)$ is the particle velocity, ρ is the volume density of mass, κ is the compressibility, $\hat{F}_k(\mathbf{x},\omega)$ is the volume force density and $\hat{Q}(\mathbf{x},\omega)$ is the volume injection rate density. The medium in both states is chosen to be the same.

The fundamental interaction quantity between the two states in Rayleigh's reciprocity theorem is:

$$\partial_m\left(\hat{P}^a\hat{V}_m^b - \hat{P}^b\hat{V}_m^a\right) = \hat{V}_m^b\partial_m\hat{P}^a + \hat{P}^a\partial_m\hat{V}_m^b - \hat{V}_m^a\partial_m\hat{P}^b - \hat{P}^b\partial_m\hat{V}_m^a \, . \tag{1.1-8}$$

For state A equation (1.1-5) is multiplied by $\delta_{m,k}\hat{V}_m^b$ and equation (1.1-6) by $\hat{P}^b$, and for state B equation (1.1-5) is multiplied by $\delta_{m,k}\hat{V}_m^a$ and equation (1.1-6) by $\hat{P}^a$ Substitute these results in equation (1.1-8) and the result is given by

$$\partial_m\left(\hat{P}^a\hat{V}_m^b - \hat{P}^b\hat{V}_m^a\right) = \hat{F}_m^a\hat{V}_m^b + \hat{Q}^b\hat{P}^a - \hat{F}_m^b\hat{V}_m^a - \hat{Q}^a\hat{P}^b \, . \tag{1.1-9}$$

Equation (1.1-9) is the local form of Rayleigh's reciprocity theorem.
Integrating equation (1.1-9) over the domain D and using Gauss's theorem in the left hand side leads to Rayleigh's reciprocity theorem in its global form.

$$\int_{x\in\partial D}\left(\hat{P}^a\hat{V}_m^b-\hat{P}^b\hat{V}_m^a\right)dA_m=\int_{x\in D}\left(\hat{F}_m^a\hat{V}_m^b+\hat{Q}^b\hat{P}^a-\hat{F}_m^b\hat{V}_m^a-\hat{Q}^a\hat{P}^b\right)dV\ , \qquad (1.1\text{-}10)$$

where the boundary surface of domain D is denoted by ∂D and dA_m is the vectorial elementary area on ∂D oriented away from D.

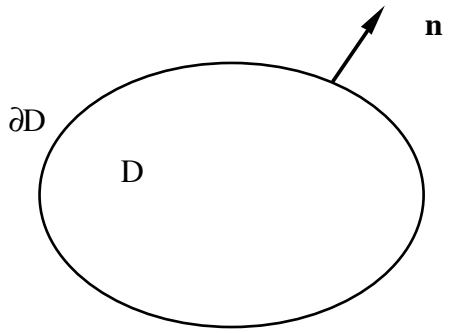

Figure 1.1 : Domain of application of the reciprocity theorem

In two-dimensional wave motions, the geometrical configuration as well as the field quantities involved are assumed to be independent of one of the Cartesian coordinates. As such the two-dimensional theory can be considered as a special case of the three-dimensional one (Tan, 1975).

In two-dimensions Rayleigh's reciprocity theorem in its global form is given by:

$$\int_{x\in\partial D}\left(\hat{P}^a\hat{V}_\alpha^b-\hat{P}^b\hat{V}_\alpha^a\right)n_\alpha dS=\int_{x\in D}\left(\hat{F}_\alpha^a\hat{V}_\alpha^b+\hat{Q}^b\hat{P}^a-\hat{F}_\alpha^b\hat{V}_\alpha^a-\hat{Q}^a\hat{P}^b\right)dA\ , \qquad (1.1\text{-}11)$$

in which n_α denotes the unit vector normal to ∂D pointing away from D (shown in Figure 1.1). Rayleigh's reciprocity theorem can be regarded as the most fundamental theorem of acoustic wave-field theory. Physically it describes the interaction between two acoustic wave states, a feature that is characteristic for any type of measurement situation. The global form of the theorem forms the basis for the construction of solutions of acoustic wave field problems.

1.2 GREEN'S FUNCTION IN A TWO-DIMENSIONAL SPACE

The Green's function method is developed to solve boundary value problems. The usefulness of a Green's function solution is that the Green's function is the solution of the differential equation with a delta distribution as the inhomogeneous term. Once the Green's

function is determined, the solution of the boundary value problem for different inhomogeneous terms $f(x)$ is obtained by a single integration (Greenberg, 1971).

1.2.1 Green's function for the Helmholtz equation

The Green's function necessary for the scattering problem in two-dimensions is defined by the inhomogeneous wave-equation. The inhomogeneous wave equation, Fourier transformed with respect to time is given by,

$$\partial_\alpha \partial_\alpha \hat{G}(\mathbf{x}) + k^2 \hat{G}(\mathbf{x}) = -\delta(\mathbf{x}-\mathbf{x}') \quad . \tag{1.2-1}$$

So the temporal Fourier transformed Green's function is a solution of the inhomogeneous Helmholtz equation. The Green's function can be solved from equation (1.2-1) by transforming it with respect to the spatial coordinates.

The transformation of (1.2-1) gives, using the spatial Fourier transform of equation (1.1-3):

$$\left(-k_\alpha k_\alpha + k^2\right)\tilde{G} = -\exp\left[-jk_\beta x'_\beta\right] ,$$

$$\tilde{G}(\mathbf{k}) = \frac{\exp\left[-jk_\beta x'_\beta\right]}{\left(k_\alpha k_\alpha - k^2\right)} . \tag{1.2-2}$$

The backtransform of expression (1.2-2), for the Green's function is, using (1.1-4),

$$\hat{G}(\mathbf{x}\,|\mathbf{x}') = \left(\frac{1}{2\pi}\right)^2 \int_{-\infty}^{+\infty} dk_1 \int_{-\infty}^{+\infty} \frac{\exp\left[jk_\beta\left(x_\beta - x'_\beta\right)\right]}{\left(k_\alpha k_\alpha - k^2\right)} dk_2 . \tag{1.2-3}$$

The first integration with respect to k_2 is done by applying the theorem of residues. By changing the path of integration in accordance with Cauchy's theorem an expression for the integral is derived.

The wavenumber k is chosen to have a small positive imaginary part in order to move the poles on the real axis below or above the real axis. The integral has two poles $k_2^+ = \left(k^2 - k_1^2\right)^{\frac{1}{2}}$ and $k_2^- = -\left(k^2 - k_1^2\right)^{\frac{1}{2}}$, one above the positive real axis and one below the negative real axis. The original path of integration is the real axis, since positive poles are slightly above it, the path of

integration passes below it. The paths of integration for the positive pole and the negative pole are shown in Figure 1.2 .

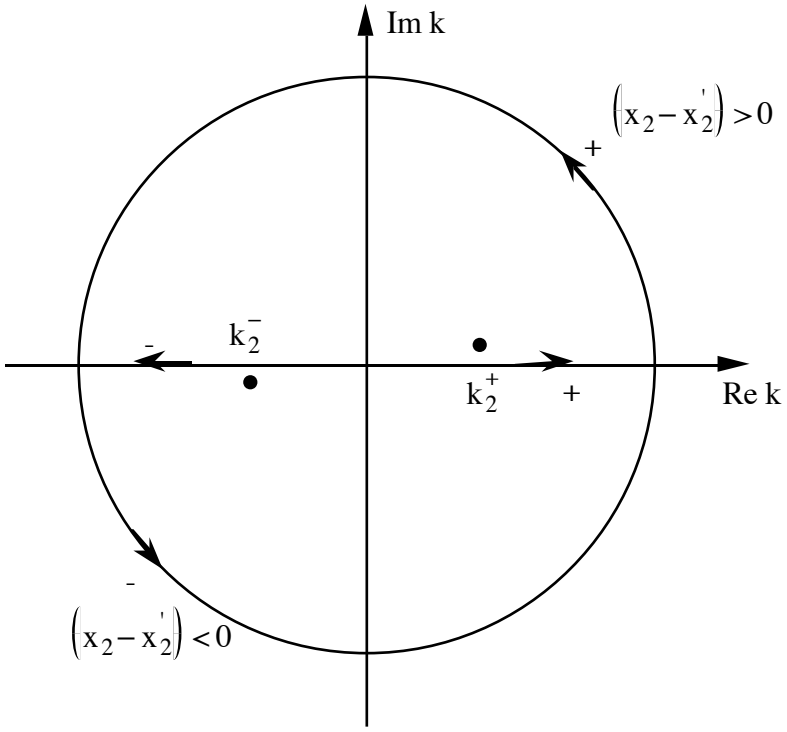

Figure 1.2 : Paths of integration that leads to a converging wave solution

The integration can now be carried out with Cauchy's theorem of residues. If $\left(x_2 - x_2'\right) > 0$ the contour for the positive pole is closed by a semicircle of large radius in the upper half plane. If $\left(x_2 - x_2'\right) < 0$ the contour for the negative pole is closed by a semicircle of large radius in the lower half plane. If the radius of the semicircle goes to infinity, the contribution of the integral along the semicircle tends to zero on account of Jordan's lemma.
The residue of the integrand at k_2^+, where $\left(x_2 - x_2'\right) > 0$, is

$$\mathrm{Res}\left(k_2^+\right) = \lim_{k_2 \to k_2^+} \frac{2\pi j\left(k_2 - \left(k^2 - k_1^2\right)^{\frac{1}{2}}\right)\exp\left(jk_1\left(x_1 - x_1'\right) + jk_2\left(x_2 - x_2'\right)\right)}{\left(k_2^2 - \left(k^2 - k_1^2\right)\right)},$$

$$\mathrm{Res}\left(k_2^+\right) = \frac{2\pi j \exp\left(jk_1\left(x_1 - x_1'\right) + jk_2^+\left(x_2 - x_2'\right)\right)}{2\left(k^2 - k_1^2\right)^{\frac{1}{2}}}. \qquad (1.2\text{-}4)$$

The residue of the integrand at k_2^- , where $\left(x_2 - x_2^{'}\right) < 0$, is

$$\mathrm{Res}\left(k_2^-\right) = \frac{2\pi j \ \exp\left(jk_1\left(x_1 - x_1^{'}\right) + jk_2^-\left(x_2 - x_2^{'}\right)\right)}{2\left(k^2 - k_1^2\right)^{\frac{1}{2}}} . \qquad (1.2\text{-}5)$$

The integral over k_2 is equal to the sum of the residues for positive values ($\left(x_2 - x_2^{'}\right) > 0$) plus the residue for negative values ($\left(x_2 - x_2^{'}\right) < 0$) .This results finally in

$$\hat{\mathrm{G}}\left(\mathbf{x} \mid \mathbf{x}^{'}\right) = \frac{j}{4\pi} \int_{-\infty}^{+\infty} \frac{\exp\left[jk_1\left(x_1 - x_1^{'}\right) + j\gamma \left| x_2 - x_2^{'} \right|\right]}{\gamma} dk_1 , \qquad (1.2\text{-}6)$$

where

$$\gamma = \left(k^2 - k_1^2\right)^{\frac{1}{2}} \qquad \text{and } \mathrm{im}(\gamma) > 0.$$

The result of this integration can be recognized as the zero order Hankel function of the first kind.

$$\equiv \ \frac{j}{4}\mathrm{H}_0^{(1)}\left(k\left[\left(x_1 - x_1^{'}\right)^2 + \left(x_2 - x_2^{'}\right)^2\right]^{\frac{1}{2}}\right) \ = \ \frac{j}{4}\mathrm{H}_0^{(1)}(kr) , \qquad (1.2\text{-}7)$$

where

$$r = \left[\left(x_1 - x_1^{'}\right)^2 + \left(x_2 - x_2^{'}\right)^2\right]^{\frac{1}{2}} ,$$

and $\frac{j}{4}\mathrm{H}_0^{(1)}(kr)$ is used as a short notation for the zero order Hankel function of the first kind.

The recognition of equation (1.2-6) as the Hankel function is explained in detail in the following references: Skudrzyk, E., *The foundations of acoustics,* 1971 section 27.9.2 or: Morse, P.M. and H. Feshbach, *Methods of theoretical physics* , 1953 , p. 623 and p.823.

The occurrence of the Hankel function, which is a linear combination of two Bessel functions, is explained by the fact that the Helmholtz equation in polar coordinates is Bessel's equation.

Asymptotic behavior of $H_0^{(1)}(kr)$ at big values

$$H_0^{(1)}(kr) \cong \sqrt{\frac{2}{\pi kr}} \exp\left(j\left(kr - \frac{\pi}{4}\right)\right) \qquad \text{as } kr \to \infty . \tag{1.2-8a}$$

Asymptotic behavior of $H_0^{(1)}(kr)$ at small values

$$H_0^{(1)}(kr) \cong 2j\ln(kr) \qquad \text{if } kr \to 0 , \tag{1.2-8b}$$

which represents a singularity at $r = 0$; which is the position of the point source.

1.2.2 The injection source Green's function

The wave equations (1.1-5) and (1.1-6) for the injection source Green's state are

$$\partial_\alpha \hat{P}^q + \hat{\zeta}\hat{V}_\alpha^q = 0 , \tag{1.2-9}$$

$$\partial_\beta \hat{V}_\beta^q + \hat{\eta}\hat{P}^q = \hat{s}\,\delta(\mathbf{x} - \mathbf{x}') . \tag{1.2-10}$$

The following relation for the injection source Green's state is used (Ottes, 1987):

$$\left(\hat{P}^q, \hat{V}_\alpha^q\right) = \hat{s}\left(\hat{G}^q, \hat{\Gamma}_\alpha^q\right) , \tag{1.2-11}$$

in which $\hat{s}$ is the spectrum of the volume injection function at the point $\mathbf{x}'$.

Substituting relation (1.2-11) in equations (1.2-9) and (1.2-10), eliminating of $\hat{P}^q$, and canceling out the source signature gives:

$$\partial_\beta \partial_\beta \hat{G}^q + k^2 \hat{G}^q = -\hat{\zeta}\,\delta(\mathbf{x} - \mathbf{x}') , \tag{1.2-12}$$

where the fact is used that

$$\hat{\zeta}\hat{\eta} = -\omega^2 \kappa\rho = \frac{-\omega^2}{c^2} = -k^2 . \tag{1.2-13}$$

Equation (1.2-12) is the inhomogeneous Helmholtz equation from paragraph 1.2.1. The solution of equation (1.2-12) is given by $\hat{\zeta}\frac{j}{4}H_0^{(1)}(kr)$ which follows from equation (1.2-7).

So the resulting injection source Green's function for the 'pressure' tensor of order zero is:

$$\hat{G}^{q}(\mathbf{x}\,|\,\mathbf{x}') = \hat{\zeta}\frac{j}{4}H_0^{(1)}(kr)\ . \tag{1.2-14}$$

The 'particle velocity' tensor for this Green's state is calculated with the use of equation (1.2-9)

$$\hat{\Gamma}_{\alpha}^{q}(\mathbf{x}\,|\,\mathbf{x}') = -\hat{\zeta}^{-1}\partial_{\alpha}\hat{G}^{q}(\mathbf{x}\,|\,\mathbf{x}') = -\partial_{\alpha}\frac{j}{4}H_0^{(1)}(kr)\ . \tag{1.2-15}$$

1.2.3 The force source Green's function

Wave equations (1.1-5) and (1.1-6) for the force source Green's state are given by

$$\partial_{\alpha}\hat{P}^{f} + \hat{\zeta}\hat{V}_{\alpha}^{f} = \hat{s}_{\alpha}\delta(\mathbf{x}-\mathbf{x}')\,, \tag{1.2-16}$$

$$\partial_{\beta}\hat{V}_{\beta}^{f} + \hat{\eta}\hat{P}^{f} = 0\,, \tag{1.2-17}$$

where $\hat{s}_{\alpha}$ is an arbitrary constant vector representing the spectrum of the directional source signature. The Green's solution depends linearly on the components of $\hat{s}_{\alpha}$.

To express this dependence the tensors $\hat{\Gamma}_{\alpha,\beta}^{f}$ and $\hat{G}_{\beta}^{f}$ are introduced, which are related to the original $\hat{\Gamma}_{\alpha}^{f}$ and $\hat{G}^{f}$ through $\hat{\Gamma}_{\alpha}^{f} = \hat{s}_{\beta}\hat{\Gamma}_{\alpha,\beta}^{f}$ and $\hat{G}^{f} = \hat{s}_{\beta}\hat{G}_{\beta}^{f}$.

The following relation for the force source Green's state is used (Ottes, 1987):

$$\left\{\hat{P}^{f}\,,\,\hat{V}_{\alpha}^{f}\right\} = \hat{s}_{\beta}\left\{\hat{G}_{\beta}^{f}\,,\,\hat{\Gamma}_{\alpha,\beta}^{f}\right\}. \tag{1.2-18}$$

The relation between the force source Green's state and the injection source Green's state can be found by using Rayleigh's reciprocity theorem. This is done by taking state *A* as the force source Green's state and taking state *B* as the injection source Green's state. The relation between the two states is:

$$\hat{G}_{\alpha}^{f}(\mathbf{x}\,|\,\mathbf{x}') = -\hat{\Gamma}_{\alpha}^{q}(\mathbf{x}\,|\,\mathbf{x}') \tag{1.2-19}$$

which holds for any choice of $\hat{s}_{\beta}$.

$\hat{\Gamma}_{\alpha,\beta}^{f}$ can be solved from relation (1.2-18) and equation (1.2-16) and is given by:

$$\hat{\Gamma}^{\mathrm{f}}_{\alpha,\beta}(\mathbf{x}\mid\mathbf{x}') = \hat{\zeta}^{-1}\left(\delta_{\alpha,\beta}\delta(\mathbf{x}-\mathbf{x}') - \partial_\alpha \hat{\mathrm{G}}^{\mathrm{f}}_{\beta}(\mathbf{x}\mid\mathbf{x}')\right) , \tag{1.2-20}$$

which holds for any choice of $\hat{s}_\beta$.

Substituting equation (1.2-19) in equation (1.2-20) results in

$$\hat{\Gamma}^{\mathrm{f}}_{\alpha,\beta}(\mathbf{x}\mid\mathbf{x}') = \hat{\zeta}^{-1}\left(\delta_{\alpha,\beta}\delta(\mathbf{x}-\mathbf{x}') + \partial_\alpha \hat{\Gamma}^{\mathrm{q}}_{\beta}(\mathbf{x}\mid\mathbf{x}')\right) . \tag{1.2-21}$$

Finally substituting equation (1.2-15) in equation (1.2-21) gives

$$\hat{\Gamma}^{\mathrm{f}}_{\alpha,\beta}(\mathbf{x}\mid\mathbf{x}') = \hat{\zeta}^{-1}\left(\delta_{\alpha,\beta}\delta(\mathbf{x}-\mathbf{x}') - \frac{j}{4}\partial_\alpha\partial_\beta \mathrm{H}_0^{(1)}(kr)\right) . \tag{1.2-22}$$

Equation (1.2-22) is an expression for the particle velocity Green's tensor for the force source state.

1.3 SCATTERING BY A STRIP

The problem of scattering objects in a domain D is solved with the use of Rayleigh's reciprocity theorem and the properties of the Green's function. By letting the point of observation approach the boundary of the obstacle an integral equation results. This result is a very convenient formulation for the scattering problem.

In the scattering problem the total field is defined as the scattered field plus the incident field,

$$\hat{P} = \hat{P}^{sc} + \hat{P}^{in} , \tag{1.3-1a}$$

$$\hat{V}_r = \hat{V}_r^{sc} + \hat{V}_r^{in} . \tag{1.3-1b}$$

1.3.1 Representation for the scattered pressure field.

To derive a representation for the pressure filed in Rayleigh's reciprocity theorem state *A* is chosen as the injection source Green's state (with relation (1.2-11))

$$\hat{P}^a(\mathbf{x}) = \hat{s}\,\hat{\mathrm{G}}^{\mathrm{q}}(\mathbf{x}\mid\mathbf{x}') , \qquad \hat{Q}^a(\mathbf{x}) = \hat{s}\,\delta(\mathbf{x}'-\mathbf{x}) , \tag{1.3-2}$$

$$\hat{V}^a_\alpha(\mathbf{x}) = \hat{s}\,\hat{\Gamma}^{\mathrm{q}}_\alpha(\mathbf{x}\mid\mathbf{x}') , \qquad \hat{F}^a_\alpha(\mathbf{x}) = 0 , \tag{1.3-3}$$

and state *B* as the total field which satisfies the acoustic wave equations with a volume source function $\widehat{Q}(\mathbf{x})$

$$\widehat{P}^{b}(\mathbf{x}) = \widehat{P}(\mathbf{x}'), \qquad \widehat{Q}^{b}(\mathbf{x}) = \widehat{Q}(\mathbf{x}'), \tag{1.3-4}$$

$$\widehat{V}_{\alpha}^{b}(\mathbf{x}) = \widehat{V}_{\alpha}(\mathbf{x}'), \qquad \widehat{F}_{\alpha}^{b}(\mathbf{x}) = 0 \ . \tag{1.3-5}$$

With these states Rayleigh's reciprocity theorem of equation (1.1-11) results in equation (1.3-6), where the source signature *s* is eliminated,

$$\int_{x\in\partial D} \left(\widehat{G}^{q}(\mathbf{x} \mid \mathbf{x}')\widehat{V}_{\alpha}(\mathbf{x}') - \widehat{P}(\mathbf{x}')\,\widehat{\Gamma}_{\alpha}^{q}(\mathbf{x}|\mathbf{x}') \right) n_{\alpha} dS(\mathbf{x}') = \int_{x\in D} \left(\widehat{Q}(\mathbf{x})\,\widehat{G}^{q}(\mathbf{x} \mid \mathbf{x}') \right) dA(\mathbf{x}') - \int_{x\in D} \delta(\mathbf{x}-\mathbf{x}')\widehat{P}(\mathbf{x}')\, dA(\mathbf{x}') \tag{1.3-6}$$

Solving the last integral on the right hand-side of equation (1.3-6) results in:

$$\chi_{D}(\mathbf{x})\widehat{P}(\mathbf{x}) = \int_{x\in D} \left(\widehat{Q}(\mathbf{x}')\,\widehat{G}^{q}(\mathbf{x} \mid \mathbf{x}') \right) dA' - \int_{x\in\partial D} \left(\widehat{G}^{q}(\mathbf{x} \mid \mathbf{x}')\widehat{V}_{\alpha}(\mathbf{x}') - \widehat{P}(\mathbf{x}')\,\widehat{\Gamma}_{\alpha}^{q}(\mathbf{x} \mid \mathbf{x}') \right) n_{\alpha} dS' \tag{1.3-7}$$

with the characteristic function $\chi_{D}(\mathbf{x})$ of domain D defined as

$$\chi_{D}(\mathbf{x}) = \left\{ 1, \tfrac{1}{2}, 0 \right\} \quad \text{when} \quad \mathbf{x} \in \left\{ D, \partial D, \overline{D} \right\} . \tag{1.3-8}$$

Since $\widehat{G}^{q}(\mathbf{x} \mid \mathbf{x}')$ is the field at $\mathbf{x}$ due to a point source at $\mathbf{x}'$ equation (1.3-7) states that the total field at $\mathbf{x}$ is the summation of the fields from all the elementary sources $\widehat{Q}(\mathbf{x}')dV'$ plus the waves reflected by the boundary surfaces. So equation (1.3-7) is a representation of the *total pressure field outside the scattering domain.*

From the above considerations it is concluded that the domain integral over domain D is the incident field. This reduces equation (1.3-7) further to.,

$$\chi_{D}(\mathbf{x})\,\widehat{P}(\mathbf{x}) = \widehat{P}^{in}(\mathbf{x}) - \int_{x\in\partial D} \left(\widehat{G}^{q}(\mathbf{x} \mid \mathbf{x}')\widehat{V}_{\alpha}(\mathbf{x}') - \widehat{P}(\mathbf{x}')\,\widehat{\Gamma}_{\alpha}^{q}(\mathbf{x} \mid \mathbf{x}') \right) n_{\alpha} dS' \ . \tag{1.3-9}$$

If there is only one strip in the unbounded domain D then the boundary ∂D consists of a boundary at infinity and a boundary at the strip as shown in Figure 1.3 (the normal vectors **n** at the boundary are pointing away from the embedding D).

The integration at infinity vanishes in an unbounded medium if all waves are outgoing. This leaves only the surface integral over the strip

$$\chi_{\mathrm{D}}(\mathbf{x})\,\widehat{P}(\mathbf{x}) = \widehat{P}^{\,in}(\mathbf{x}) - \int_{x\in\partial \mathrm{D}^{sc}} \left(\widehat{\mathrm{G}}^{\mathrm{q}}(\mathbf{x}\mid\mathbf{x}')\widehat{V}_{\alpha}(\mathbf{x}') - \widehat{P}(\mathbf{x}')\,\widehat{\Gamma}^{\mathrm{q}}_{\alpha}(\mathbf{x}\mid\mathbf{x}') \right) n_{\alpha} dS' \,. \quad (1.3\text{-}10)$$

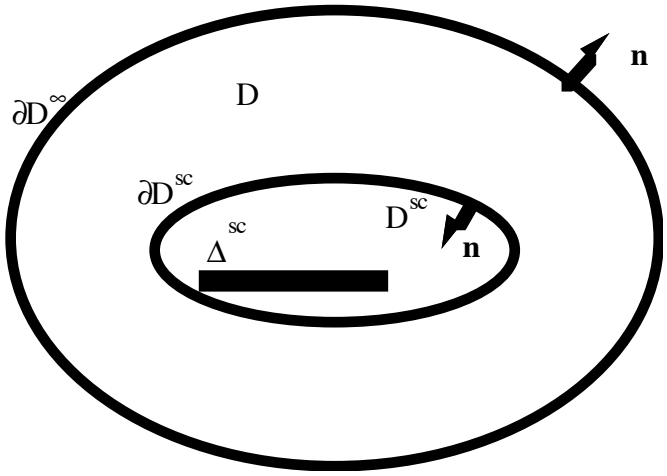

Figure 1.3 : Rayleigh's reciprocity theorem applied to domain D with a strip embedded in it

To make equation (1.3-10) more clear the same equation is derived by considering the scattered field and the incident field contributions separate. This will be set out in the remainder of this section.

An expression for the *scattered field outside the scattering domain* is derived by applying Rayleigh's reciprocity theorem with state *A* as the injection source Green's state

$$\widehat{P}^{\,a}(\mathbf{x}) = \hat{s}\,\widehat{\mathrm{G}}^{\mathrm{q}}(\mathbf{x}\mid\mathbf{x}')\,, \qquad \widehat{Q}^{\,a}(\mathbf{x}) = \hat{s}\,\delta(\mathbf{x}'-\mathbf{x})\,, \quad (1.3\text{-}11)$$

$$\widehat{V}^{\,a}_{\alpha}(\mathbf{x}) = \hat{s}\,\widehat{\Gamma}^{\mathrm{q}}_{\alpha}(\mathbf{x}\mid\mathbf{x}')\,, \qquad \widehat{F}^{\,a}_{\alpha}(\mathbf{x}) = 0\,, \quad (1.3\text{-}12)$$

and state *B* as the source-free scattered field inside domain D

$$\widehat{P}^{\,b}(\mathbf{x}) = \widehat{P}^{\,sc}(\mathbf{x}')\,, \qquad \widehat{Q}^{\,b}(\mathbf{x}) = 0\,, \quad (1.3\text{-}13)$$

$$\widehat{V}^{\,b}_{\alpha}(\mathbf{x}) = \widehat{V}^{\,sc}_{\alpha}(\mathbf{x}')\,, \qquad \widehat{F}^{\,b}_{\alpha}(\mathbf{x}) = 0\,. \quad (1.3\text{-}14)$$

Substituting these states in (1.1-11), Rayleigh's reciprocity theorem then yields

$$\hat{P}^{sc}(\mathbf{x}) = -\int_{x\in\partial D^{sc}} \left(\hat{G}^{q}(\mathbf{x}\mid\mathbf{x}')\hat{V}_{\alpha}^{sc}(\mathbf{x}') - \hat{P}^{sc}(\mathbf{x}')\hat{\Gamma}_{\alpha}^{q}(\mathbf{x}\mid\mathbf{x}') \right) n_{\alpha} dS' \quad x \in D . \quad (1.3\text{-}15)$$

An expression for the *incident field inside the scattering domain* is derived by applying Rayleigh's reciprocity theorem to domain D^{sc} with state *A* as the injection source Green's state.

$$\hat{P}^{a}(\mathbf{x}) = \hat{s}\,\hat{G}^{q}(\mathbf{x}\mid\mathbf{x}') , \qquad \hat{Q}^{a}(\mathbf{x}) = \hat{s}\,\delta(\mathbf{x}'-\mathbf{x}) , \quad (1.3\text{-}16)$$

$$\hat{V}_{\alpha}^{a}(\mathbf{x}) = \hat{s}\,\hat{\Gamma}_{\alpha}^{q}(\mathbf{x}\mid\mathbf{x}') , \qquad \hat{F}_{\alpha}^{a}(\mathbf{x}) = 0 , \quad (1.3\text{-}17)$$

and state *B* as the source-free incident field in domain D^{sc}

$$\hat{P}^{b}(\mathbf{x}) = \hat{P}^{in}(\mathbf{x}') , \qquad \hat{Q}^{b}(\mathbf{x}) = 0 , \quad (1.3\text{-}18)$$

$$\hat{V}_{\alpha}^{b}(\mathbf{x}) = \hat{V}_{\alpha}^{in}(\mathbf{x}') , \qquad \hat{F}_{\alpha}^{b}(\mathbf{x}) = 0 . \quad (1.3\text{-}19)$$

Substituting these states in Rayleigh's reciprocity theorem (1.1-11) gives

$$\hat{P}^{in}(\mathbf{x}) = \int_{x\in\partial D^{sc}} \left(\hat{G}^{q}(\mathbf{x}\mid\mathbf{x}')\hat{V}_{\alpha}^{in}(\mathbf{x}') - \hat{P}^{in}(\mathbf{x}')\hat{\Gamma}_{\alpha}^{q}(\mathbf{x}\mid\mathbf{x}') \right) n_{\alpha} dS' \quad x \in D . \quad (1.3\text{-}20)$$

The unit vector **n** points towards D^{sc} as shown in Figure 1.3.

Combining equation (1.3-15) and equation (1.3-20), and realizing that the total field is the incident field plus the scattered field, results in the following equation:

$$\hat{P}^{sc}(\mathbf{x}) = -\int_{x\in\partial D^{sc}} \left(\hat{G}^{q}(\mathbf{x}\mid\mathbf{x}')\hat{V}_{\alpha}(\mathbf{x}') - \hat{P}(\mathbf{x}')\hat{\Gamma}_{\alpha}^{q}(\mathbf{x}\mid\mathbf{x}') \right) n_{\alpha} dS' \qquad \text{when } \mathbf{x}\in D \quad (1.3\text{-}22)$$

Equation (1.3-22) is equal to equation (1.3-10) for a point outside the sacttering domain. In these equations; $n_{\alpha}\hat{V}_{\alpha}(\mathbf{x})$ can be regarded as the surface density of equivalent injection rate ('monopole source'), and $n_{\alpha}\hat{P}(\mathbf{x})$ can be regarded as the surface density of equivalent force ('dipole source').

1.3.2 Representation for the scattered particle velocity field.

In this paragraph the same steps are followed as for the representation for the pressure field. Choose in Rayleigh's reciprocity theorem state *A* as the force source Green's state (with relation (1.2-18)) ,

$$\hat{P}^{a}(\mathbf{x}) = \hat{s}_{\beta}\hat{\mathrm{G}}^{\mathrm{f}}_{\beta}(\mathbf{x} \mid \mathbf{x}') \quad , \qquad \hat{Q}^{a}(\mathbf{x}) = 0 \; , \tag{1.3-23}$$

$$\hat{V}^{a}_{\alpha}(\mathbf{x}) = \hat{s}_{\beta}\hat{\Gamma}^{\mathrm{f}}_{\alpha,\beta}(\mathbf{x} \mid \mathbf{x}') \; , \qquad \hat{F}^{a}_{\alpha}(\mathbf{x}) = \hat{s}_{\alpha}\delta(\mathbf{x}' - \mathbf{x}) \; , \tag{1.3-24}$$

and state *B* as the total field which satisfies the acoustic wave equations with a volume source function $\hat{Q}(\mathbf{x})$,identical to equations (1.3-4) and (1.3-5).
With these states Rayleigh's reciprocity theorem, (1.1-11), results in equation (1.3-25)

$$\begin{aligned} &\int_{x\in\partial\mathrm{D}} \left(\hat{s}_{\beta}\hat{\mathrm{G}}^{\mathrm{f}}_{\beta}(\mathbf{x} \mid \mathbf{x}')\hat{V}_{\alpha}(\mathbf{x}') - \hat{P}(\mathbf{x}')\hat{s}_{\beta}\hat{\Gamma}^{\mathrm{f}}_{\alpha,\beta}(\mathbf{x} \mid \mathbf{x}') \right) n_{\alpha} dS(\mathbf{x}') = \\ &\int_{x\in\mathrm{D}} \left(\hat{Q}(\mathbf{x})\hat{s}_{\beta}\hat{\mathrm{G}}^{\mathrm{f}}_{\beta}(\mathbf{x} \mid \mathbf{x}') \right) dA(\mathbf{x}') + \int_{x\in\mathrm{D}} \hat{s}_{\alpha}\delta(\mathbf{x} - \mathbf{x}')\hat{V}_{\alpha}(\mathbf{x}')\, dA(\mathbf{x}') \end{aligned} \tag{1.3-25}$$

Solving the surface integrals on the right-hand side this results in

$$\chi_{\mathrm{D}}(\mathbf{x})\hat{V}_{\alpha}(\mathbf{x}) = -\hat{V}^{in}_{\alpha}(\mathbf{x}) + \int_{x\in\partial\mathrm{D}} \left(\hat{\mathrm{G}}^{\mathrm{f}}_{\alpha}(\mathbf{x} \mid \mathbf{x}')\hat{V}_{\beta}(\mathbf{x}') - \hat{P}(\mathbf{x}')\hat{\Gamma}^{\mathrm{f}}_{\alpha,\beta}(\mathbf{x} \mid \mathbf{x}') \right) n_{\beta} dS' \quad , \tag{1.3-26}$$

which holds for any choice of the source signature $\hat{s}_{\beta}$.

Equation (1.3-26) is a representation of the *total particle velocity field outside the scattering domain*. It is noticed that equation (1.3-26) has the same structure as equation (1.3-9).
If there is only one strip in the unbounded domain D then the boundary ∂D consists of a boundary at infinity and a boundary at the strip. On account of the radiation condition the boundary integral at infinity vanishes. This leaves only the boundary integral over the strip.

$$\chi_D(\mathbf{x})\hat{V}_\alpha(\mathbf{x}) = -\hat{V}_\alpha^{in}(\mathbf{x}) + \int_{x\in\partial D^{sc}} \left(\hat{G}^f_\alpha(\mathbf{x}\mid\mathbf{x}')\hat{V}_\beta(\mathbf{x}') - \hat{P}(\mathbf{x}')\hat{\Gamma}^f_{\alpha,\beta}(\mathbf{x}\mid\mathbf{x}') \right) n_\beta dS' \quad . \qquad (1.3\text{-}27)$$

The representation for the scattered field in the domain D (see Figure 1.3) is derived using the same arguments which lead from (1.3-11) to (1.3-22) in paragraph 1.3.1 . The particle velocity counterpart of equation (1.3-22) is

$$\hat{V}_\alpha^{sc}(\mathbf{x}) = \int_{x\in\partial D^{sc}} \left(\hat{G}^f_\alpha(\mathbf{x}\mid\mathbf{x}')\hat{V}_\beta(\mathbf{x}') - \hat{P}(\mathbf{x}')\hat{\Gamma}^f_{\alpha,\beta}(\mathbf{x}\mid\mathbf{x}') \right) n_\beta dS' \qquad \text{when } \mathbf{x}\in D. \qquad (1.3\text{-}28)$$

With this last equation all expressions for the scattered field problem are derived and can be used to solve the scattered field by a strip. In section 1.4 and section 1.5 these equations, with prescribed boundary conditions, are used to solve this scattering problem.

1.4 SCATTERING BY A PERFECTLY COMPLIANT STRIP

The scattering problem by a strip is carried out in two dimensions by applying line sources as excitation sources, and extending the strip along the direction of the line source (the x_3 direction) to infinity (see Figure 1.4 below).

To specify the position in the configuration the coordinates (x_1, x_2), with respect to a fixed orthogonal Cartesian reference frame, with origin O and the two mutually perpendicular base vectors (i_1, i_2), of unit length each is employed. In this reference frame i_2 is chosen to point vertically downward.

The strip under consideration is denoted by Δ^{sc}. The strip is taken to be located at $-a < x_1 < a$, $x_2 = 0$, $-\infty < x_3 < \infty$. The strip is embedded in an unbounded, homogeneous, isotropic fluid.

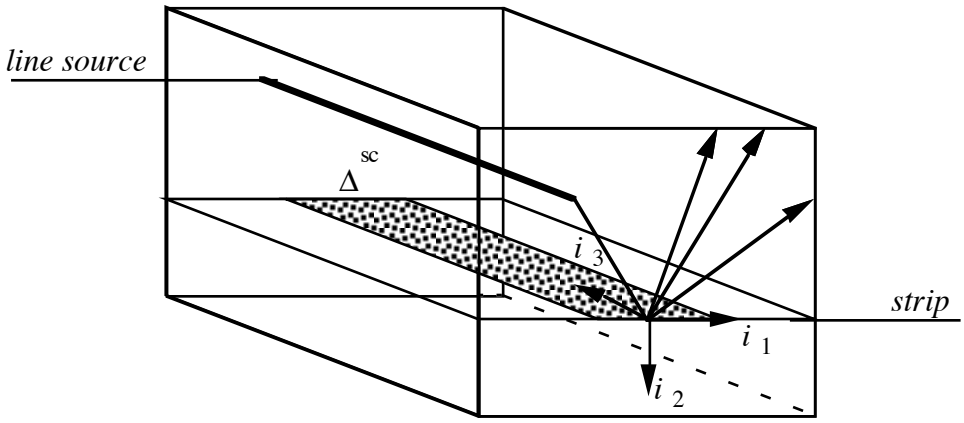

Figure 1.4 : scattering by a strip reduced to two dimensions

If the scattering object of vanishing thickness is a perfectly compliant strip, then the acoustic pressure vanishes on either side of the strip.

The boundary conditions for such a perfectly compliant strip are:

$$\lim_{x_2 \uparrow 0} \widehat{P}(\mathbf{x}) = 0 \quad \text{and} \quad \lim_{x_2 \downarrow 0} \widehat{P}(\mathbf{x}) = 0 \qquad \text{when} \quad -a < x_1 < a \,. \qquad (1.4\text{-}1)$$

Using equation (1.3-1a), the definition of the total field, this implies

$$\lim_{x_2 \uparrow 0} \widehat{P}^{sc}(\mathbf{x}) = -\lim_{x_2 \uparrow 0} \widehat{P}^{in}(\mathbf{x}) \quad \text{and} \quad \lim_{x_2 \downarrow 0} \widehat{P}^{sc}(\mathbf{x}) = -\lim_{x_2 \downarrow 0} \widehat{P}^{in}(\mathbf{x}) \quad \text{when} \quad -a < x_1 < a \,. \qquad (1.4\text{-}2)$$

The integral representation for the pressure field of the scattered wave on the strip is derived by surrounding the strip by a closed curve existing of four surfaces at a small distance from the strip.

The following surfaces are introduced around the strip (see Figure 1.5):

$$D^{sc,-} = \left\{ \mathbf{x} \in \Re^2 ; (x_1) \in \Delta^{sc}, x_2 = -\varepsilon ; \varepsilon > 0 \right\}$$
$$D^{sc,+} = \left\{ \mathbf{x} \in \Re^2 ; (x_1) \in \Delta^{sc}, x_2 = \varepsilon ; \varepsilon > 0 \right\}$$

at an arbitrary small distance ε from the strip.

In which $\Delta^{sc} =$ is a bounded domain representing the strip and $\mathbf{n}^-$ and $\mathbf{n}^+$ are the unit vectors along the normals of the surfaces $D^{sc,-}$ and $D^{sc,+}$ both oriented *towards* D. Around the edges of the strip the circles C_1 and C_2 of radius ε are introduced.

The field around the circles C_1 and C_2 must require the "edge condition". This means that through any surface, and in particular around an edge of the strip, only a finite amount of power can be transported (Tan, 1975).

Figure 1.5 : the surfaces $D^{sc,-}$, $D^{sc,+}$, C_1 and C_2 around the strip

Application of the reciprocity theorem to the bounded domain *external* to the scattering domain, making use of equation (1.3-22) and equation (1.2-15) (the expression for the particle velocity Green's tensor), gives:

$$\hat{P}^{sc}(\mathbf{x}) = \int_{x \in \partial D^{sc}} \left(\hat{G}^q(\mathbf{x} \mid \mathbf{x}') \hat{V}_\alpha(\mathbf{x}') + \hat{P}(\mathbf{x}') \hat{\zeta}^{-1} \partial_\alpha \hat{G}^q(\mathbf{x} \mid \mathbf{x}') \right) n_\alpha dS' . \qquad (1.4\text{-}3)$$

In equation (1.4-3) the minus sign is changed, compared with equation (1.3-22), on account of the different direction of the unit vector along the normal of the scattering boundary.

The boundary of the scatterer is divided into the four surfaces which were introduced in Figure 1.5 Introducing the particle velocity field in the n_α^- direction, and the pressure field at this surface as $\hat{V}_\alpha^-$, $\hat{P}^-$ and in the n_α^+ direction as $\hat{V}_\alpha^+$, $\hat{P}^+$. Equation (1.4-3) can be rewritten as

$$\begin{aligned}\hat{P}^{sc}(\mathbf{x}) = &\int_{x\in D^{-,sc}} \left(\hat{G}^q(\mathbf{x}\mid\mathbf{x}')\hat{V}_\alpha^-(\mathbf{x}') + \hat{P}^-(\mathbf{x}')\hat{\zeta}^{-1}\partial_\alpha\hat{G}^q(\mathbf{x}\mid\mathbf{x}')\right) n_\alpha^- dS' + \\ &\int_{x\in D^{+,sc}} \left(\hat{G}^q(\mathbf{x}\mid\mathbf{x}')\hat{V}_\alpha^+(\mathbf{x}') + \hat{P}^+(\mathbf{x}')\hat{\zeta}^{-1}\partial_\alpha\hat{G}^q(\mathbf{x}\mid\mathbf{x}')\right) n_\alpha^+ dS' + \\ &\int_{x\in C_1+C_2} \left(\hat{G}^q(\mathbf{x}\mid\mathbf{x}')\hat{V}_\alpha(\mathbf{x}') + \hat{P}(\mathbf{x}')\hat{\zeta}^{-1}\partial_\alpha\hat{G}^q(\mathbf{x}\mid\mathbf{x}')\right) n_\alpha dS' \quad .\end{aligned} \tag{1.4-4}$$

By virtue of the "edge condition" the boundary integrals over C_1 and C_2 vanishes in the limit when $\varepsilon \to 0$, so the last integral in equation (1.4-4) vanishes in the limit.

Using the boundary condition in equation (1.4-4), and taking the two boundaries along the length of the strip, $D^{sc,-}$ and $D^{sc,+}$, together, the result is:

$$\hat{P}^{sc}(\mathbf{x}) = \int_{x\in\left\{D^{-,sc}+D^{+,sc}\right\}} \hat{G}^q(\mathbf{x}\mid\mathbf{x}')\left(V_\alpha^-(\mathbf{x}')n_\alpha^- + V_\alpha^+(\mathbf{x}')n_\alpha^+\right) dS' \quad . \tag{1.4-5}$$

The equivalent injection surface source is defined as (after de Hoop, 1988)

$$\partial q(\mathbf{x}) = n_\alpha^-\hat{V}_\alpha^-(\mathbf{x}) + n_\alpha^+\hat{V}_\alpha^+(\mathbf{x}) \qquad \text{when} \qquad \mathbf{x}\in\Delta^{sc} . \tag{1.4-6}$$

The incident field is continuous across the strip so,

$$n_\alpha^-\hat{V}_\alpha^{-,in}(\mathbf{x}) + n_\alpha^+\hat{V}_\alpha^{+,in}(\mathbf{x}) = 0 \qquad \text{when} \qquad \mathbf{x}\in\Delta^{sc} . \tag{1.4-7}$$

Equation (1.4-6) can, on account of equation (1.4-7), be rewritten as

$$\partial q(\mathbf{x}) = n_\alpha^- \hat{V}_\alpha^{-,sc}(\mathbf{x}) + n_\alpha^+ \hat{V}_\alpha^{+,sc}(\mathbf{x}) \qquad \text{when} \qquad \mathbf{x} \in \Delta^{sc} . \tag{1.4-8}$$

∂q is the unknown quantity in this scattering problem.

Squeezing the boundary integral over the strip into a lamina of vanishingly small thickness by letting $D^{sc,-}$ and $D^{sc,+}$ approach the strip, where **x** is a point *outside* the strip, the result is

$$\hat{P}^{sc}(\mathbf{x}) = \int_{x_1' = -a}^{x_1' = +a} \hat{G}^q(\mathbf{x} \mid \mathbf{x}') \partial q(\mathbf{x}') \, dx_1' . \tag{1.4-9}$$

The integration variable is now running over the strip area.

Letting the point of observation approach the strip and making use of equation (1.4-2), where **x** is now a position *on* the boundary

$$\hat{P}^{in}(\mathbf{x}) = -\int_{x_1' = -a}^{x_1' = +a} \hat{G}^q(\mathbf{x} \mid \mathbf{x}') \partial q(\mathbf{x}') \, dx_1' . \tag{1.4-10}$$

Equation (1.4-10) is an integral equation which must be solved for the field on the strip.

The two-dimensional injection source Green's function (1.2-14), which is the known function under the integral, is repeated in equation (1.4-11) for a position on the strip

$$\hat{G}^q(x_1, 0) = \hat{\zeta} \frac{j}{4} H_0^{(1)}\left(k \left| x_1 - x_1' \right|\right) = \hat{\zeta} \frac{j}{4\pi} \int_{-\infty}^{+\infty} \frac{\exp\left[jk_1 \left(x_1 - x_1'\right)\right]}{\sqrt{\left(k^2 - k_1^2\right)}} dk_1 . \tag{1.4-11}$$

In equation (1.4-11) the zero in the argument of the Green's function represents the x_2 position of the strip. Equation (1.4-11) is substituted in equation (1.4-10)

$$\hat{p}^{in}(x_1, 0) = -\hat{\zeta} \frac{j}{4} \int_{x_1' = -a}^{x_1' = +a} H_0^{(1)}\left(k \left| x_1 - x_1' \right|\right) \partial q(x_1') \, dx_1' . \tag{1.4-12}$$

Equation (1.4-12) can be recognized as a convolution; in a short-hand notation it can be written as

$$\hat{p}^{in}(x_1,0) = -\hat{\zeta}\frac{j}{4}\mathrm{H}_0^{(1)}(k|x_1|) * \partial q(x_1)\chi_a(x_1) \quad . \tag{1.4-13}$$

With the characteristic function of the strip region $A\ (-a<x<a)$ defined as

$$\begin{aligned} \chi_a(x_1) &= 1 \qquad |x_1| < a \\ &= 0 \qquad |x_1| > a \quad . \end{aligned} \tag{1.4-14}$$

The asterisk $*$ denotes convolution with respect to the x_1 coordinate.

Equation (1.4-12) is a linear integral equation of the first kind from which ∂q is to be solved. This equation can be solved only with the aid of numerical methods. The fact that the integral equation is a convolution makes the use of a spatial Fourier transform in the numerical calculation of the problem possible. The structure of the Green's function in equation (1.4-11) can be recognized as a spatial Fourier backtransform which makes the use of a Fourier transform even more useful. The advantage of the convolution structure can efficiently computed using FFT routines (for more details about the calculation in the wavenumber domain see Chapter 5).

1.5 SCATTERING BY A PERFECTLY RIGID STRIP

The same scattering configuration as in section 1.4 is used again in this section. If the scattering object of vanishing thickness is an immovable perfectly rigid strip, the normal component of the particle velocity field vanishes on either side of the strip.

So the boundary conditions for a perfectly rigid strip are:

$$\lim_{x_2\uparrow 0}\hat{V}_2(\mathbf{x}) = 0 \quad \text{and} \quad \lim_{x_2\downarrow 0}\hat{V}_2(\mathbf{x}) = 0 \quad . \tag{1.5-1}$$

Using equation (1.3-1b), the definition of the total field, this implies

$$\lim_{x_2\uparrow 0}\hat{V}_2^{sc}(\mathbf{x}) = -\lim_{x_2\uparrow 0}\hat{V}_2^{in}(\mathbf{x}) \quad \text{and} \quad \lim_{x_2\downarrow 0}\hat{V}_2^{sc}(\mathbf{x}) = -\lim_{x_2\downarrow 0}\hat{V}_2^{in}(\mathbf{x}) \quad . \tag{1.5-2}$$

The integral representation for the particle velocity field of the scattered wave is derived by surrounding the strip by the same closed curve as in section 1.4 , consisting of the four surfaces at a small distance from the strip shown in Figure 1.5 .

Application of the reciprocity theorem to the bounded domain *external* to the scattering domain, making use of equation (1.3-28), the representation of the particle velocity field outside the scattering domain, is given by

$$\widehat{V}_\alpha^{sc}(\mathbf{x}) = \int_{x \in \partial \mathrm{D}^{sc}} \left(\widehat{\mathrm{G}}_\alpha^{\mathrm{f}}(\mathbf{x} \mid \mathbf{x}') \widehat{V}_\beta(\mathbf{x}') - \widehat{P}(\mathbf{x}') \widehat{\Gamma}_{\alpha,\beta}^{\mathrm{f}}(\mathbf{x} \mid \mathbf{x}') \right) n_\beta \, dS' \,. \tag{1.5-3}$$

In equation (1.5-3) the minus sign is changed, compared with equation (1.3-28), on account of the different direction of the unit vector along the normal of the scattering boundary (see Figure 1.5). Using the boundary condition and letting $\varepsilon \to 0$, and again applying the "edge condition", equation (1.5-3) reduces to (using the same arguments as in section 1.4):

$$\widehat{V}_2^{sc}(\mathbf{x}) = \int_{x \in \left\{ \mathrm{D}^{-,sc} + \mathrm{D}^{+,sc} \right\}} \left(\widehat{P}^{-}(\mathbf{x}') n_2^{-} + \widehat{P}^{+}(\mathbf{x}') n_2^{+} \right) \widehat{\Gamma}_{2,2}^{\mathrm{f}}(\mathbf{x} \mid \mathbf{x}') \, dS' \,. \tag{1.5-4}$$

In equation (1.5-4) only the components in the x_2 direction, along the normal of the strip, of the particle velocity field have been taken into account. The reason for this is that the problem can only be solved in the x_2 direction, because the boundary condition is only prescribed in the x_2 direction.

The equivalent surface force source is defined as

$$\partial f_2(\mathbf{x}) = n_2^{-} \widehat{P}^{-}(\mathbf{x}) + n_2^{+} \widehat{P}^{+}(\mathbf{x}) \qquad \text{when} \qquad \mathbf{x} \in \Delta^{sc} \,. \tag{1.5-5}$$

The incident field is continuous across the strip

$$\widehat{P}^{-,in}(\mathbf{x}) = \widehat{P}^{+,in}(\mathbf{x}) \qquad \text{when} \qquad \mathbf{x} \in \Delta^{sc} \,. \tag{1.5-6}$$

Equation (1.5-6) used in equation (1.5-5) results in

$$\partial f_2(\mathbf{x}) = n_2^{-} \widehat{P}^{-,sc}(\mathbf{x}) + n_2^{+} \widehat{P}^{+,sc}(\mathbf{x}) \qquad \text{when} \qquad \mathbf{x} \in \Delta^{sc} \,, \tag{1.5-7}$$

where ∂f_2 is the unknown quantity in this scattering problem.

Squeezing the boundary integral over the strip into a lamina of vanishingly small thickness by letting $D^{sc,-}$ and $D^{sc,+}$ approach the strip, where **x** is a point *outside* the strip,

$$\hat{V}_2^{sc}(\mathbf{x}) = \int_{x_1' = -a}^{x_1' = +a} \partial f_2(\mathbf{x}') \hat{\Gamma}_{2,2}^{f}(\mathbf{x} \mid \mathbf{x}')\, dx_1' \quad . \tag{1.5-8}$$

The integration variable is now running over the strip area.

Letting the point of observation approach the strip and making use of equation (1.5-2), where **x** is now a position *on* the boundary,

$$\hat{V}_2^{in}(\mathbf{x}) = -\int_{x_1' = -a}^{x_1' = +a} \partial f_2(\mathbf{x}') \hat{\Gamma}_{2,2}^{f}(\mathbf{x} \mid \mathbf{x}')\, dx_1' \quad . \tag{1.5-9}$$

In equation (1.5-9) the Green's tensor for the particle velocity field is given by equation (1.2-22). The Dirac function in equation (1.2-22) has no contribution in the domain of consideration. So the Green's tensor, for the domain of observation, is given by:

$$\hat{\Gamma}_{2,2}^{f}(\mathbf{x} \mid \mathbf{x}') = -\hat{\zeta}^{-1} \frac{j}{4} \partial_2^2 H_0^{(1)}(\mathbf{x} \mid \mathbf{x}') \quad . \tag{1.5-10}$$

The functional dependence of the Hankel function of the x_2 coordinate occurs in an absolute value. Therefore the sign of the differentiated result depends on the value of the difference $(x_2 - x_2')$ and represents a singularity (branch point) in the integral. In order to avoid singularity problems with the differential operator acting on the Hankel function the differential operator is taken outside the integral, which is possible because the differential operator does not affect the integral.

Substituting equation (1.5-10) the expression for the Green's function into equation (1.5-9) gives:

$$\hat{V}_2^{in}(\mathbf{x}) = \hat{\zeta}^{-1} \frac{j}{4} \partial_2^2 \int_{x_1' = -a}^{x_1' = +a} \partial f_2(\mathbf{x}') H_0^{(1)}(\mathbf{x} \mid \mathbf{x}')\, dx_1' \quad . \tag{1.5-11}$$

The zero order Hankel function of the first kind differentiated twice with respect to x_2 is given by

$$\partial_2^2 \hat{H}_0^{(1)}(\mathbf{x}\,|\mathbf{x}') = \frac{1}{\pi}\int_{-\infty}^{+\infty} \frac{\partial_2^2 \exp\left[jk_1\left(x_1 - x_1'\right) + j\gamma\left|x_2 - x_2'\right|\right]}{\gamma}\, dk_1 , \tag{1.5-12}$$

$$\partial_2^2 \hat{H}_0^{(1)}(\mathbf{x}\,|\mathbf{x}') = \frac{-1}{\pi}\int_{-\infty}^{+\infty} \gamma \exp\left[jk_1\left(x_1 - x_1'\right) + j\gamma\left|x_2 - x_2'\right|\right] dk_1 . \tag{1.5-13}$$

Applying twice the differential operator with respect to the x_2 coordinate does not affect the sign of the differentiated result and can therefore be calculated without loss of generality. Substituting equation (1.5-13) in equation (1.5-11) gives equation (1.5-14).

$$\hat{V}_2^{in}(x_1, 0) = -\hat{\zeta}^{-1}\frac{j}{4\pi}\int_{x_1' = -a}^{x_1' = +a} \left\{\int_{-\infty}^{+\infty} \gamma \exp\left[jk_1\left(x_1 - x_1'\right)\right] dk_1\right\} \partial f_2\left(x_1'\right) dx_1' , \tag{1.5-14}$$

where the zero, in the argument of the particle velocity field, stands for the x_2 position on the strip. Equation (1.5-14) is a linear integral equation of the first kind from which ∂f_2 is to be solved. This equation can be solved only with the aid of numerical methods.

Equation (1.5-14) can also be rewritten in a convolutional form

$$\hat{V}_2^{in}(x_1, 0) = -\frac{j}{4\pi}\hat{\zeta}^{-1}\left\{\int_{-\infty}^{+\infty} \gamma \exp\left[jk_1(x_1)\right] dk_1\right\} * \partial f_2(x_1)\,\chi_a(x_1) . \tag{1.5-15}$$

The integral in the integral equation can be recognized as a spatial Fourier back-transform with respect to the k_1 coordinate. It will therefore be useful to calculate integral equation (1.5-14) in the wavenumber domain. In doing so the convolutional form of equation (1.5-14) is changed to a simple product in the wave number domain. Using in the numerical calculation FFT routines will efficiently use this property, in Chapter 5 these ideas are worked out in detail.

After solving equation (1.5-15) numerically the unknown function in the integral equation is known. From this known field an expression for the pressure field outside the scattering domain can be derived using equation (1.3-10)

$$\widehat{P}(\mathbf{x}) = \widehat{P}^{in}(\mathbf{x}) + \int_{x \in \partial D^{sc}} \partial f_2^{sc}(\mathbf{x}') \widehat{\Gamma}_{\alpha}^{q}(\mathbf{x} \mid \mathbf{x}') \, d\mathbf{x}' \,. \tag{1.5-16}$$

Where the Green's function for the particle velocity field is given by equation (1.2-15).

Chapter 2

SCATTERING BY A STRIP IN A TWO-DIMENSIONAL HALFSPACE

2.0 INTRODUCTION

In Chapter 1 the fact was used that in an unbounded medium the boundary integral at infinity vanishes if all waves are outgoing. In a half space this is not the case and boundary conditions on the half-space must be prescribed to solve the scattering problem. The boundary condition that the pressure is zero at the boundary surface is treated in this chapter.

In section 2.1 Rayleigh's reciprocity theorem is adapted to this situation and an extra surface integral appears in it. In section 2.2 the Green's function is calculated in such a way that the extra boundary integral in the reciprocity theorem vanishes. Physically this means that boundary conditions on a surface can be thought of as being equivalent to source distributions on this surface. This method is known as the method of images. With this Green's function the same equations which were derived in section 1.4 and 1.5 are used again in section 2.3 for the prescribed boundary conditions on the disk. The surface of the halfspace is chosen as the x_1 axis. The strip is symmetric with respect to the x_2. axis.

2.1 RAYLEIGH'S RECIPROCITY THEOREM

2.1.1 Representation for the pressure field

Starting with equation (1.3-9): Rayleigh's reciprocity theorem for the pressure field

$$\chi_D(\mathbf{x})\,\widehat{P}(\mathbf{x}) = \widehat{P}^{in} - \int_{\mathbf{x}\in\partial D} \left(\widehat{G}^{q}(\mathbf{x} \mid \mathbf{x}')\widehat{V}_{\alpha}(\mathbf{x}') - \widehat{P}(\mathbf{x}')\,\widehat{\Gamma}^{q}_{\alpha}(\mathbf{x} \mid \mathbf{x}') \right) \mathbf{n}_{\alpha}\, dS' \,. \qquad (2.1\text{-}1)$$

As seen in Figure 2.1 the boundary integral consists now of three parts. The boundary integral of the semicircle at infinity vanishes on account of Jordan's lemma leaving the two boundary integrals which are shown in equation (2.1-2).

$$\int_{x\in\partial D}\left(\hat{G}^{q}(\mathbf{x}\mid\mathbf{x}')\hat{V}_{\alpha}(\mathbf{x}')-\hat{P}(\mathbf{x}')\hat{\Gamma}^{q}_{\alpha}(\mathbf{x}\mid\mathbf{x}')\right)\mathbf{n}_{\alpha}dS' = \int_{x\in\partial D^{sc}}\left(\hat{G}^{q}(\mathbf{x}\mid\mathbf{x}')\hat{V}_{\alpha}(\mathbf{x}')-\hat{P}(\mathbf{x}')\hat{\Gamma}^{q}_{\alpha}(\mathbf{x}\mid\mathbf{x}')\right)\mathbf{n}_{\alpha}dS' +$$

$$\int_{x\in\partial D|_{x_2=0}}\left(\hat{G}^{q}(\mathbf{x}\mid\mathbf{x}')\hat{V}_{\alpha}(\mathbf{x}')-\hat{P}(\mathbf{x}')\hat{\Gamma}^{q}_{\alpha}(\mathbf{x}\mid\mathbf{x}')\right)\mathbf{n}_{\alpha}dS' \qquad (2.1\text{-}2)$$

In Figure 2.1 the halfspace configuration with the different boundaries is shown. The boundary integral around the scattering object is treated in the same manner as in section 1.4 and 1.5. In this chapter only the boundary integral over the x_1 axis is treated.

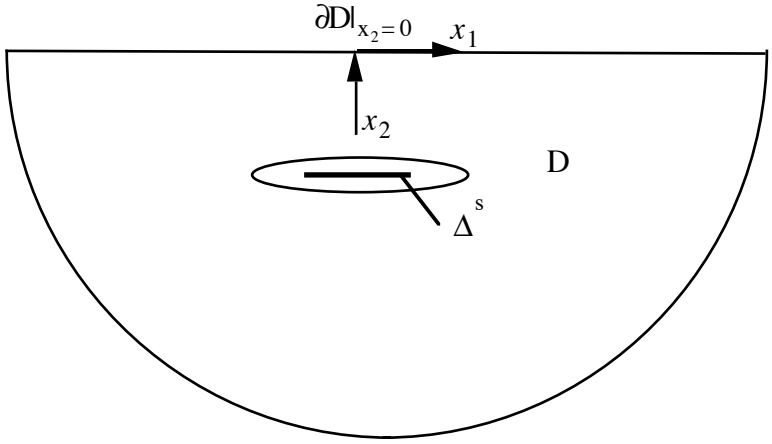

Figure 2.1 : Rayleigh's reciprocity theorem in a half space $\partial D = \partial D^{s} + \partial D^{\infty} + \partial D|_{x_2=0}$

The boundary condition on the surface is that the pressure at the surface x_2=0 is zero so the last boundary integral at the right handside of equation (2.1-2) reduces to :

$$\int_{x\in\partial D|_{x_2=0}}\hat{G}^{q}(\mathbf{x}\mid\mathbf{x}')\hat{V}_{\alpha}(\mathbf{x}')\,\mathbf{n}_{\alpha}dS' , \qquad (2.1\text{-}3)$$

If we choose the Green's function zero if $x_2 = 0$, then the whole surface integral over the x_1 axis vanishes. The same equations for the scattering problem which where derived in Chapter 1 can then be used again only now with a different Green's function.

2.1.2 Representation for the particle velocity field

Starting with equation (1.3-27) ; Rayleigh's reciprocity theorem for the particle velocity field

$$\chi_D(\mathbf{x})\hat{V}_\alpha(\mathbf{x}) = -\hat{V}^{in}_\alpha(\mathbf{x}) + \int_{x\in\partial D} \left(\hat{G}^f_\alpha(\mathbf{x} \mid \mathbf{x}')\hat{V}_\beta(\mathbf{x}') - \hat{P}(\mathbf{x}')\hat{\Gamma}^f_{\alpha,\beta}(\mathbf{x} \mid \mathbf{x}') \right) \mathbf{n}_\beta dS' \,. \qquad (2.1\text{-}4)$$

As mentioned above the boundary integral consists of three parts. The boundary integral of the semicircle vanishes leaving two boundary integrals. The pressure at the surface $x_2 = 0$ is zero so the boundary integral over the x_1 axis reduces to:

$$\int_{x\in\partial D|_{x_2=0}} \hat{G}^f_\alpha(\mathbf{x} \mid \mathbf{x}')\hat{V}_\beta(\mathbf{x}')\ \mathbf{n}_\beta dS' \,. \qquad (2.1\text{-}5)$$

The force source Green's function is again chosen zero at the surface of the halfspace to let the boundary integral over the surface vanish.

2.2 CALCULATING THE GREEN'S FUNCTION

Choosing the Green's function with the same boundary conditions as the wave field, the extra boundary integral of equation (2.1-2) vanishes. The calculated Green's function then contains a term representing the waves reflected by the boundary plane. In this section the Green's function for the inhomogeneous Helmholtz equation is derived. From this Green's function the injection source and force source Green's functions can be calculated using former results derived in Chapter 1.

In order to let the surface integral vanish the Green's function of the inhomogeneous Helmholtz equation, (1.2-1), for a halfspace must satisfy:

$$\hat{G}(x_1, x_2) = 0 \qquad \text{when } x_2 = 0. \qquad (2.2\text{-}1)$$

To solve this problem a quest is made. The guest must contain the Green's function in the unbounded medium and a term which represents the effects of the halfspace. The following quest for the Green`s function is made:

$$\hat{G}(x_1, x_2) = \frac{j}{4\pi} \int_{-\infty}^{+\infty} \frac{\exp\left[jk_1(x_1 - x_1') + j\gamma \left| x_2 - x_2' \right| \right]}{\gamma} dk_1 + \frac{j}{4\pi} \int_{-\infty}^{+\infty} A(\gamma) \exp\left[jk_1(x_1 - x_1') + j\gamma\ |x_2| \right] dk_1 \,, \qquad (2.2\text{-}2)$$

in which $\gamma = \left(k^2 - k_1^2\right)^{\frac{1}{2}}$.

A(γ) is the unknown function which has to be determined. The last integral in the right-hand side, which is added to the original Green's function in the unbounded domain, represents the boundary effects of the half-space. This integral cannot have any singularities inside the half-space, because it has no sources inside the halfspace.

The boundary condition on the surface of the halfspace is:

$$\hat{G}(x_1,0) = \frac{j}{4\pi}\int_{-\infty}^{+\infty} \frac{\exp\left[jk_1\left(x_1 - x_1'\right) + j\gamma\left|x_2'\right|\right]}{\gamma} dk_1 + \frac{j}{4\pi}\int_{-\infty}^{+\infty} A(\gamma)\exp\left[jk_1\left(x_1 - x_1'\right)\right] dk_1 = 0 \ . \qquad (2.2\text{-}3)$$

Solving *A(γ)* from (2.2-3) gives

$$A(\gamma) = \frac{-\exp\left[j\gamma\left|x_2'\right|\right]}{\gamma} \ . \qquad (2.2\text{-}4)$$

So the Green's function is given by:

$$\hat{G}(x_1,x_2) = \frac{j}{4\pi}\int_{-\infty}^{+\infty} \left(\frac{\exp\left[jk_1\left(x_1 - x_1'\right) + j\gamma\left|x_2 - x_2'\right|\right]}{\gamma} - \frac{\exp\left[jk_1\left(x_1 - x_1'\right) + j\gamma\left|x_2 + x_2'\right|\right]}{\gamma} \right) dk_1 \qquad .(2.2\text{-}5)$$

The expression of this Green's function can again be recognized as a Fourier backtransform. For further details about the backtransform see Chapter 5. Using a notation with Hankel functions equation (2.2-5) can be rewritten as

$$\hat{G}\left(\mathbf{x} \mid \mathbf{x}'\right) = \frac{j}{4}H_0^{(1)}\left(k\left[\left(x_1 - x_1'\right)^2 + \left(x_2 - x_2'\right)^2\right]^{\frac{1}{2}}\right) - \frac{j}{4}H_0^{(1)}\left(k\left[\left(x_1 - x_1'\right)^2 + \left(x_2 + x_2'\right)^2\right]^{\frac{1}{2}}\right) \qquad (2.2\text{-}6)$$

or

$$\hat{G}\left(\mathbf{x} \mid \mathbf{x}'\right) = \frac{j}{4}H_0^{(1)}(kr) - \frac{j}{4}H_0^{(1)}\left(kr^+\right) , \qquad (2.2\text{-}7)$$

with the distances

$$r = \left[\left(x_1 - x_1' \right)^2 + \left(x_2 - x_2' \right)^2 \right]^{\frac{1}{2}}, \tag{2.2-8}$$

and

$$r^+ = \left[\left(x_1 - x_1' \right)^2 + \left(x_2 + x_2' \right)^2 \right]^{\frac{1}{2}}, \tag{2.2-9}$$

The effect of the boundary plane can be intepretated as a set of image sources, symmetrically placed with respect to the boundary plane which is clearly shown by equation (2.2-7). Both the source and it's 'image' radiating into the unbounded space. The portion of the wavefield from the image source constitutes the reflected waves and carries the energy reflected from the boundary surface. The method by which the Green's function is calculated is known in the literature as the method of images (Morse and Ingard, 1968).

The Green's function for the injection source and the force source can be calculated using relations (1.2-14) and (1.2-15) for the injection source and equations (1.2-19) and (1.2-21) for the force source.

2.3 SCATTERING IN A HALFSPACE

In this section the scattering of a perfectly compliant strip and a perfectly rigid strip in a halfspace is discussed. Equation (1.4-10) and equation (1.5-9) are used as a starting point.

2.3.1 Scattering by a perfectly compliant strip

Equation (1.4-10), the integral equation for the compliant strip, is repeated in equation (2.3-1)

$$\hat{P}^{in}(\mathbf{x}) = -\int_{x_1' = -a}^{x_1' = +a} \hat{G}^q(\mathbf{x} \mid \mathbf{x}') \partial q(\mathbf{x}') \, dx_1' . \tag{2.3-1}$$

Using the results from the injection source Green's function in paragraph 1.2.2 and equation (2.2-7) the injection source Green's function for the halfspace can be written as.

$$\hat{G}^{q}(\mathbf{x} \mid \mathbf{x}') = \hat{\zeta}\frac{j}{4\pi}\int_{-\infty}^{+\infty}\left\{\frac{\exp\left[jk_1\left(x_1 - x_1'\right) + j\gamma\left|x_2 - x_2'\right|\right]}{\gamma} - \frac{\exp\left[jk_1\left(x_1 - x_1'\right) + j\gamma\left|x_2 + x_2'\right|\right]}{\gamma}\right\}dk_1 \tag{2.3-2}$$

For a position on the strip $x_2 = x_2'$ holds. Substituting this position in equation(2.3-2) and using this result in equation (2.3-1) gives

$$\hat{P}^{in}(\mathbf{x}) = -\hat{\zeta}\frac{j}{4\pi}\int_{x_1' = -a}^{x_1' = +a}\int_{-\infty}^{+\infty}\left\{\frac{\exp\left[jk_1\left(x_1 - x_1'\right)\right]}{\gamma}\left(1 - \exp\left[-2j\gamma\left|x_2\right|\right]\right)\right\}dk_1\,\partial q(x_1)\,dx_1' \,. \tag{2.3-3}$$

Since x_2 in equation (2.3-3) is a constant, equation (2.3-3) represents a convolution with respect to x_1. This fact can be used in the numerical calculation of the integral equation. In a short hand notation, using an asterisk ($*$) as convolution operator, equation (2.3-3) can be written as

$$\hat{P}^{in}(\mathbf{x}) = -\hat{\zeta}\frac{j}{4\pi}\int_{-\infty}^{+\infty}\left\{\frac{\exp\left[jk_1(x_1)\right]}{\gamma}\left(1 - \exp\left[-2j\gamma\left|x_2\right|\right]\right)\right\}dk_1 * \partial q(x_1)\,\chi_a(x_1) \,. \tag{2.3-4}$$

With the characteristic function of the strip region defined as in equation (1.4-13). In Chapter 5 the spatial Fourier transform is used to calculate the convolution in the wavenumber domain (a simple product).

2.3.2 Scattering by a perfectly rigid strip

Equation (1.5-9), the integral equation for a rigid strip, is repeated in equation (2.3-5)

$$\hat{V}_2^{in}(\mathbf{x}) = -\int_{x_1' = -a}^{x_1' = +a}\partial f_2(\mathbf{x}')\,\hat{\Gamma}_{2,2}^{f}(\mathbf{x} \mid \mathbf{x}')\,dx_1' \,. \tag{2.3-5}$$

The expression of the Green's tensor in equation (2.3-5) is given by equation (1.2-22). The Dirac function in the expression of the Green's function (equation (1.2-2)) can be omitted because the position of the Dirac function is not included in the domain of observation. Using equation (2.2-5), the resulting expression for the Green's function is then given by:

$$\hat{\Gamma}^{f}_{2,2}(\mathbf{x}\mid\mathbf{x}') = -\hat{\zeta}^{-1}\frac{j}{4\pi}\partial_2^2\int_{-\infty}^{+\infty}\left\{\frac{\exp\left[jk_1(x_1-x_1')+j\gamma(x_2'-x_2)\right]}{\gamma}\left(1-\exp\left[2j\gamma(x_2)\right]\right)\right\}dk_1, \qquad (2.3\text{-}6a)$$

when $x_2 < x_2'$. If $x_2 > x_2'$ the Green's function is given by

$$\hat{\Gamma}^{f}_{2,2}(\mathbf{x}\mid\mathbf{x}') = -\hat{\zeta}^{-1}\frac{j}{4\pi}\partial_2^2\int_{-\infty}^{+\infty}\left\{\frac{\exp\left[jk_1(x_1-x_1')+j\gamma(x_2-x_2')\right]}{\gamma}\left(1-\exp\left[2j\gamma(x_2')\right]\right)\right\}dk_1. \qquad (2.3\text{-}6b)$$

The result of equation (1.5-13), the Hankel function differentiated two times with respect to the x_2 direction, is used in equation (2.3-6), where **x** is now a position on the strip ($x_2 = x_2'$)

$$\hat{\Gamma}^{f}_{2,2}(\mathbf{x}\mid\mathbf{x}') = \hat{\zeta}^{-1}\frac{j}{4\pi}\int_{-\infty}^{+\infty}\gamma\exp\left[jk_1(x_1-x_1')\right]\left(1-\exp\left[2j\gamma(x_2')\right]\right)dk_1. \qquad (2.3\text{-}7)$$

The integral in equation (2.3-7) is recognized as a spatial Fourier back-transform with respect to the k_1 coordinate.

Equation (2.3-7) can be substituted in equation (2.3-5) which results in

$$\hat{V}_2^{in}(\mathbf{x}) = \hat{\zeta}^{-1}\frac{j}{4\pi}\int_{x_1'=-a}^{x_1'=+a}\left\{\int_{-\infty}^{+\infty}\gamma\exp\left[jk_1(x_1-x_1')\right]\left(1-\exp\left[2j\gamma(x_2)\right]\right)dk_1\right\}\partial f_2(x_1')\,dx_1'. \qquad (2.3\text{-}8)$$

In a short hand notation, using an asterisk ($*$) as convolution operator, equation (2.3-8) can be written as

$$\hat{V}_2^{in}(\mathbf{x}) = \hat{\zeta}^{-1}\frac{j}{4\pi}\left\{\int_{-\infty}^{+\infty}\gamma\exp\left[jk_1(x_1)\right]\left(1-\exp\left[2j\gamma(x_2)\right]\right)dk_1\right\} * \partial f_2(x_1)\,\chi_a(x_1) \quad . \tag{2.3-9}$$

In the numerical calculation of the problem the integral equations of (2.3-8) are calculated in the wavenumber domain in order to take advantage of the convolutional structure of the equation.

Chapter 3

SOURCE AND RECEIVER

3.0 INTRODUCTION

This chapter summarizes some earlier results and puts them in relation to the whole scattering configuration. The calculation of the source and receiver positions are easily derived from former results. In section 3.1 the total field at an observation point is calculated using Rayleigh's reciprocity theorem. The incident field, which stands in equation (1.4-10) for a compliant strip and in equation (1.5-9) for a rigid strip, is calculated in section 3.2 in the case where the incident field is a 2-dimensional point source (which in fact is the Green's function of Section 1.2). In section 3.3 a simple example is worked out which uses the results from earlier sections.

3.1 RECEIVER

The total pressure field at an arbitrary point in the embedding is calculated by using equation (1.3-9). Where **x** is the receiver position and the integral is running over the domain of the strip

$$\chi_{\mathrm{D}}(\mathbf{x})\hat{P}(\mathbf{x}) = \hat{P}^{in}(\mathbf{x}) - \int_{x\in\partial\mathrm{D}^{\mathrm{sc}}} \left(\hat{\mathrm{G}}^{\mathrm{q}}(\mathbf{x}\mid\mathbf{x}')\hat{V}_{\alpha}^{sc}(\mathbf{x}') - \hat{P}^{sc}(\mathbf{x}')\hat{\Gamma}_{\alpha}^{\mathrm{q}}(\mathbf{x}\mid\mathbf{x}') \right) n_{\alpha} dS' \,. \tag{3.1-1}$$

The total particle velocity field at an arbitrary point in the embedding is calculated by using equation (1.3-26). Where **x** is the receiver position and the integral is running over the domain of the strip

$$\chi_{\mathrm{D}}(\mathbf{x})\hat{V}(\mathbf{x}) = -\hat{V}^{in}(\mathbf{x}) + \int_{x\in\partial\mathrm{D}^{\mathrm{sc}}} \left(\hat{\mathrm{G}}^{\mathrm{f}}_{\alpha}(\mathbf{x}\mid\mathbf{x}')\hat{V}_{\beta}^{sc}(\mathbf{x}') - \hat{P}^{sc}(\mathbf{x}')\hat{\Gamma}^{\mathrm{f}}_{\alpha,\beta}(\mathbf{x}\mid\mathbf{x}') \right) n_{\beta} dS' \,. \tag{3.1-2}$$

$\partial q = \hat{V}_{\alpha}^{sc} n_{\alpha}$ and $\partial f_{\alpha} = \hat{P}^{sc} n_{\alpha}$ are calculated numerically from equations (1.4-12) and (1.5-14) for an unbounded medium and from equations (2.3-3) and (2.3-8) for a halfspace. In Chapter 1 and 2 the Green's functions for equations (3.1-1) and (3.1-2) were calculated. So both equations can be solved, with the knowledge of the incident field on the strip, and the scattered field can be calculated everywhere in space.

3.2 LINE SOURCE

In the integral equations of Chapter 1 and 2 the known function is given by the incident pressure or velocity field. It is therefore necessary to describe the incident field at the strip position in order to solve the integral equations numerically. In all calculations a line injection source is chosen as the incident field.

Each line element of the line injection source is considered to be an isotropic point source. The expression for an isotropic injection point source is given by:

$$\frac{\exp(jkR)}{4\pi R} \qquad \text{with} \qquad R = \left[\left(x_1 - x_1^{so}\right)^2 + \left(x_2 - x_2^{so}\right)^2 + \left(x_3 - x_3^{so}\right)^2 \right]^{\frac{1}{2}} . \tag{3.2-1}$$

Integrating the 3-dimensional point source over one direction (for example x_3) results in the 2-dimensional line source

$$\int_{-\infty}^{+\infty} \frac{\exp(jkR)}{4\pi R} dx_3 \equiv \frac{j}{4} H_0^{(1)}\left(k \left[\left(x_1 - x_1^{so}\right)^2 + \left(x_2 - x_2^{so}\right)^2 \right]^{\frac{1}{2}} \right) = \frac{j}{4} H_0^{(1)}(kr) \quad , \tag{3.2-2}$$

with the distance

$$r = \left[\left(x_1 - x_1^{so}\right)^2 + \left(x_2 - x_2^{so}\right)^2 \right]^{\frac{1}{2}} , \tag{3.2-3}$$

and $\left(x_1^{so}, x_2^{so}, x_3^{so}\right)$ is the position of the point source.

3.2.1 The incident pressure field

In equation (1.4-11) and equation (2.3-3), the integral equation for a compliant strip in an unbounded medium and for a halfspace, respectively, the known function is given by the incident pressure field. If the incident pressure field is the 2-dimensional line source, equation (3.2-2), the Hankel function can be used.

The Hankel function can be expressed as an inverse spatial Fourier transform, which will be shown in the next equations. Starting with equation (1.2-6) , the expression of the Hankel function

$$H_0^{(1)}\left(k\left[\left(x_1 - x_1^{so}\right)^2 + \left(x_2^{so}\right)^2 \right]^{\frac{1}{2}} \right) = \frac{1}{\pi} \int_{-\infty}^{\infty} \frac{\exp\left[jk_1\left(x_1 - x_1^{so}\right) \right] \exp j\left[\left(k^2 - k_1^2\right)^{\frac{1}{2}} \left| x_2^{so} \right| \right]}{\left(k^2 - k_1^2\right)^{\frac{1}{2}}} dk_1 \quad , \qquad (3.2\text{-}4)$$

where the fact is used that in the integral equation the position on the strip is for $x_2 = 0$ in the bouded medium. The incident pressure field is then given by the expression

$$\hat{P}^{in}(x_1,0) = \hat{S}(\omega) \frac{j}{4\pi} \int_{-\infty}^{\infty} \frac{\exp\left[jk_1\left(x_1 - x_1^{so}\right) \right] \exp j\left[\left(k^2 - k_1^2\right)^{\frac{1}{2}} \left| x_2^{so} \right| \right]}{\left(k^2 - k_1^2\right)^{\frac{1}{2}}} dk_1 \qquad (3.2\text{-}5)$$

In equation (3.2-5) $\hat{S}(\omega)$ represents the spectrum of the source signature.
As was pointed out in earlier chapters, the Hankel function can be recognized as a Fourier back-transform

$$H_0^{(1)}\left(k\left[\left(x_1 - x_1^{so}\right)^2 + \left(x_2^{so}\right)^2 \right]^{\frac{1}{2}} \right) = F^{-1}\left\{ \frac{2 \exp j\left[-k_1 x_1^{so} + \left(k^2 - k_1^2\right)^{\frac{1}{2}} \left| x_2^{so} \right| \right]}{\left(k^2 - k_1^2\right)^{\frac{1}{2}}} \right\} . \qquad (3.2\text{-}6)$$

So to compute the incident pressure field a Fourier backtransform can be used.

3.2.1 The incident particle velocity field

In equation (1.5-14) and equation (2.3-8), the integral equation for a rigid strip in an unbounded medium and a bounded medium, respectively, the known function is given by the second component of the incident particle velocity field. To calculate the incident particle velocity field the following relation is used, which is derived from equation (1.1-5) without a source.

$$\hat{V}_2^{in} = -\hat{\zeta}^{-1} \partial_2 \hat{P}^{in} \quad . \qquad (3.2\text{-}7)$$

The first order derivative of the Hankel function, which is an expression for the incident pressure field, is given by

$$\partial_2 \hat{H}_0^{(1)}(\mathbf{x}\,|\mathbf{x}') = \frac{-j}{\pi} \int_{-\infty}^{+\infty} \exp\left[jk_1 (x_1 - x_1^{so}) + j\left(k^2 - k_1^2\right)^{\frac{1}{2}} \left| x_2^{so} \right| \right] dk_1 \,, \qquad (3.2\text{-}8)$$

where it is assumed that the source lies above the strip. Substituting equation (3.2-8) into equation (3.2-7) gives the expression for the incident particle velocity field:

$$\hat{V}_2^{in}(x_1, 0) = \hat{S}(\omega)\, \hat{\zeta}^{-1} \frac{j}{4\pi} \int_{-\infty}^{+\infty} \exp\left[jk_1 (x_1 - x_1^{so}) + j\left(k^2 - k_1^2\right)^{\frac{1}{2}} \left| x_2^{so} \right| \right] dk_1 \quad . \qquad (3.2\text{-}9)$$

Equation (3.2-8) can also be intepreted as a Fourier back transform. So the expression of the first order derivative of the incident pressure field can again be calculated using an inverse Fourier transform.

3.3 AN EXAMPLE

The example is worked out for just one situation and most of the attention is paid to the use of the Fourier transform in the problem. The following example is worked out: the two dimensional strip problem as described in section 1.4 with the boundary condition of a perfectly compliant strip a line source as incident field, described in section 3.2, and a receiver with position $\mathbf{x}^{rc}$. The total configuration is shown in figure 3.1.

The scattered pressure field at the strip is calculated from equation (1.4-12)

$$\hat{p}^{in}(x_1, 0) = -\hat{\zeta} \frac{j}{4} \int_{x_1' = -a}^{x_1' = +a} H_0^{(1)}\left(k \left| x_1 - x_1' \right| \right) \partial q(x_1')\, dx_1' \quad . \qquad (3.3\text{-}1)$$

Substituting for the incident field at the strip the line source at position $\left(x_1^{so}, x_2^{so}\right)$, and substituting equation (3.2-8), into equation (3.3-1) yields

$$\hat{S}(\omega)\, \mathrm{F}^{-1}\left\{ \frac{2 \exp j\left[\left(k^2 - k_1^2\right)^{\frac{1}{2}} \left| x_2^{so} \right| - k_1 x_1^{so} \right]}{\left(k^2 - k_1^2\right)^{\frac{1}{2}}} \right\} = -\hat{\zeta} \frac{j}{4} \int_{x_1' = -a}^{x_1' = +a} H_0^{(1)}\left(k \left| x_1 - x_1' \right| \right) \partial q(x_1')\, dx_1' \qquad (3.3\text{-}2)$$

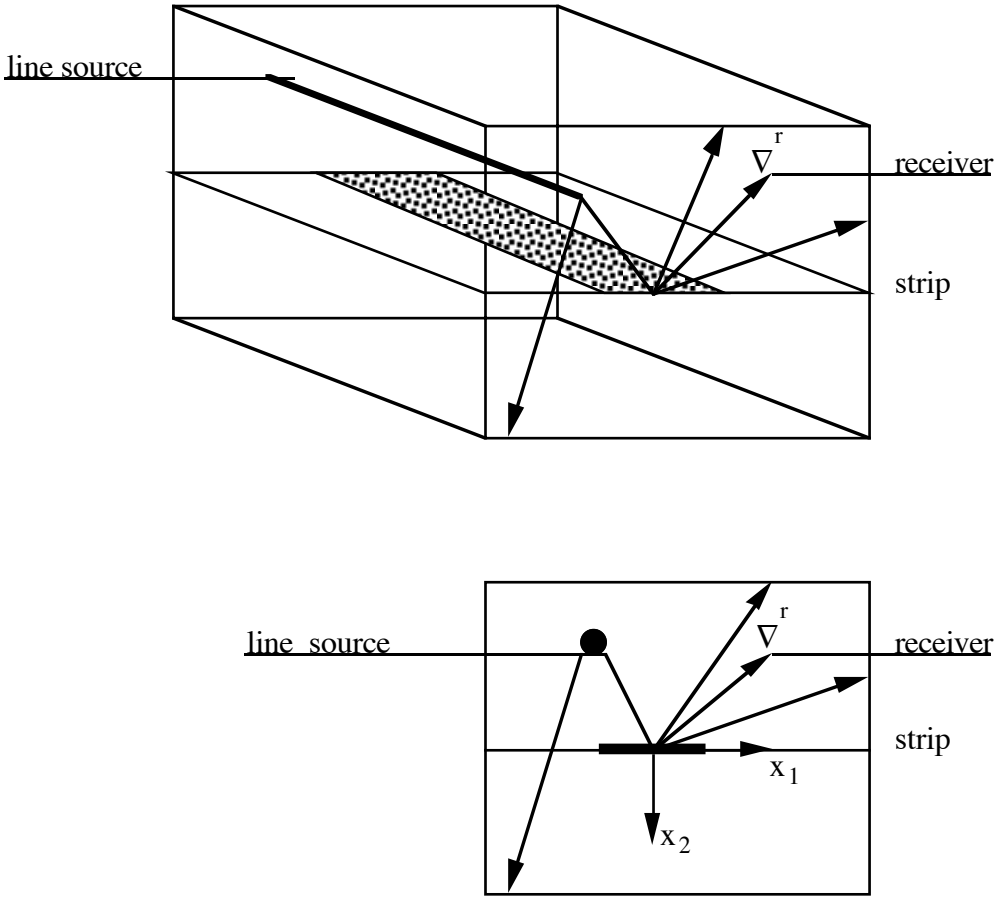

Figure 3.1 scattering by a strip with line source and receiver.

From equation (3.3-2) ∂q is calculated numerically. The Hankel function in the integral of equation (3.3-2) is also calculated in the wavenumber domain. The total numerical procedure is discussed in Chapters 4 and 5. The solution of equation (3.3-2) is substituted into equation (3.1-1) where **x** is a position at the receiver, and the direct incident field is given by equation (3.2-2)

$$\widehat{P}\left(\mathbf{x}^{rc}\right)=\widehat{S}\left(\omega\right)\frac{j}{4}\mathrm{H}_0^{(1)}\left(k\left[\left(x_1^{rc}-x_1^{so}\right)^2+\left(x_2^{rc}-x_2^{so}\right)^2\right]^{\frac{1}{2}}\right)-\frac{j}{4}\int_{x_1'=-a}^{x_1'=a}\mathrm{H}_0^{(1)}\left(k\left|x_1^{rc}-x_1'\right|\right)\partial q\left(x_1'\right)dx_1' \quad .(3.3\text{-}3)$$

Equation (3.3-3) is the result for the scattered field of the strip plus the total field at one receiver position. Where $\mathbf{x}^{rc}$ is the receiver position. It can be written in terms of inverse Fourier transforms using the special structure of the Hankel function.

$$\widehat{P}\left(x_1, x_2^{rc}\right) = \widehat{S}\left(\omega\right) \frac{j}{4} \mathrm{F}^{-1}\left\{ \frac{2 \exp j\left[\left(k^2 - k_1^2\right)^{\frac{1}{2}} \left| x_2^{so} - x_2^{rc} \right| - k_1 x_1^{so} \right]}{\left(k^2 - k_1^2\right)^{\frac{1}{2}}} \right\} -$$

$$\frac{j}{4} \mathrm{F}^{-1}\left\{ \frac{2 \exp j\left[\left(k^2 - k_1^2\right)^{\frac{1}{2}} \left| x_2^{rc} \right| \right]}{\left(k^2 - k_1^2\right)^{\frac{1}{2}}} \mathrm{F}\left\{ \partial q^{sc}\left(x_1\right) \chi_d\left(x_1\right) \right\} \right\} . \qquad (3.3\text{-}4)$$

For a perfectly compliant strip and for the halfspace configuration the equations have the same structure as in this example. In this example it can be seen how the spatial Fourier backtransforms have been used to express the Hankel function and to calculate the convolution in the wavenumber domain.

Chapter 4

ITERATIVE SCHEMES BASED ON MINIMIZATION OF A UNIFORM ERROR CRITERION

4.0 INTRODUCTION

In the present chapter the iterative solution of the integral equations of acoustic scattering problems, which were derived in Chapter 1, is discussed. To have a measure for the accuracy, the global root-mean-square error in the equality sign of the integral equation has to be satisfied for the exact solution. For a given sequence of expansion functions, which are used to represent the unknown field values in the domain of the scatterer, the minimization of the relevant error leads to a particular method of moments. In the iterative schemes the integrated-square error, with respect to the original operator equation, is taken as a measure of deviation of the approximate solution from the exact one. The iterative schemes in this chapter are all developed by van den Berg (1989).

The general form of the operator equation is introduced as

$$\int_{x' \in D} L(x,x')\, u(x')\, dx' = f(x) \quad \text{when } x \in D. \tag{4.0-1}$$

In this equation, u is the unknown field quantity in the contrasting space frequency domain, f is a known field related to the incident field and L is the kernel of the integral equation, which is related to the field at x radiated by a source at x'. In general u and f are vector valued, L yields the proper matrix relationship, and D is the domain for which (4.0-1) holds .To write equation (4.0-1) in an operator form, the linear operator L acting on a function $u \in D$ is introduced by

$$Lu = \int_{x' \in D} L(x,x')\, u(x')\, dx' . \tag{4.0-2}$$

Then equation (4.0-1) is equivalent to

$$Lu = f \quad \text{when } x \in D. \tag{4.0-3}$$

Further, the inner product of two integrable functions u and v defined on D is taken as the number

$$\langle u,v \rangle = \int_{x \in D} u(x)\bar{v}(x)\, dx , \tag{4.0-4}$$

where the overbar denotes complex conjugate. The norm of a function u is in accordance with equation (4.0-4), defined as

$$\|u\| = \langle u, u \rangle^{\frac{1}{2}} . \tag{4.0-5}$$

The Hilbert adjoint operator L^* of L is defined as that one for which

$$\langle Lu, v \rangle = \langle u, L^* v \rangle \tag{4.0-6}$$

for all functions u and v defined on D. If $L^* = L$, the operator is selfadjoint. However in most scattering problems the operator is not selfadjoint .

4.1 DIRECT MINIMIZATION OF THE ERROR

A direct (non-iterative) approximation of the solution of the operator equation (4.0-3) is discussed in this section. To construct an approximate solution, the unknown function u is expanded in terms of a given, approximately chosen, sequence of linearly independent expansion functions $\{ \phi_n ; n = 1,\ldots,N \}$ that are defined on D. Let, for some N ≥ 1

$$u_N = \sum_{n=1}^{N} \alpha_n^{(N)} \phi_n , \tag{4.1-1}$$

and define the residual as

$$r_N = f - Lu_N . \tag{4.1-2}$$

Then the problem is to determine, *for given N*, the sequence of expansion coefficients $\{ \alpha_n^{(N)} ; n = 1,\ldots,N \}$ such that $\langle r_N, r_N \rangle$ is minimized. The relevant values of $\{ \alpha_n^{(N)} \}$ are denoted as the optimum values $\{ \alpha_n^{(opt)} \}$. Assuming that the optimum exists, let

$$\alpha_n^{(N)} = \alpha_n^{opt} + \delta \alpha_n \quad \text{for } n = 1,\ldots,\text{N} \tag{4.1-3}$$

where $\delta \alpha_n$ is arbitrary. Further let

$$r_N^{opt} = f - \sum_{n=1}^{N} \alpha_n^{opt} L\phi_n \ , \tag{4.1-4}$$

then

$$\langle r_N, r_N \rangle = \langle r_N^{opt}, r_N^{opt} \rangle - 2\mathrm{Re}\left(\sum_{m=1}^{N} \overline{\delta\alpha_m} \langle r_N^{opt}, L\phi_m \rangle \right) + \langle \sum_{n=1}^{N} \delta\alpha_n L\phi_n , \sum_{m=1}^{N} \delta\alpha_m L\phi_m \rangle \ . \tag{4.1-5}$$

The last term on the right-hand side of equation (4.1-4) is always positive if $\{\delta\alpha_1, \ldots, \delta\alpha_N\} \neq \{0,\ldots,0\}$. Hence if

$$\langle r_N^{opt}, L\phi_m \rangle = 0 \qquad \text{for } m = 1,...,N \ . \tag{4.1-6}$$

Then for $\{\delta\alpha_1, \ldots, \delta\alpha_N\} = \{0,\ldots,0\}$ the quantity $\langle r_N^{opt}, r_N^{opt} \rangle$ is the absolute minimum of $\langle r_N, r_N \rangle$. From equation (4.1-5) and (4.1-1) it also follows that

$$\langle r_N^{opt}, Lu_N \rangle = 0 \ . \tag{4.1-7}$$

For the measure of the deviation the global root-mean-square error is defined as

$$\mathrm{ERR_N} = \langle r_N, r_N \rangle^{\frac{1}{2}} = \| r_N \| \ . \tag{4.1-8}$$

Note that $\mathrm{ERR_N} \geq 0$ and that $\mathrm{ERR_N} = 0$ if and only if $u^{app} = u$

The normalized root-mean-square error is defined as

$$\widehat{\mathrm{ERR}}_\mathrm{N} = \frac{\| r_N \|}{\| f \|} \ . \tag{4.1-9}$$

The error defined in equations (4.1-7) and (4.1-8) is used as a measure for the accuracy in the iterative schemes to be dealt with in later sections.

For problems of realistic size and complexity the value N soon becomes so large that the storage requirements exceed even the capacity of present-day large computer systems. The problem of excessive computation time and computer storage requirements for a direct numerical solution of the system of equations can be circumvented by using suitable iterative techniques. Another advantage of iterative techniques is that the system of equations is not solved to a higher degree of accuracy than is needed.

4.2 RECURSIVE MINIMIZATION OF THE ERROR

In an iterative procedure the elements of the sequence of expansion functions are recursively generated from the operator equation to be solved, one in each iteration step. At step N there are N presumably linearly independent expansion functions generated. The minimization of the error will be employed to generate the system of linear algebraic equations.

Take

$$u_0 = 0 \ ,$$
$$u_N = u_{N-1} + u_N^{cor} \quad \text{for } N = 1,\ldots \tag{4.2-1}$$

where u_N is the N'th approximation to the solution of the operator equation. And the correction to u_N is given by

$$u_N^{cor} = \sum_{n=1}^{N} \alpha_n^{(N)} \phi_n \quad \text{for } N = 1,\ldots \tag{4.2-2}$$

in which $\left\{ \phi_n \, ; n = 1,\ldots,N \right\}$ are the recursively generated sequence of expansion functions of u_N^{cor}. From equation (4.1-2) it follows that the residuals are found to be

$$r_0 = f \quad ,$$
$$r_N = r_{N-1} - L u_N^{cor} \ . \tag{4.2-3}$$

On account of equation (4.1-5), minimization of the norm of the residuals which is repeated here, and substitution of equations (4.2-2) and (4.2-3) into it leads to a system of linear equations in the N expansion coefficients.

$$\left\langle r_N^{opt}, L\phi_m \right\rangle = 0 \qquad \text{for } m = 1,...,N \ , \tag{4.2-4}$$

$$\sum_{n=1}^{N} \alpha_n^{(N)} \left\langle L\phi_n, L\phi_m \right\rangle = \left\langle r_{N-1}, L\phi_m \right\rangle \text{ for } m = 1,\ldots,N \ . \tag{4.2-5}$$

At the N-th step r_{N-1} is known.

On account of equation (4.2-4) only the right-hand side of equation (4.2-5) for $m = N$ may differ from zero if not all the expansion coefficients are zero, so

$$\left\langle r_{N-1}, L\phi_N \right\rangle \neq 0 \ . \tag{4.2-6}$$

If equation (4.2-6) is satisfied then the expansion coefficients $\left\{ \alpha_n^{(N)} ; n = 1,\ldots,N \right\}$ can be solved from equation (4.2-5). Equation (4.2-6) is denoted, after van den Berg, as the *improvement condition*.

From equation (4.2-5) it is observed that all $\alpha_n^{(N)}$ are proportional to $\alpha_N^{(N)}$ therefore the sequence of expansion functions $\left\{ \psi_N ; N = 1,\ldots \right\}$ is introduced as

$$\psi_N = \frac{u_N^{cor}}{\alpha_N^{(N)}} \quad \text{for } N = 1,\ldots \quad , \tag{4.2-7}$$

or according to equation (4.2-1),

$$\begin{aligned} &\psi_1 = \phi_1 \ , \\ &\psi_N = \phi_N + \sum_{n=1}^{N-1} \frac{\alpha_n^{(N)}}{\alpha_N^{(N)}} \phi_n \quad \text{for } N = 2,\ldots \end{aligned} \tag{4.2-8}$$

ψ_N is expressed as a linear combination of $\left\{ \phi_n ; n = 1,\ldots,N \right\}$. Since the reverse is also true, ϕ_n can be expressed as a linear combination of $\left\{ \psi_n ; n = 1,\ldots,N \right\}$. In view of this equation (4.2-8) can be rewritten as

$$\begin{aligned} &\psi_1 = \phi_1 \ , \\ &\psi_N = \phi_N + \sum_{n=1}^{N-1} \beta_n^{(N)} \phi_n \quad \text{for } N = 2,\ldots \end{aligned} \tag{4.2-9}$$

The coefficients $\left\{ \beta_n^{(N)} ; n = 1,\ldots,N-1 \right\}$ can be determined. Since any ψ_N is as a linear combination of the expansion functions $\left\{ \phi_n ; n = 1,\ldots,N \right\}$ equation (4.2-4) leads to

$$\left\langle r_N, L\psi_m \right\rangle = 0 \qquad \text{for } m = 1,...,N \ . \tag{4.2-10}$$

Combining equation (4.2-3) and equation (4.2-7) with (4.2-10) gives the orthogonality equation

$$\left\langle L\psi_n, L\psi_m \right\rangle = 0 \qquad \text{for } m \neq n \ . \tag{4.2-11}$$

Applying the operator L on equation (4.2-9) and substituting this in equation (4.2-11) gives the solution for the coefficients $\left\{ \beta_n^{(N)} ; n = 1,\ldots,N-1 \right\}$,

$$\beta_n^{(N)} = \frac{-\left\langle L\,\phi_N, L\,\psi_n \right\rangle}{\| L\,\psi_n \|^2} \qquad \text{for} \quad n = 1,\ldots,N-1 \ . \tag{4.2-12}$$

The sequence of $\left\{ \psi_N ; N = 1,\ldots \right\}$ can now be constructed.
The value of u_N^{cor} follows from equation (4.2-7),

$$u_N^{cor} = \alpha_N^{(N)}\,\psi_N \qquad \text{for } N = 1,... \tag{4.2-13}$$

which leads to

$$\left\langle L u_N^{cor}, L\psi_N \right\rangle = \alpha_N^{(N)} \left\langle L\psi_N, L\psi_N \right\rangle . \tag{4.2-14}$$

From equation (4.2-3) it also follows that

$$\left\langle L u_N^{cor}, L\psi_N \right\rangle = \left\langle r_{N-1} - r_N, L\psi_N \right\rangle . \tag{4.2-15}$$

Since ψ_N is as a linear combination of $\left\{ \phi_n ; n = 1,\ldots,N \right\}$ application of equation (4.2-4) leads to the result

$$\left\langle L u_N^{cor}, L\psi_N \right\rangle = \left\langle r_{N-1}, L\psi_N \right\rangle = \left\langle r_{N-1}, L\phi_N \right\rangle . \tag{4.2-16}$$

Combining equation (4.2-16) with equation (4.2-14) the result is

$$\alpha_N^{(N)} = \frac{\left\langle r_{N-1}, L\psi_N \right\rangle}{\| L\psi_N \|^2} \ . \tag{4.2-17}$$

With this result the determination of u_N^{cor} has been completed and the iterative scheme based on error minimization has been defined.

In the case that the function ϕ_N, that is generated at the N -th step of iteration, is linearly related to the residual r_{N-1} at the previous step. Then

$$\phi_N = T r_{N-1} \quad \text{for } N = 1, \ldots \tag{4.2-18}$$

where T is a bounded linear operator on D.
A computational scheme with this operator T is be derived.

4.2.a Computational scheme for an arbitrary operator T

The scheme starts with the initial values

$$u_0 = 0, \; r_0 = f, \quad \mathrm{ERR}_0 = \| f \| \tag{4.2-19}$$

Next, the scheme puts

$$\begin{aligned}
&\psi_1 = T r_0 \\
&\mathrm{B}_1 = \| L \psi_1 \|^2 \\
&\alpha_1^{(1)} = \frac{\langle r_0 , L T r_0 \rangle}{\mathrm{B}_1} \\
&u_1 = u_0 + \alpha_1^{(1)} \psi_1 \\
&r_1 = r_0 - \alpha_1^{(1)} L \psi_1 \\
&\mathrm{ERR}_1 = \| \mathrm{r}_1 \|
\end{aligned} \tag{4.2-20}$$

and computes successively for $N = 2,...$

$$\beta_n^{(N)} = -\frac{\langle L T r_{N-1}, L \psi_n \rangle}{\mathrm{B}_n} \qquad \text{for} \quad n = 1, \ldots, N-1$$

$$\psi_N = T\, r_{N-1} + \sum_{n=1}^{N-1} \beta_n^{(N)}\, \psi_n$$

$$\mathrm{B}_N = \| L\, \psi_N \|^2$$

$$\alpha_N^{(N)} = \frac{\langle r_{N-1},\, LTr_{N-1} \rangle}{\mathrm{B}_N}$$

$$u_N = u_{N-1} + \alpha_N^{(N)}\, \psi_N$$

$$r_N = f - L\, u_N = r_{N-1} - \alpha_N^{(N)}\, L\, \psi_N$$

$$\mathrm{ERR}_N = \| \mathrm{r}_N \| \ .$$

(4.2-21)

The important orthogonality relations that hold are

$$\langle L\, \psi_n,\, L\, \psi_m \rangle = 0 \quad \text{for } m \neq n$$

$$\langle L\, Tr_n,\, L\, Tr_m \rangle = 0 \quad \text{for } m \neq n$$

$$\langle r_N,\, L\, \psi_m \rangle = 0 \quad \text{for } m = 1,\ldots,N$$

$$\langle r_N,\, L\, Tr_m \rangle = 0 \quad \text{for } m = 1,\ldots,N-1 \ .$$

(4.2-22)

In this scheme the computer storage and computation time required for each step of iteration increases with an increasing number of iterations.

4.3 SELFADJOINT OPERATOR *LT*

In the case the operator *LT* is selfadjoint the computational scheme of section 4.2 is changed. Selfadjoint operators have the property

$$\langle r_{N-1},\, L\, Tr_{N-1} \rangle = \langle L\, Tr_{N-1},\, r_{N-1} \rangle \ . \qquad (4.3\text{-}1)$$

The last orthogonality relation of (4.2-22) for selfadjoint operators can be written as

$$\left\langle r_n\,,\, L\,Tr_m \right\rangle = \left\langle L\,Tr_n\,,\, r_m \right\rangle = 0 \quad \text{for} \quad m \neq n \quad . \tag{4.3-2}$$

Equation (4.2-17) combined with equation (4.2-18) gives

$$\alpha_N^{(N)} = \frac{\left\langle r_{N-1}\,,\, LTr_{N-1} \right\rangle}{\| L\,\psi_n \|^2} \quad . \tag{4.3-3}$$

From equation (4.2-3) and equation (4.2-8)

$$L\,\psi_n = -\frac{r_n - r_{n-1}}{\alpha_n^{(n)}} \quad \text{for} \quad n = 1,\ldots,N \quad . \tag{4.3-4}$$

Using equation (4.3-3), (4.3-4), and (4.2-18) in equation (4.2-12), the expression for $\beta_n^{(N)}$ becomes

$$\beta_n^{(N)} = \frac{\left\langle LTr_{N-1}\,,\, r_{n-1} \right\rangle - \left\langle LTr_{N-1}\,,\, r_{n-1} \right\rangle}{\left\langle LTr_{n-1}\,,\, r_{n-1} \right\rangle} \quad \text{for} \quad n = 1,\ldots,N-1 \quad . \tag{4.3-5}$$

Take into account orthogonality relation (4.3-2)

$$\beta_n^{(N)} = \begin{cases} 0 & \text{for} \quad n = 1,\ldots,N-2 \\ \dfrac{\left\langle LTr_{N-1}\,,\, r_{N-1} \right\rangle}{\left\langle LTr_{N-2}\,,\, r_{N-2} \right\rangle} & \text{for} \quad n = N-1 \end{cases} \tag{4.3-6}$$

Hence, only $\beta_{N-1}^{(N)}$ differs from zero and has to be determined.

When the operator *L* is not selfadjoint the choice of *T* can lead to a combined operator which is selfadjoint. A selfadjoint operator has a simple iteration scheme, which is an advantage to the iteration scheme of equations (4.2-19) - (4.2-22), and is shown at the end of this section. Therefore the choice

$$\phi_N = L^* r_{N-1} \tag{4.3-7}$$

or

$$T = L^* \tag{4.3-8}$$

is made.
The operator

$$LT = LL^* = L^* L \tag{4.3-9}$$

is selfadjoint and the simple iteration scheme at end of this section can be used.
For selfadjoint operators with T replaced by L^* the orthogonality relation (4.3-2) simplifies to

$$\left\langle L^* r_{m-1}, L^* r_{n-1} \right\rangle = \left\langle \phi_m, \phi_n \right\rangle = 0 \quad \text{for } m \neq n \quad . \tag{4.3-10}$$

Hence, the expansion functions generated according to equation (4.3-7) form an orthogonal sequence.
And the improvement condition (4.2-6) is automatically satisfied which follows from

$$\left\langle r_{N-1}, L\phi_N \right\rangle = \left\langle L^* r_{N-1}, \phi_N \right\rangle = \left\langle \phi_N, \phi_N \right\rangle = \left\langle L^* r_{N-1}, L^* r_{N-1} \right\rangle \neq 0 \quad . \tag{4.3-11}$$

4.3.a Computational scheme for a selfadjoint operator LT

The scheme starts with the initial values

$$u_0 = 0, \; r_0 = f, \quad \mathrm{ERR}_0 = \| f \| \tag{4.3-12}$$

Next, the scheme puts

$$\mathrm{A}_1 = \left\langle r_0 , LTr_0 \right\rangle$$

$$\psi_1 = T\, r_0$$

$$\mathrm{B}_1 = \| L\psi_1 \|^2$$

$$u_1 = u_0 + \frac{\mathrm{A}_1}{\mathrm{B}_1}\psi_1$$

$$r_1 = r_0 - \frac{\mathrm{A}_1}{\mathrm{B}_1} L\psi_1$$

$$\mathrm{ERR}_1 = \| \mathrm{r}_1 \|$$

(4.3-13)

and computes successively for $N = 2,...$

$$\mathrm{A}_N = \langle r_N, LTr_{N-1} \rangle$$

$$\psi_N = T\, r_{N-1} + \frac{\mathrm{A}_1}{\mathrm{A}_{N-1}} \psi_{N-1}$$

$$\mathrm{B}_N = \| L\, \psi_N \|^2$$

$$u_N = u_{N-1} + \frac{\mathrm{A}_N}{\mathrm{B}_N} \psi_N$$

$$r_N = f - L\, u_N = r_{N-1} - \frac{\mathrm{A}_N}{\mathrm{B}_N} L\, \psi_N$$

$$\mathrm{ERR}_N = \| \mathrm{r}_N \| \, .$$

(4.3-14)

This scheme is known as the conjugate-gradient scheme for a non-selfadjoint operator L (after van den Berg, 1989). The computation time and computer storage required for each step of iteration remains the same for all iterations.

4.4 CONVERGENCE

4.4.1 Convergence for the recursive scheme

To investigate the convergence of the iterative self adjoint scheme the following properties of the operators are introduced.
The norm of the operator L is defined as

$$\| L \| = \frac{\| Lu \|}{\| u \|} \quad \text{for all } u \in \mathrm{D} / \{ u \neq 0 \} \, , \tag{4.4-1}$$

with the consequence that

$$\| Lu \| \leq \| L \| \| u \| \qquad \text{for all } u \in \mathrm{D} \,. \tag{4.4-2}$$

The norm for the inverse operator L^{-1} is given by

$$\| L^{-1} \| = \frac{\| L^{-1} v \|}{\| v \|} \quad \text{for all } v \in \mathrm{D} / \{ v \neq 0 \} \,. \tag{4.4-3}$$

Taking $v = Lu$, it follows that

$$\| L^{-1} \| = \frac{\| u \|}{\| Lu \|} \quad \text{for all } u \in \mathrm{D} / \{ u \neq 0 \} \,, \tag{4.4-4}$$

with the consequence that

$$\| Lu \| \geq \frac{\| u \|}{\| L^{-1} \|} \qquad \text{for all } u \in \mathrm{D} \,. \tag{4.4-5}$$

Combining equations (4.4-2) and (4.4-5) , the result is

$$0 < \frac{\| u \|}{\| L^{-1} \|} \leq \| Lu \| \leq \| L \| \,.\, \| u \| < \infty \tag{4.4-6}$$

for all non-zero $u \in \mathrm{D}$. The left and right inequality are a consequence of the assumption that the operator L and L^{-1} are bounded.

It can be shown that (van den Berg, 1989)

$$\| L \| = \| L^{*} \| \,, \tag{4.4-7}$$

and

$$\| L^{*} L \| = \| L L^{*} \| = \| L \|^{2} \,. \tag{4.4-8}$$

In order to investigate the convergence of the recursive scheme of section 4.2 the quantity ERR_N^2 is considered. Using equation (4.2-3), (4.2-13) and the orthogonality relation (4.2-10)

$$\mathrm{ERR}_N^2 = \langle r_N , r_N \rangle = \left\langle r_N , r_{N-1} - \alpha_N^{(N)} L \psi_N \right\rangle = \langle r_N , r_{N-1} \rangle \,. \tag{4.4-9}$$

Again using equation (4.2-3), (4.2-13) and (4.2-16)

$$\langle r_N, r_N \rangle = \left\langle r_{N-1} - \alpha_N^{(N)} L\psi_N \, , r_{N-1} \right\rangle = \langle r_{N-1}, r_{N-1} \rangle - \alpha_N^{(N)} \langle L\phi_N, r_{N-1} \rangle . \qquad (4.4\text{-}10)$$

With the expression for $\alpha_N^{(N)}$ of equation (4.2-17) this result in

$$\langle r_N, r_N \rangle = \langle r_{N-1}, r_{N-1} \rangle - \frac{\langle L\phi_N, r_{N-1} \rangle^2}{\| L\,\psi_N \|^2} . \qquad (4.4\text{-}11)$$

Equation (4.4-11) shows that $\langle r_N, r_N \rangle < \langle r_{N-1}, r_{N-1} \rangle$ and hence the error at step N is always smaller than the error at step N-1, provided that the improvement condition of equation (4.2-6) is satisfied. Consider the expression for the norm of $L\,\psi_N$. Using equation (4.2-9) and the orthogonality relation (4.2-11) it follows that

$$\begin{aligned} \| L\,\psi_N \|^2 &= \langle L\,\psi_N \, , L\,\phi_N \rangle \\ &= \langle L\,\phi_N \, , L\,\phi_N \rangle + \sum_{n=1}^{N-1} \beta_n^{(N)} \langle L\,\psi_n , L\,\phi_N \rangle . \end{aligned} \qquad (4.4\text{-}12)$$

Substituting of the expression of $\beta_n^{(N)}$ equation (4.2-12) in it

$$\| L\,\psi_N \|^2 = \langle L\,\phi_N \, , L\,\phi_N \rangle - \sum_{n=1}^{N-1} \frac{\langle L\,\psi_n , L\,\phi_N \rangle^2}{\| L\,\psi_n \|^2} , \qquad (4.4\text{-}13)$$

$$\| L\,\psi_N \|^2 \le \| L\,\phi_N \|^2 . \qquad (4.4\text{-}14)$$

Using this result in equation (4.4-11) the inequality (4.4-15) is the result

$$\| r_N \|^2 \le \| r_{N-1} \|^2 - \frac{\langle L\phi_N, r_{N-1} \rangle^2}{\| L\,\phi_N \|^2} . \qquad (4.4\text{-}15)$$

In the case that $\phi_N = Tr_{N-1}$ equation (4.4-15) can be rewritten as

$$\| r_N \|^2 \leq \| r_{N-1} \|^2 - \frac{\langle LTr_{N-1}, r_{N-1} \rangle^2}{\| LTr_{N-1} \|^2} . \tag{4.4-16}$$

For a certain class of bounded operators L and T, convergence of the iteration scheme can be proved. The relevant class is characterized by the property that there exist a constant $c \neq 0$ such that

$$\left| \langle LTr_{N-1}, r_{N-1} \rangle \right| \geq |c| \, \| r_{N-1} \|^2 . \tag{4.4-17}$$

This requirement implies that the improvement condition of equation (4.2-6), $\langle LTr_{N-1}, r_{N-1} \rangle \neq 0$, is satisfied. Equation (4.4-17) is a stronger condition. The Cauchy-Schwarz inequality gives

$$\left| \langle LTr_{N-1}, r_{N-1} \rangle \right|^2 \leq \| LTr_{N-1} \|^2 \, \| r_{N-1} \|^2 . \tag{4.4-18}$$

Using the definition of the norm of a bounded operator (4.4-2) and apply this definition to the bounded operator LT gives

$$\| LTr_{N-1} \| \leq \| LT \| \, \| r_{N-1} \| . \tag{4.4-19}$$

Using this equation (4.4-19) in equation (4.4-18) the inequality (4.4-20) is the result

$$\left| \langle LTr_{N-1}, r_{N-1} \rangle \right|^2 \leq \| LT \|^2 \, \| r_{N-1} \|^4 . \tag{4.4-20}$$

Comparing equation (4.4-20) with equation (4.4-17), it follows that the value of c lies in the range $0 < |c| \leq \| LT \| < \infty$.

Using equation (4.4-17) and (4.4-19) in equation (4.4-16) the inequality can be written as

$$\| r_N \|^2 \leq \left(1 - \frac{|c|^2}{\| LT \|^2} \right) \| r_{N-1} \|^2 \quad \text{for } N = 1, \ldots . \tag{4.4-21}$$

Repeated application of equation (4.4-21) gives

$$\| r_N \|^2 \leq \left(1 - \frac{|c|^2}{\| LT \|^2}\right)^N \| r_0 \|^2 \quad . \tag{4.4-22}$$

From equation (4.4-22) it follows that, if there exists some nonzero c such that equation (4.4-17) holds, the error converges monotonically to zero as $N \to \infty$. The rate of convergence depends on the values of $\frac{|c|}{\| LT \|}$; the closer this value is to unity, the faster the convergence.

4.4.2 Convergence for the selfadjoint and positive operator LT

If LT is selfadjoint and positive ($\langle u, LTu \rangle > 0$ for all $u \neq 0$ defined on D then there exists a positive selfadjoint operator $(LT)^{\frac{1}{2}}$ such that

$$\langle u, LTu \rangle = \left\langle (LT)^{\frac{1}{2}} u , (LT)^{\frac{1}{2}} u \right\rangle = \| (LT)^{\frac{1}{2}} u \|^2 \tag{4.4-23}$$

for all $u \in$ D. Replacing L in equation (4.4-5) by $(LT)^{\frac{1}{2}}$ and using that

$$\left((LT)^{\frac{1}{2}}\right)^{-1} = (LT)^{-\frac{1}{2}} \tag{4.4-24}$$

it follows that,

$$\| (LT)^{\frac{1}{2}} u \| \geq \frac{\| u \|}{\| (LT)^{-\frac{1}{2}} \|} . \tag{4.4-25}$$

Using $\| (LT)^{-\frac{1}{2}} u \| = \| (LT)^{-1} u \|^{\frac{1}{2}}$ equations (4.4-23) and (4.4-25) lead to

$$\langle u, LTu \rangle \geq \frac{\| u \|^2}{\| (LT)^{-1} \|} . \tag{4.4-26}$$

Comparing equation (4.4-17) with equation (4.4-26) the constant c exists and is given by

$$|c| = \frac{1}{\| (LT)^{-1} \|} . \tag{4.4-27}$$

In view of the leftmost inequality of equation (4.4-6), with L replaced by LT, c has a nonzero value. Using this result in equation (4.4-22) the final result is

$$\| r_N \|^2 \leq \left(1 - \frac{1}{\| (LT)^{-1} \|^2 \, \| LT \|^2} \right)^N \| r_0 \|^2 \quad . \tag{4.4-28}$$

From equation (4.4-6), with L replaced by LT, it follows that

$$0 < \frac{1}{\| (LT)^{-1} \| \; \| LT \|} \leq 1 \quad . \tag{4.4-29}$$

Equation (4.4-28) and equation (4.4-29) demonstrate the convergence of the scheme If LT is close to the identity operator, the left-hand side of equation (4.4-28) becomes close to 1 and very rapid convergence is expected.

4.5 PRECONDITIONING ($T = P$)

If T is chosen equal to L^{-1}, the inverse of L, then the recursive scheme of section 4.2 will terminate in the first iteration; the solution is than the exact solution. This fact can be used if T is chosen equal to a suitable preconditioning operator P, where the operator LP more closely resembles the identity operator than L itself does. The success of the method depends on the availability of an approximate inverse to the operator L. In the schemes we take then:

$$\phi_N = P \, r_{N-1} \tag{4.5-1}$$

or

$$T = P \; . \tag{4.5-2}$$

The relevant iteration scheme follows by replacing the operator T by the preconditioning operator P.

When the operator LP is not selfadjoint the recursive scheme for $T = P$ must be used, in which the computer storage of the expansion functions required for each step of iteration increases with an increasing number of iterations. To make use of the simple iteration scheme of equations (4.3-12) - (4.3-14) operator T is chosen as

$$T = P \, P^* L^* \tag{4.5-3}$$

or

$$\phi_N = P\,P^*\,L^*\,r_{N-1} \quad . \tag{4.5-4}$$

The operator

$$LT = L\,P\,P^*\,L^* = (LP)\,(LP)^* \cdot \tag{4.5-5}$$

is selfadjoint. This is a conjugate-gradient scheme for a preconditioned non-selfadjoint operator *L*.

To show that application of a preconditioning scheme converges faster than a non-preconditioned scheme. Use equation (4.4-28) where *T* is chosen equal to L^*. Equation (4.4-28) can then be rewritten as

$$\| r_N \|^2 \le \left(1 - \frac{1}{\| L^{-1} \|^4 \, \| L \|^4} \right)^N \| r_0 \|^2 \quad , \tag{4.5-6}$$

where $\| \left(LL^* \right)^{-1} \| = \| L^{-1} \|^2$ and $\| LL^* \| = \| L \|^2$ have been used.
In the preconditioning procedure by taking $T = P\,P^*\,L^*$ equation (4.4-28) can be rewritten as

$$\| r_N \|^2 \le \left(1 - \frac{1}{\| (LP)^{-1} \|^4 \, \| LP \|^4} \right)^N \| r_0 \|^2 \quad , \tag{4.5-7}$$

where $\| \left(LPL^*P^* \right)^{-1} \| = \| LP^{-1} \|^2$ and $\| LPL^*P^* \| = \| LP \|^2$ have been used. Comparing equation (4.5-6) with equation (4.5-7) it can be seen that the preconditioned scheme converges indeed faster than the preconditioned scheme as soon as *LP* is closer to the identity operator than *L* itself is.

Chapter 5

NUMERICAL IMPLEMENTATION

5.0 INTRODUCTION

As was pointed out before, the Hankel function, and the derivatives of the Hankel function, can be written in a structure which is in itself a Fourier backtransform. This structure is used to calculate the operator expressions in the iterative procedure of Chapter 4 and the integral equations needed to describe the wavefield in the domain of interest.

In section 5.1 the convolutional structure of the integral equations for the unbounded medium and the halfspace, derived in Chapter 1 and 2, is used to derive a structure which can easily be implemented in the computer. In section 5.2 the preconditioning operators, which are used in the numerical calculation, of the operators in section 5.1 are calculated. In section 5.3 some fundamental properties of the discrete Fourier transform are discussed. In section 5.4 the problem of branch points is investigated. And in section 5.5 the Fourier transform in relation to causal signals is explained.

5.1 THE OPERATOR EXPRESSION *LU*

The operator expressions, derived in sections 1.4 and 1.5 for the unbounded medium and in section 2.3 for the halfspace, occur in a convolutional structure. So a Fourier transform, with respect to the integration variable, changes the convolution into a simple product in the wavenumber domain.

5.1.1a Perfectly compliant strip in an unbounded medium

The operator L acting on the unknown function ($u = \partial q$) is given by equation (5.1-1) (from equation (1.4-10))

$$Lu = -\hat{\zeta}\frac{j}{4}\int_{x_1'=-a}^{x_1'=+a} H_0^{(1)}\left(k\left|x_1-x_1'\right|\right)\partial q\left(x_1'\right)dx_1' \quad . \tag{5.1-1}$$

Letting the integral running from minus infinity to plus infinity and thereby introducing the characteristic function of the strip region into equation (5.1-1) results in

$$Lu = -\hat{\zeta}\frac{j}{4}\int_{x_1'=-\infty}^{x_1'=+\infty} \mathrm{H}_0^{(1)}\left(k\left|x_1 - x_1'\right|\right)\partial q\left(x_1'\right)\,\chi_a\left(x_1'\right)dx_1' \,. \tag{5.1-2}$$

Transforming equation (5.1-2) with respect to the spatial coordinates gives, where F denotes Fourier transform,

$$\mathrm{F}\{Lu\} = -\hat{\zeta}\frac{j}{4}\,\mathrm{F}\left\{\mathrm{H}_0^{(1)}\left(k\left|x_1\right|\right)\right\}\mathrm{F}\left\{\chi_a\left(x_1\right)\partial q\left(x_1\right)\right\}, \tag{5.1-3}$$

with the spatial Fourier transform of the Hankel function as

$$\mathrm{F}\left\{\mathrm{H}_0^{(1)}\left(k\left|x_1\right|\right)\right\} = \int_{x_1=-\infty}^{x_1=\infty}\exp\left(-jk_1x_1\right)\mathrm{H}_0^{(1)}\left(k\left|x_1\right|\right)dx_1 \,. \tag{5.1-4}$$

Substituting equation (1.4-11), the expression for the Hankel function on the strip, into equation (5.1-4) gives

$$\mathrm{F}\left\{\mathrm{H}_0^{(1)}\left(k\left|x_1\right|\right)\right\} = \int_{x_1=-\infty}^{x_1=\infty}\exp\left(-jk_1x_1\right)\left\{\frac{1}{\pi}\int_{k_1=-\infty}^{k_1=\infty}\frac{\exp\left(jk_1x_1\right)}{\left(k^2-k_1^2\right)^{\frac{1}{2}}}\,dk_1\right\}dx_1 \tag{5.1-5}$$

The Hankel function can be recognized as a Fourier back-transform as seen in equation (5.1-5)

$$\mathrm{F}\left\{\mathrm{H}_0^{(1)}\left(k\left|x_1\right|\right)\right\} = \mathrm{F}\left\{\mathrm{F}^{-1}\left\{\frac{2}{\left(k^2-k_1^2\right)^{\frac{1}{2}}}\right\}\right\} = 2\left(k^2-k_1^2\right)^{-\frac{1}{2}} \,. \tag{5.1-6}$$

With this result equation (5.1-3) reduces to the simple expression

$$\mathrm{F}\{Lu\} = -\hat{\zeta}\frac{j}{2}\left(k^2-k_1^2\right)^{-\frac{1}{2}}\mathrm{F}\left\{\chi_a\left(x_1\right)\partial q\left(x_1\right)\right\} \,. \tag{5.1-7}$$

Or, transforming back

$$Lu = -\hat{\zeta}\frac{j}{2}\mathrm{F}^{-1}\left\{\left(k^2 - k_1^2\right)^{-\frac{1}{2}}\mathrm{F}\left\{\chi_a(x_1)\,\partial q(x_1)\right\}\right\}. \qquad (5.1\text{-}8)$$

The operator expression LU can be computed efficiently using FFT routines to evaluate the forward and inverse Fourier transformations in equation (5.1-8). A similar computation can be carried out for the adjoint operator L^* and the preconditioning operator P.

5.1.1b Perfectly rigid strip in an unbounded medium

The operator expression is given by equation (1.5-14) and is repeated in equation (5.1-9)

$$Lu = -\hat{\zeta}^{-1}\frac{j}{4\pi}\int_{x_1'=-a}^{x_1'=+a}\left\{\int_{-\infty}^{+\infty}\gamma\exp\left[jk_1\left(x_1 - x_1'\right)\right]dk_1\right\}\partial f_2\left(x_1'\right)dx_1', \qquad (5.1\text{-}9)$$

where $u = \partial f$. The spatial Fourier transform of the operator expression is derived using the same method as in paragraph 5.1.1 a which results in

$$\mathrm{F}\{Lu\} = -\frac{j}{2}\hat{\zeta}^{-1}\left(k^2 - k_1^2\right)^{\frac{1}{2}}\mathrm{F}\left\{\chi_a(x_1)\,\partial f(x_1)\right\}. \qquad (5.1\text{-}10)$$

5.1.2a Perfectly compliant strip in a halfspace

The operator expression is given by equation (2.3-3) with $u = \partial q$

$$Lu = -\hat{\zeta}\frac{j}{4\pi}\int_{x_1'=-a}^{x_1'=+a}\left\{\int_{-\infty}^{+\infty}\frac{\exp\left[jk_1\left(x_1 - x_1'\right)\right]}{\gamma}\left(1 - \exp\left[-2j\gamma\left|x_2\right|\right]\right)\right\}dk_1\,\partial q(x_1)\,dx_1' \qquad (5.1\text{-}11)$$

.

The Fourier transform of the exponentional function (which is the Hankel function) of the first expression on the right hand-side of equation (5.1-11) is given by equation (5.1-6). For the Fourier

transform of the second expression (which can also be expressed as a Hankel function as shown in equation (5.1-12)) a closer look is needed. Using the fact that it is a convolution with the unknown function, it can be written as follows

$$H_0^{(1)}\left(k\left[(x_1)^2 + (2x_2)^2 \right]^{\frac{1}{2}} \right) = \frac{1}{\pi} \int_{-\infty}^{\infty} \frac{\exp\left[jk_1(x_1) \right] \exp\left[j\left(k^2 - k_1^2\right)^{\frac{1}{2}} |2x_2| \right]}{\left(k^2 - k_1^2\right)^{\frac{1}{2}}} dk_1 \quad . \tag{5.1-12}$$

In equation (5.1-12) a spatial Fourier backtransform is recognized

$$H_0^{(1)}\left(k\left[(x_1)^2 + (2x_2)^2 \right]^{\frac{1}{2}} \right) = F^{-1}\left\{ \frac{2 \exp\left[j\left(k^2 - k_1^2\right)^{\frac{1}{2}} |2x_2| \right]}{\left(k^2 - k_1^2\right)^{\frac{1}{2}}} \right\} . \tag{5.1-13}$$

So the spatial Fourier transform of the operator equation (5.1-11) is given by

$$F\{Lu\} = \frac{-j\hat{\zeta}}{2} \left(\frac{1 - 2 \exp\left[j\left(k^2 - k_1^2\right)^{\frac{1}{2}} |2x_2| \right]}{\left(k^2 - k_1^2\right)^{\frac{1}{2}}} \right) F\left\{ \chi_a(x_1) \partial q(x_1) \right\} . \tag{5.1-14}$$

5.1.2b Perfectly rigid strip in a halfspace

The operator expression is given by equation (2.3-8) where $u = \partial f$

$$Lu = \hat{\zeta}^{-1} \frac{j}{4\pi} \int_{x'_1 = -a}^{x'_1 = +a} \left\{ \int_{-\infty}^{+\infty} \gamma \exp\left[jk_1(x_1 - x'_1) \right] \left(1 - \exp\left[2j\gamma(x_2) \right] \right) dk_1 \right\} \partial f_2(x'_1) \, dx'_1 . \tag{5.1-15}$$

From the configuration of the half-space it can be shown that x'_2 is always positive. The first expression of the integral of equation (5.1-15) is the Fourier backtransform of equation (5.1-10) The second expression under the integral, which represents the effect of the halfspace, is the Fourier back transform of

$$\int_{-\infty}^{+\infty} \left(k^2-k_1^2\right)^{\frac{1}{2}} \exp\left[jk_1\left(x_1-x_1'\right)+j\left(k^2-k_1^2\right)^{\frac{1}{2}}\left|2x_2'\right|\right] dk_1 = \tag{5.1-17}$$

$$\mathrm{F}^{-1}\left\{2\pi\left(k^2-k_1^2\right)^{\frac{1}{2}} \exp\left[-jk_1x_1'+j\left(k^2-k_1^2\right)^{\frac{1}{2}}\left|2x_2'\right|\right]\right\} \quad .$$

So the spatial Fourier transformed operator expression is given by

$$\mathrm{F}\{Lu\} = \hat{\zeta}^{-1}\frac{j}{2}\left(k^2-k_1^2\right)^{\frac{1}{2}}\left(1-\exp\left[j\left(k^2-k_1^2\right)^{\frac{1}{2}}\left|2x_2'\right|\right]\right)\mathrm{F}\{\chi_a(x_1)\,\partial f(x_1)\} \tag{5.1-18}$$

5.2 THE PRECONDITIONING OPERATOR

The preconditioned conjugate-gradient scheme converges faster than the non-preconditioned scheme which was shown in section 4.5 . The advantage of the conjugate gradient scheme is that the orthogonalization of the expansion functions is automatically enforced and storage of these expansion functions of all previous iterations is superfluous. So by using a preconditioning operator in a conjugate gradient scheme the iteration will converge fast to the desired solution.

5.2.1a Perfectly compliant strip in an unbounded medium

Equation (5.1-7) can be used to construct a preconditioning operator that is under certain circumstances an approximate inverse operator. The equation inverse to equation (5.1-7) is

$$\mathrm{F}\{\chi_a(x_1)\,\partial q(x_1)\} = 2j\,\hat{\zeta}^{-1}\left(k^2-k_1^2\right)^{\frac{1}{2}}\mathrm{F}\{Lu\} \quad . \tag{5.2-1}$$

The value of $\chi_a(x_1)\,\partial q(x_1)$ *cannot* be obtained by an inverse Fourier transform (direct deconvolution) of equation (5.2-1) to the spatial domain, since *LU* is only known for $x \in (-a, a)$ and not outside this interval. Let the operator *P* for any *v* defined on $x \in (-a, a)$ be defined as

$$\mathrm{F}\{Pv\} = 2j\,\hat{\zeta}^{-1}\left(k^2-k_1^2\right)^{\frac{1}{2}}\mathrm{F}\{\chi_a(x_1)\,\partial q(x_1)\} \quad . \tag{5.2-2}$$

Inverse Fourier transformation then yields

$$Pv = 2j\hat{\zeta}^{-1}\,\mathrm{F}^{-1}\left\{\left(k^2 - k_1^2\right)^{\frac{1}{2}}\mathrm{F}\left\{\chi_a(x_1)\partial q(x_1)\right\}\right\} \quad . \tag{5.2-3}$$

Now P is an approximate inverse of L in all cases where Lu is relatively small outside the interval $x \in (-a, a)$. The preconditioning operator expression Pv can also be computed using FFT routines. A similar computation can be carried out for the adjoint operator P^*.

5.2.1b Perfectly rigid strip in an unbounded medium

The preconditioning operator of equation (5.1-10) is given by

$$\mathrm{F}\{Pv\} = 2j\hat{\zeta}^{1}\left(k^2 - k_1^2\right)^{-\frac{1}{2}}\ \mathrm{F}\left\{\chi_a(x_1)\,\partial f(x_1)\right\} \quad . \tag{5.2-4}$$

5.2.2a Perfectly compliant strip in a halfspace

The preconditioning operator of equation (5.1-14) is given by

$$\mathrm{F}\{Pv\} = -2j\hat{\zeta}^{-1}\left(\frac{\left(k^2 - k_1^2\right)^{\frac{1}{2}}}{2\exp j\left[\left(k^2 - k_1^2\right)^{\frac{1}{2}}|2x_2|\right] - 1}\right)\mathrm{F}\left\{\chi_a(x_1)\,\partial q(x_1)\right\} \quad . \tag{5.2-5}$$

5.2.2b Perfectly rigid strip in a halfspace

The preconditioning operator of equation (5.1-18) is given by

$$\mathrm{F}\{Pv\} = -2j\hat{\zeta}\left(k^2 - k_1^2\right)^{-\frac{1}{2}}\left(1 - \exp\left[j\left(k^2 - k_1^2\right)^{\frac{1}{2}}|2x_2'|\right]\right)^{-1}\ \mathrm{F}\left\{\chi_a(x_1)\,\partial f(x_1)\right\} \quad . \tag{5.2-6}$$

5.3 DISCRETE FOURIER TRANSFORM

Solving the strip problem uses Fourier transforms intensively. In this section some fundamental properties of the Discrete Fourier Transforms (DFTs) are treated. In using DFTs the computation can be carried out using Fast Fourier Transform (FFT) algorithms. A FFT algorithm can compute a Fourier transform very efficiently when the number of samples is chosen to fit the FFT algorithm scheme. In appendix A a description of the errors made in DFT's is given.
The spatial continuous Fourier transform is defined by

$$\widetilde{X}(k) = \int_{-\infty}^{\infty} X(x) \exp(-jkx)\, dx \quad . \tag{5.3-1}$$

The backtransform is then given by

$$X(x) = \frac{1}{2\pi} \int_{-\infty}^{\infty} \widetilde{X}(k) \exp(jkx)\, dk \quad . \tag{5.3-2}$$

The assumption is made that $X(x)$ is a bounded function in space, see Figure 5.1.

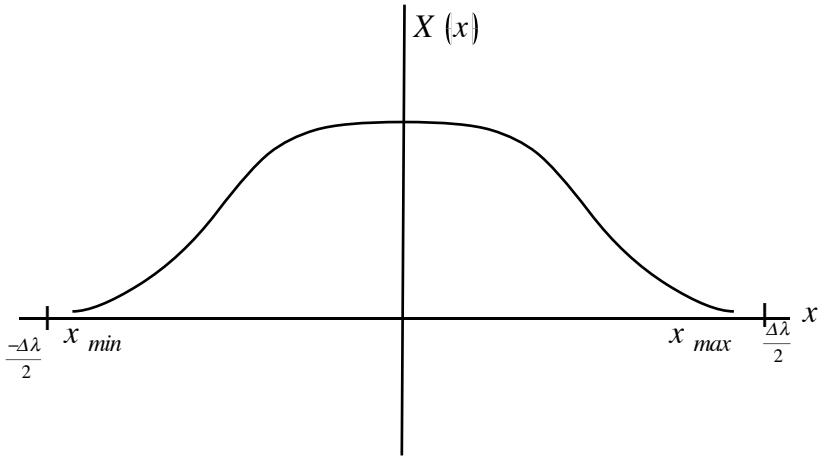

Figure 5.1 : bounded function in space

Making the wavenumber domain discrete by taking $k=n\Delta k$ equation (5.3-1) results in

$$\widetilde{X}(n\Delta k) = \int_{-\infty}^{\infty} X(t) \exp(-jn\Delta kx)\, dx \quad . \tag{5.3-3}$$

The effect of the discretization can be shown as follows, introducing the relation

$$\Delta k \Delta\lambda = 2\pi \ , \tag{5.3-4}$$

equation (5.3-3) can be rewritten as

$$\widetilde{X}_n = \sum_{m=-\infty}^{+\infty} \int_{\left(m-\frac{1}{2}\right)\Delta\lambda}^{\left(m+\frac{1}{2}\right)\Delta\lambda} X(x) \exp\left(-j\frac{2\pi}{\Delta\lambda} nx\right) dx \quad . \tag{5.3-5}$$

In equation (5.3-3) the integral is divided into integral parts which sum up to the integral running from minus infinity to infinity.

Choosing a new integration variable

$$\tau = x + m\Delta\lambda \ , \tag{5.3-6}$$

Changes the integral in (5.3-5) to

$$\widetilde{X}_n = \sum_{m=-\infty}^{+\infty} \int_{\frac{-1}{2}\Delta\lambda}^{\frac{1}{2}\Delta\lambda} X(\tau - m\Delta\lambda) \exp\left(-jn\frac{2\pi}{\Delta\lambda}(\tau - m\Delta\lambda)\right) d\tau \quad . \tag{5.3-7}$$

With the relation $\exp(-j\,2\pi nm) = 1$ this is equal to

$$\widetilde{X}_n = \int_{\frac{-1}{2}\Delta\lambda}^{\frac{1}{2}\Delta\lambda} \sum_{m=-\infty}^{+\infty} X(\tau - m\Delta\lambda) \exp\left(-jn\frac{2\pi}{\Delta\lambda}\tau\right) d\tau \quad . \tag{5.3-8}$$

So sampling in the wavenumber domain makes the originally bounded function in space periodic with period $\Delta\lambda$.

$$\sum_{m=-\infty}^{+\infty} X\left(\tau - m\Delta\lambda\right) = X_{per}\left(\tau\right) \quad . \tag{5.3-9}$$

The reverse is also true; sampling in the spatial domain makes the wavenumber domain periodic.

In order not to be aliased (having the periods of the periodic function overlapping) in the spatial domain the following inequality must hold (the Nyquist criterion)

$$\frac{\Delta\lambda}{2} < max\left|x_{min}\ ,\ x_{max}\right| \quad . \tag{5.3-10}$$

If equation (5.3-10) is satisfied the spatial domain can be made discrete without having the effect of aliasing. So the discretization number N must therefore satisfy the relation:

$$\Delta\lambda = \Delta x\ N \qquad \text{or} \qquad \Delta k\ \Delta x = \frac{2\pi}{N}\ , \tag{5.3-11}$$

equation (5.3-8) then changes into

$$\tilde{\tilde{X}}_n = \Delta x \sum_{m=\frac{-N}{2}}^{\frac{+N}{2}-1} X\left(m\Delta x\right) \exp\left(-j\frac{2\pi nm}{N}\right) \quad , \tag{5.3-12}$$

$$\tilde{\tilde{X}}_n = \Delta x \sum_{m=\frac{-N}{2}}^{\frac{+N}{2}-1} X_m \exp\left(-j\frac{nm\ 2\pi}{N}\right) \quad . \tag{5.3-13}$$

In doing so the wavenumber domain is also made periodic with period $\frac{1}{\Delta x}$ and because of the finite length of the function in the spatial domain the function in the wavenumber domain will always be aliased. In general a finite length signal in one domain is unbounded in the other (transformed) domain. So a DFT pair is always aliased in one domain.

The DFT pair is given by (from equation (5.3-13)).

$$X_m = \frac{\Delta k}{2\pi} \sum_{m=\frac{-N}{2}}^{\frac{+N}{2}-1} \widetilde{X}_n \exp\left(jnm\Delta x\Delta k\right) \qquad \text{for } m = -\frac{N}{2} \ldots\ldots \frac{N}{2} \tag{5.3-14}$$

$$\widetilde{X}_n = \Delta x \sum_{m=\frac{-N}{2}}^{\frac{+N}{2}-1} X_m \exp\left(-jnm\Delta x\Delta k\right) \qquad \text{for } n = -\frac{N}{2} \ldots\ldots \frac{N}{2} \tag{5.3-15}$$

And in order not to be aliased in *both* domains the following choice must be made

$$\Delta\lambda = \Delta x\, N \qquad\qquad \Delta k\, \Delta x = \frac{2\pi}{N} \tag{5.3-16}$$

$$|x_{max}| \le \frac{2\pi}{\Delta k} \quad \text{or} \quad |k_{max}| \le \frac{1}{2\Delta x} \quad . \tag{5.3-17}$$

In appendix A the error due to the aliased spectrum is worked out in detail.

In FFT it is favorable to choose the number of sample points in the spatial domain equal to the number of samples in the wavenumber domain. Therefore zeros are added to the original signal to arrive at the number of samples desired for the FFT. This operation is equal to applying a box function to the signal. In the wavenumber domain the spectrum is then convolved with a sinc function (the Fourier transform of a box function). So the interpolation due to the box function is done by the sinc function. Interpolating using the sinc function implements exact reconstruction of the original signal if *X* is bounded and the sampling frequency satisfies the anti-alias condition.

Adding zero's to the signal does *not* change the contents of the signal, it only makes the number of sample points bigger in the transform domain. Therefore the signal looks better in the transform domain but this is only because there are more points used to represent the spectrum of the signal.

5.4 BRANCH POINTS

Multivalued functions are not uniquely specified when the argument is given. This multiplicity of values introduces discontinuities into the function. The independent sets of the multivalued function are called the branches of the function. The line along which the discontinuities occur is called the branch line. Branch points always occur in pairs and the branch lines join the branch points. Crossing the branch line on the z-plane takes the function from one of its branches to the other. A typical multivalued function is the square root; the square root of a number may have either a plus or a minus value. From the first two sections of this chapter it can be seen that the square root $\left(k^2 - k_1^2\right)^{\frac{1}{2}}$ plays an important role in the whole analysis. This function has two branch points one at *-k* and one at *+k* (after Spiegel, 1964).

In order to cope with the branch points in the numerical inverse Fourier transformation in equation (5.1-8), slight losses in the medium surrounding the strip are introduced, in accordance with the condition of causality, by taking the angular wavenumber to have a positive imaginary part. In this way the integration path avoids the branch line and the integrated function remains on the same branch. In section 1.2 the wavenumber was already made complex in order to deal with the pole in the wavenumber domain.

By taking the wavenumber complex, equation (5.4-1), the path of integration is changed see Figure 5.2 (Morse and Ingard, 1968)

$$k = \frac{2\pi}{\lambda} + j\varepsilon = \frac{\omega + j\varepsilon c}{c} \quad . \tag{5.4-1}$$

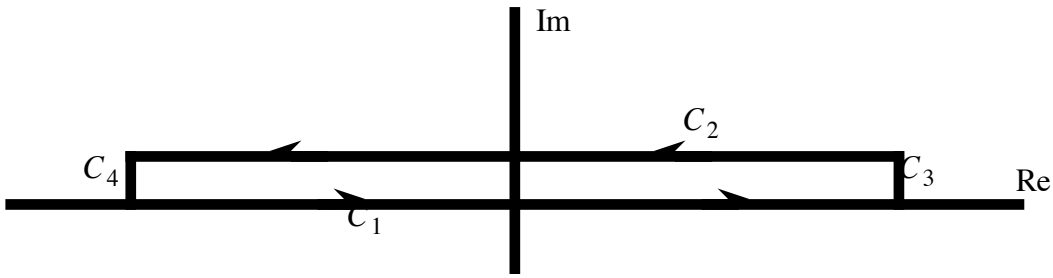

Figure 5.2: changing the path of integration along the contours $C^t = C_1 + C_2 + C_3 + C_4$

Using Cauchy's theorem it can be shown that if there are no poles inside the changed path of integration (the closed contour C^t), which is always true for causal signals, then reduces to

$$\int_{C^t} \hat{X}(\omega) \exp(-j\omega t)\, d\omega = 0 \quad . \tag{5.4-2}$$

By letting the integral along the Real-axis going to infinity the contours C_3 and C_4 vanish.

$$\int_{C_1} \hat{X}(\omega)\exp(-j\omega t)\,d\omega = -\int_{C_2} \hat{X}(\omega)\exp(-j\omega t)\,d\omega \quad . \tag{5.4-3}$$

Changing the order of the complex integral and putting in the boundaries gives

$$\int_{-\infty}^{\infty} \hat{X}(\omega)\exp(-j\omega t)\,d\omega = \int_{-\infty+j\varepsilon c}^{\infty+j\varepsilon c} \hat{X}(\omega)\exp(-j\omega t)\,d\omega \quad . \tag{5.4-4}$$

Changing the integration variable ω of the right-hand integral of equation (5.4-4) to

$$\omega' = \omega - j\varepsilon c \quad , \tag{5.4-5}$$

equation (5.4-4) can be rewritten as

$$\int_{-\infty}^{\infty} \hat{X}(\omega)\exp(-j\omega t)\,d\omega = \int_{-\infty}^{\infty} \hat{X}(\omega'+j\varepsilon c)\exp(-j(\omega'+j\varepsilon c)t)\,d\omega' \quad , \tag{5.4-6}$$

or

$$X(t) = \exp(t\varepsilon c)\int_{-\infty}^{\infty} \hat{X}(\omega'+j\varepsilon c)\exp(-j\omega' t)\,d\omega' \quad , \tag{5.4-7}$$

which is equal to

$$\exp(-t\varepsilon c)X(t) = \int_{-\infty}^{\infty} \hat{X}(\omega'+j\varepsilon c)\exp(-j\omega' t)\,d\omega' \quad . \tag{5.4-8}$$

So, introducing a complex wavenumber in the inverse Fourier transform scales the original function into a decaying function of t. According to the causality condition this is legitimate. In order to undo the effect of the complex frequency in the time space domain an inverse exponential taper is applied.

5.5 CAUSALITY

In the calculation of the scattering problem the solution is given in the space-frequency domain. To get a time signal back the frequencies must be transformed back to time. In the numerical calculation only the positive frequencies are calculated. The negative frequencies are obtained by using a relation between the positive and negative frequencies. This relationship must be chosen such that the the time signal is causal and real. In this section two kinds of relations which give back a causal time signal are discussed.

5.5.1 Complex conjugate and causality

Real time signals have some properties which can be used to construct the negative frequencies values from the values at positive frequencies. From the properties of the Fourier transform it is known that an even function has only a real transformed part, and an odd function has only an imaginary transformed part. So

even function $F \rightarrow$real
odd function $F \rightarrow$imaginary .

In the frequency domain this property is used in the following way; taking the real part even and the imaginary part odd (so the negative frequencies are the complex conjugate of the positive frequencies) the function in the frequency domain can be written as follows:

$$\hat{\mathrm{f}}(\omega) = \hat{\mathrm{f}}^{*}(-\omega) \ , \tag{5.5-1}$$

or

$$\hat{\mathrm{f}}(\omega) = \hat{\mathrm{E}}(\omega) + j\,\hat{\mathrm{O}}(\omega) \ . \tag{5.5-2}$$

Where E is an even function and O is an odd function.
Transforming this special chosen function back to time gives the following

$$\mathrm{f}(t) = \frac{1}{2\pi}\int_{\omega=-\infty}^{\omega=+\infty} \hat{\mathrm{f}}(\omega)\exp(-j\,\omega\,t)\,d\omega \ . \tag{5.5-3}$$

$$\mathrm{f}(t) = \frac{1}{2\pi}\int_{\omega=-\infty}^{\omega=+\infty} \left(\hat{\mathrm{E}}(\omega) + j\,\hat{\mathrm{O}}(\omega)\right)\left(\cos(\omega\,t) - j\sin(\omega\,t)\right)d\omega \ . \tag{5.5-4}$$

An odd function integrated over minus infinity to plus infinity is zero thus the remaining part of equation (5.5-4) is a real function which is asymmetrical. So from equation (5.5-4) it follows that the time function is real and asymmetrical. This a necessary condition for causality but it is not sufficient.

5.5.2 The Hilbert transform and causality

The Hilbert transform forces the time function to be causal. Starting in the frequency domain the Hilbert transform is obtained by setting the imaginary part of the frequencies in a special relation with the real part (after Bracewell, 1978). The original backtransform to the time domain is given by

$$f(t) = \frac{1}{2\pi}\int_{\omega=-\infty}^{\omega=+\infty} \hat{f}(\omega)\exp(-j\,\omega\,t)\,d\omega \quad . \tag{5.5-5}$$

Choosing $\hat{f}(\omega)$ zero for negative frequencies equation (5.5-5) is changed into

$$\bar{f}(t) = \frac{1}{2\pi}\int_{\omega=0}^{\omega=+\infty} \hat{f}(\omega)\exp(-j\,\omega\,t)\,d\omega \quad , \tag{5.5-6}$$

where $\bar{f}(t)$ denotes an analytic signal. Which can be rewritten as

$$\bar{f}(t) = \frac{1}{2\pi}\int_{\omega=-\infty}^{\omega=+\infty} \hat{f}(\omega)\,\hat{u}(\omega)\exp(-j\,\omega\,t)\,d\omega \quad , \tag{5.5-7}$$

where $\hat{u}(\omega)$ is the unit step function. It is also necessary to double the result to get the energy content of the frequency domain the same as in the original transform.
Multiplication in the frequency domain is equavalent to convolution in the time domain. The Fourier backtransform of the unit step function is given by

$$F\{\hat{u}(\omega)\} = \frac{1}{2}\,\delta(t) - \frac{j}{2\pi t} \quad . \tag{5.5-8}$$

So the analytic time function is given by

$$\bar{f}(t) = f(t) * \left\{\frac{1}{2}\,\delta(t) - \frac{j}{2\pi t}\right\} \quad , \tag{5.5-9}$$

Equation (5.5-9) is equal to

$$\bar{f}(t) = \frac{1}{2} f(t) - \frac{j}{2\pi} \int_{\tau=-\infty}^{\tau=+\infty} \frac{f(\tau)d\tau}{(\tau - t)} \quad . \tag{5.5-10}$$

The last expression is called the Hilbert transform of $f(t)$. And $\bar{f}(t)$ is an analytic signal. Hence all functions whith negative frequencies zero in the frequency domain have in the time domain the form

$$\bar{f}(t) = A(t) - j\,B(t) \quad , \tag{5.5-11}$$

where B is the Hilbert transform of A. In choosing the frequency function in this way the time function is always real.

Chapter 6

RESULTS

6.0 INTRODUCTION

In this chapter results are given for a set of scattering configurations in the time space domain. In the first section a 'sea configuration' is chosen to show some results related to the surface multiple removal in the marine case. In the second section of this chapter the reliability of the data is tested on several aspects of the scattering problem.

6.1 SEA CONFIGURATION

The scattering configurations are chosen such that the source and receiver distance to the strip can be compared with the source and receiver distances to the sea-bottom in the North-sea. These depth parameters are held constant in all pictures in this section. In Figure 6.1a the configuration is shown for the unbounded medium, and in Figure 6.1b for the bounded medium, where the source lies above the middle of the strip.

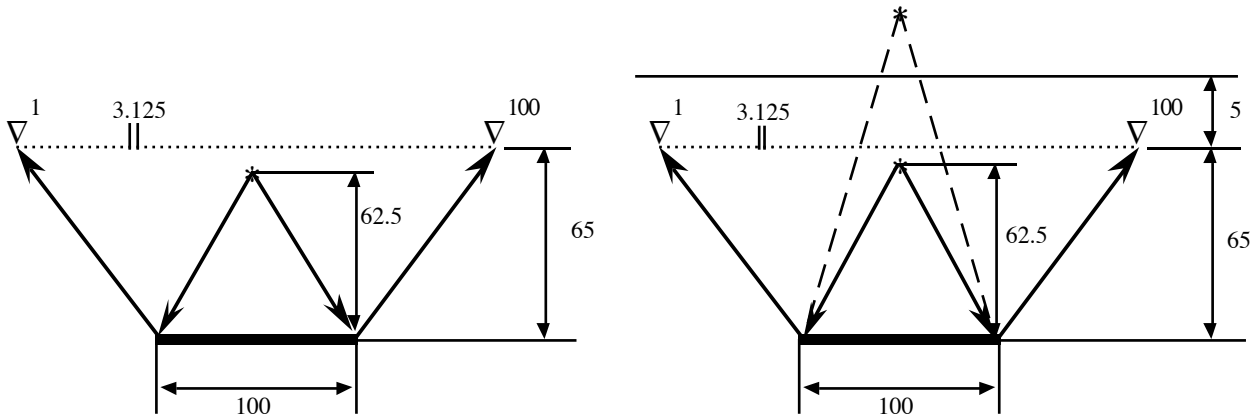

a **b**

Figure 6.1a : the scattering configuration in the unbounded medium (dimensions are in metres)

b : the scattering configuration in the bounded medium (dimensions are in metres)

In order to make a reasonable set the configuration is calculated with different source positions. The following source positions are chosen; source above the middle of the strip and successively 25,50 and 100 metres away from this middle. All these configurations are calculated for the scattered pressure field in a bounded and unbounded medium (see also Appendix B).

In this section for every configuration the bounded and unbounded situation is shown in the same figure. In order to compare the different pictures with each other, the pictures are made with a

scaling to the maximum value of the shotgather. And to show clearly the effects of the scattering configuration the same configurations are plotted with a scaling per trace. Only two kinds of configurations are shown with a scaling per trace one where the source lies above the middle of the strip and one where the source is positioned 25 away from this middle. The other calculated configurations are not shown with a scaling per trace because they give no new effects of interest for the reader. All time space pictures are made with SKS; a seismic software package.
The wavelet which is used to convolve the impulse response data with is shown in Figure 6.2.

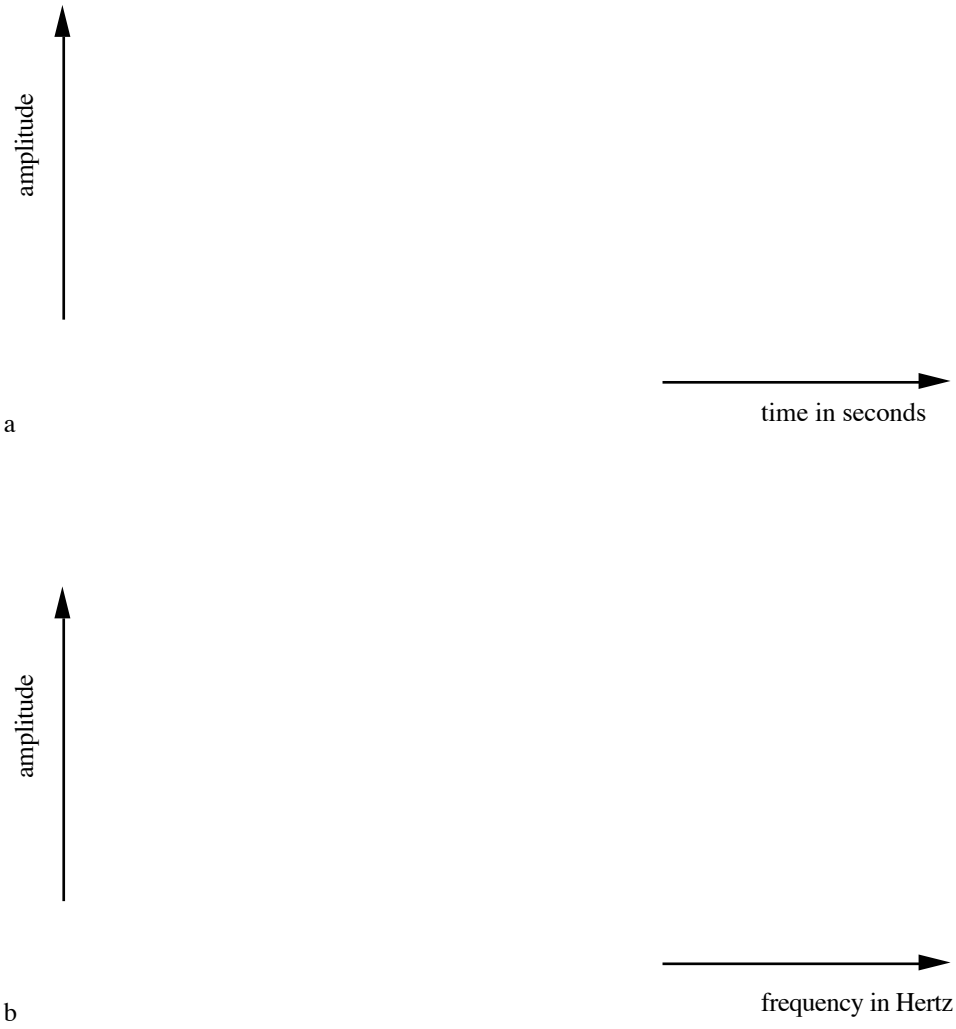

Figure 6.2a : the wavelet in the time domain

b : the amplitude spectrum of the wavelet

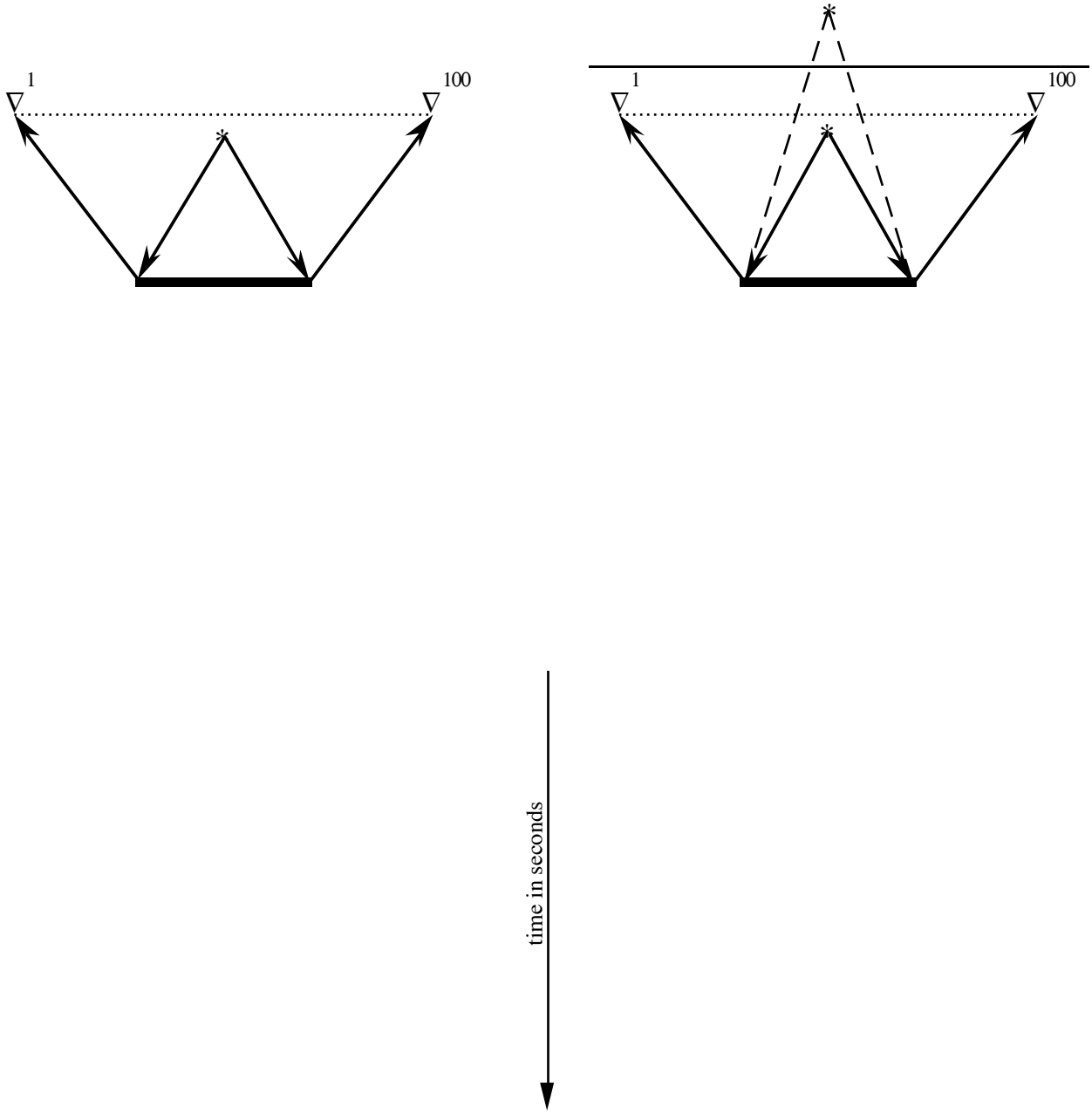

Figure 6.3 : Compliant strip in an unbounded medium (left picture) and in a bounded medium (right picture) with the source and receivers symmetrically above the strip. The scaling is to the maximum value of the shotgather.

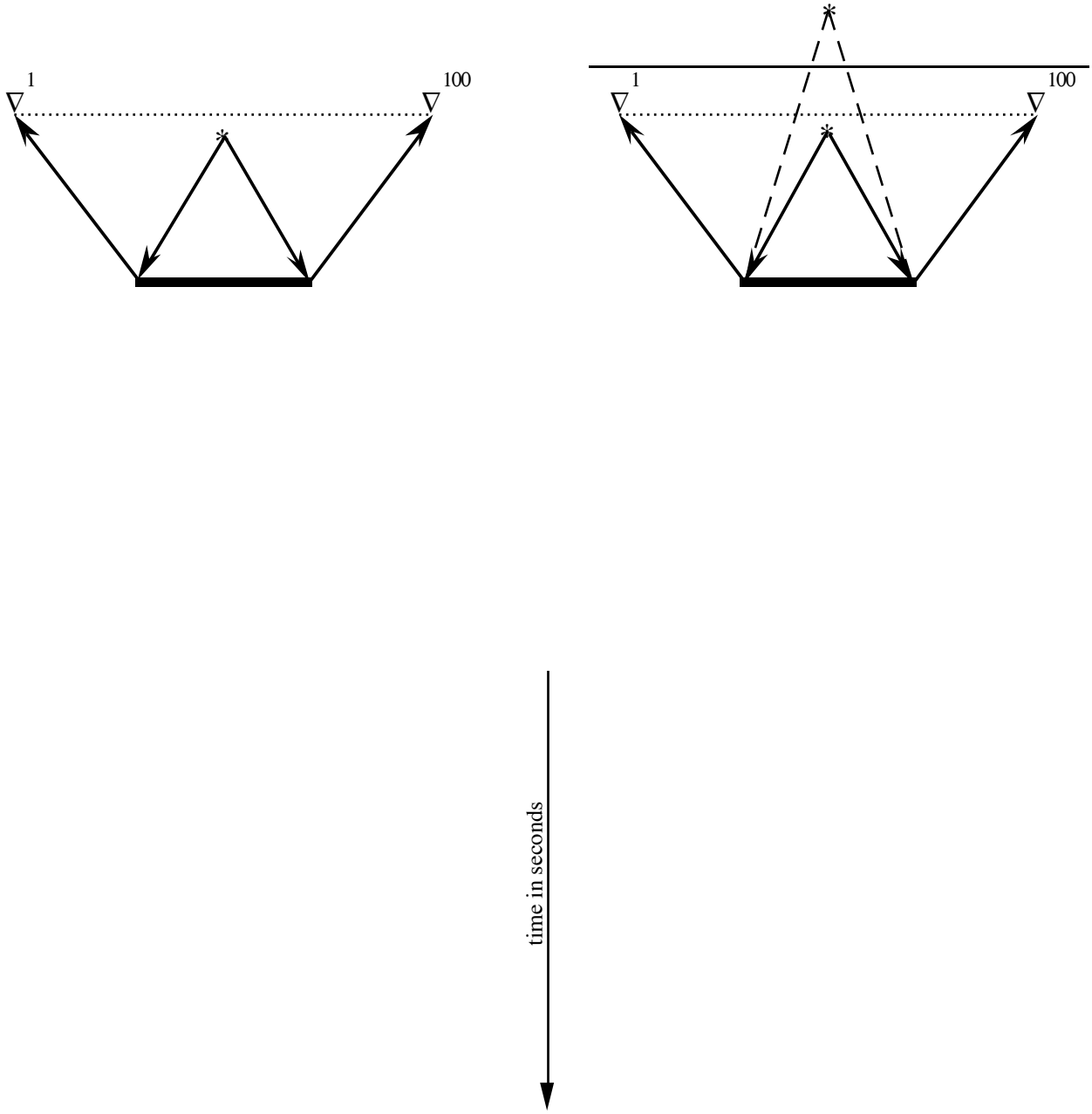

Figure 6.4 : Rigid strip in an unbounded medium (left picture) and in a bounded medium (right picture) with the source and receivers symmetrically above the strip. The scaling is to the maximum value of the shotgather.

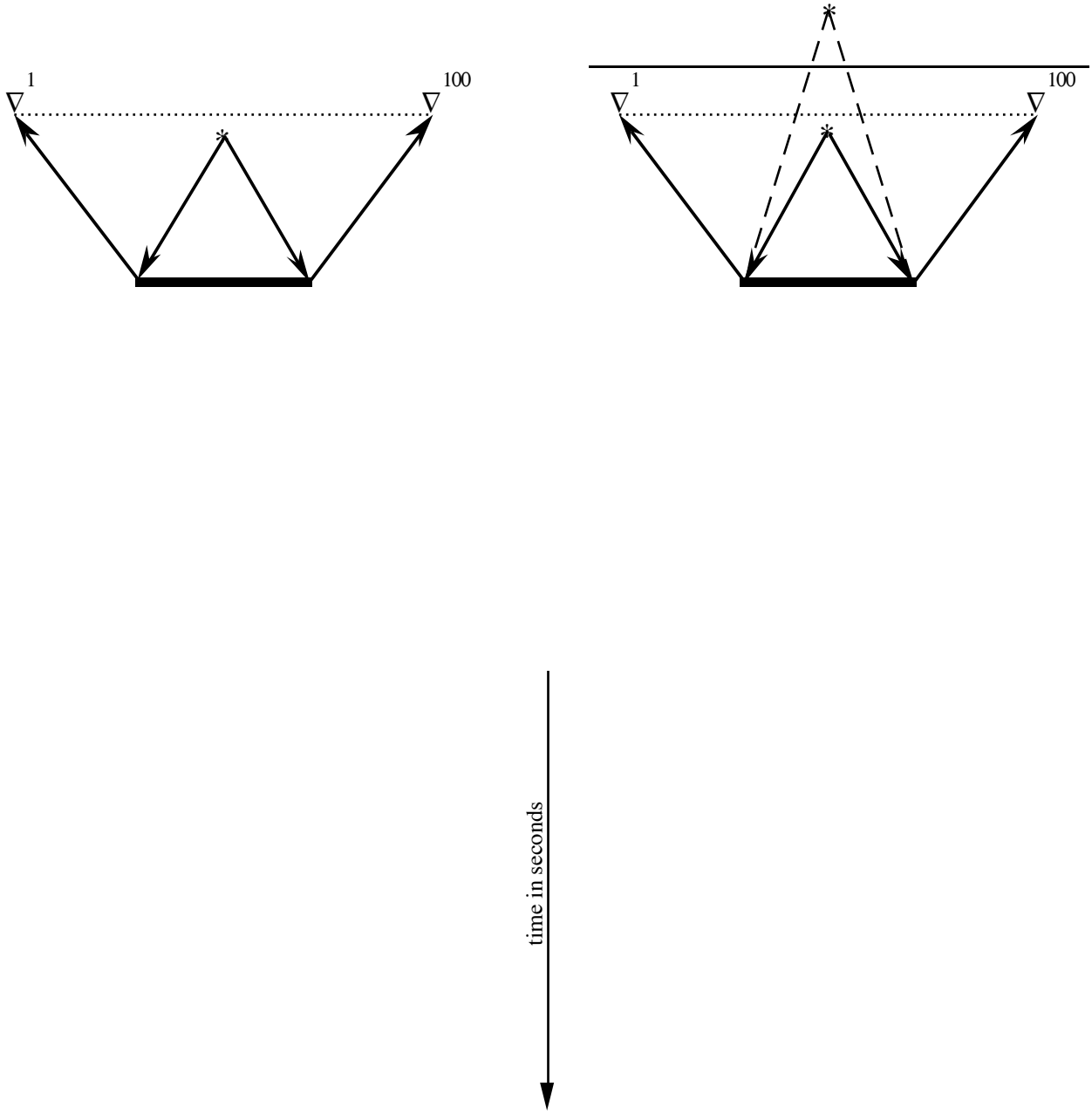

Figure 6.5 : Compliant strip in an unbounded medium (left picture) and in a bounded medium (right picture) with the source and receivers symmetrically above the strip. The scaling is done per trace.

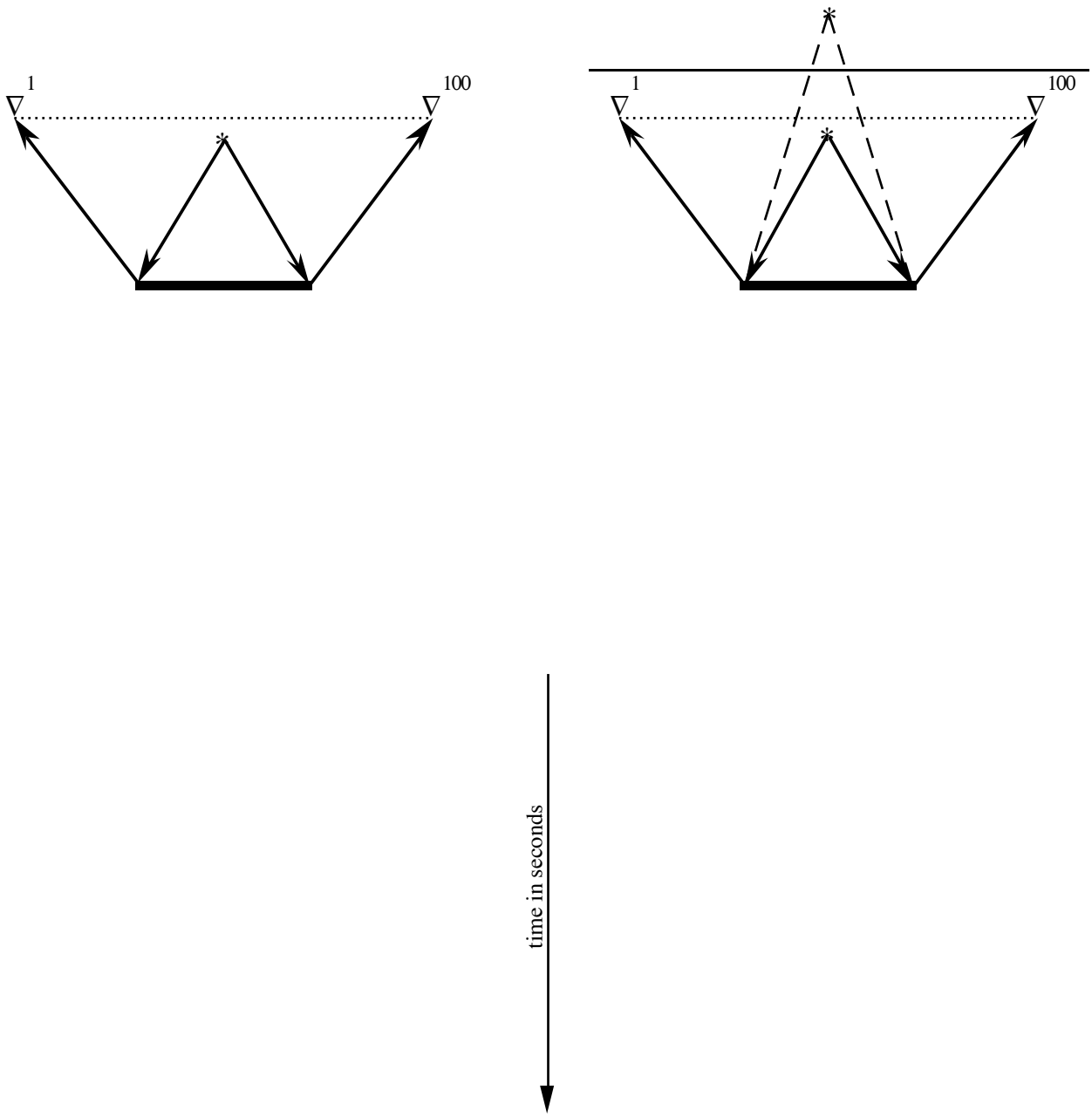

Figure 6.6 : Rigid strip in an unbounded medium (left picture) and in a bounded medium (right picture) with the source and receivers symmetrically above the strip. The scaling is done per trace.

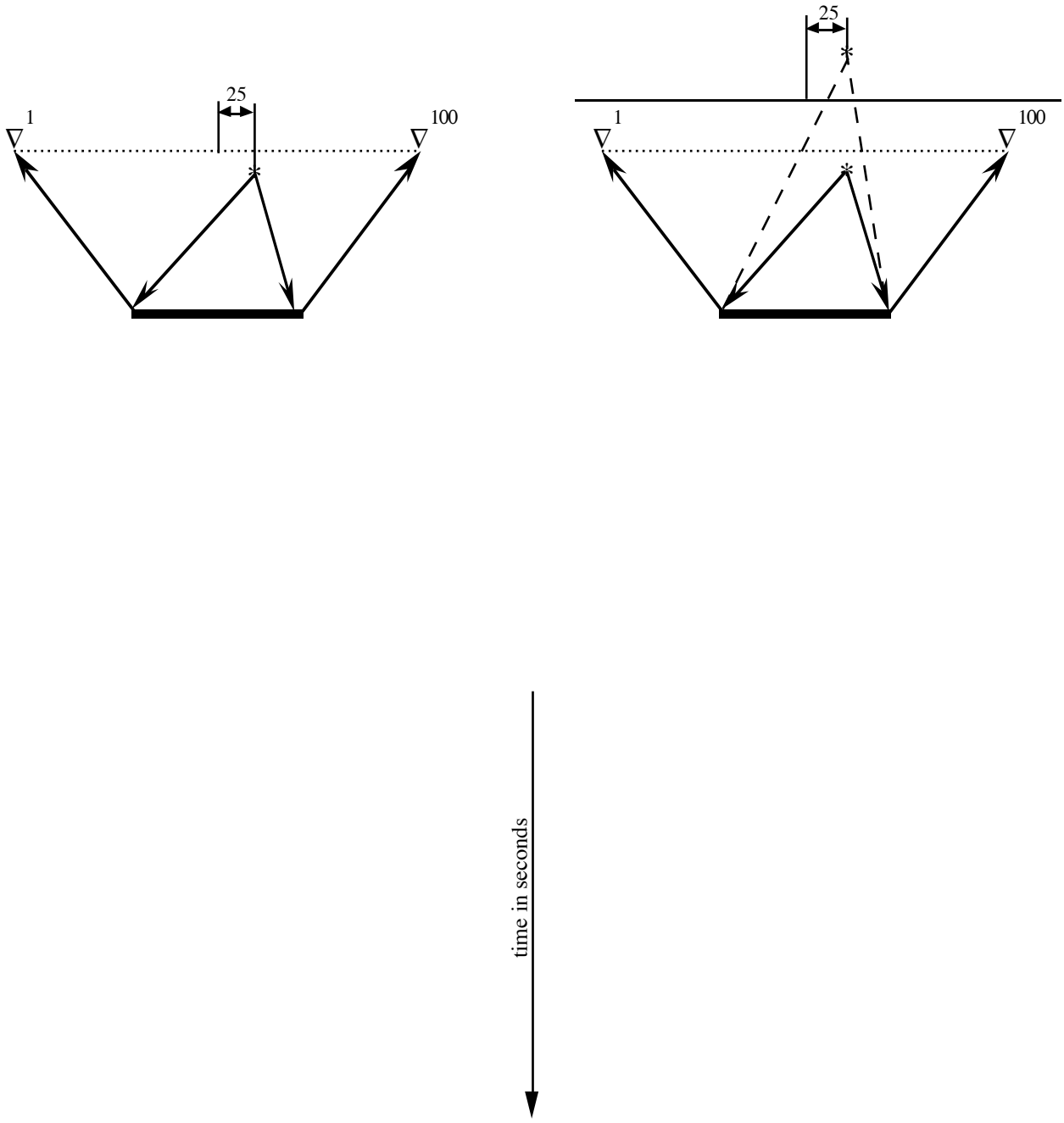

Figure 6.7 : Compliant strip in an unbounded medium (left picture) and in a bounded medium (right picture) with the source position 25 metres away from the center of the strip. The scaling is to the maximum value of the shotgather.

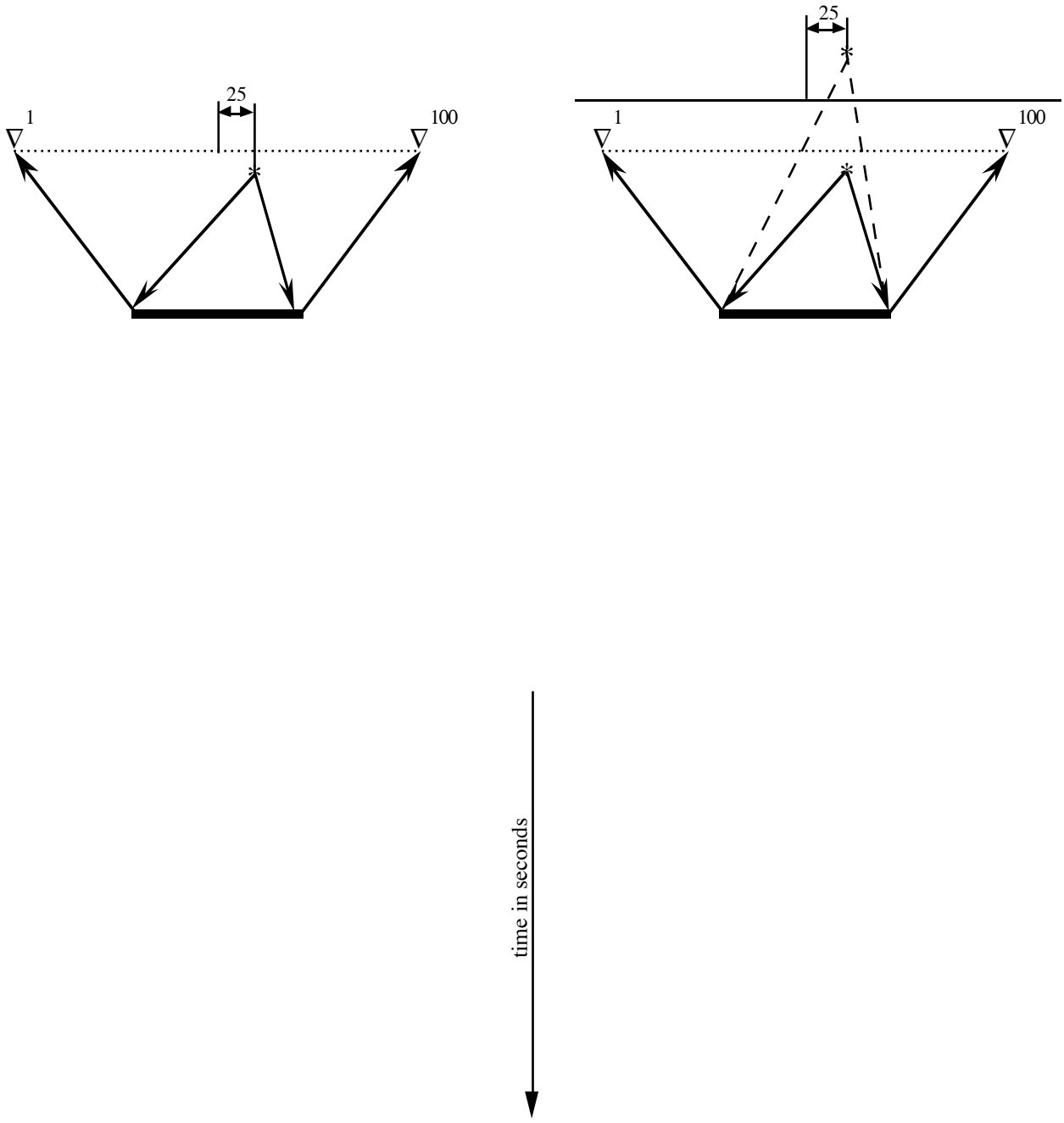

Figure 6.8 : Rigid strip in an unbounded medium (left picture) and in a bounded medium (right picture) with the source position 25 metres away from the center of the strip. The scaling is to the maximum value of the shotgather.

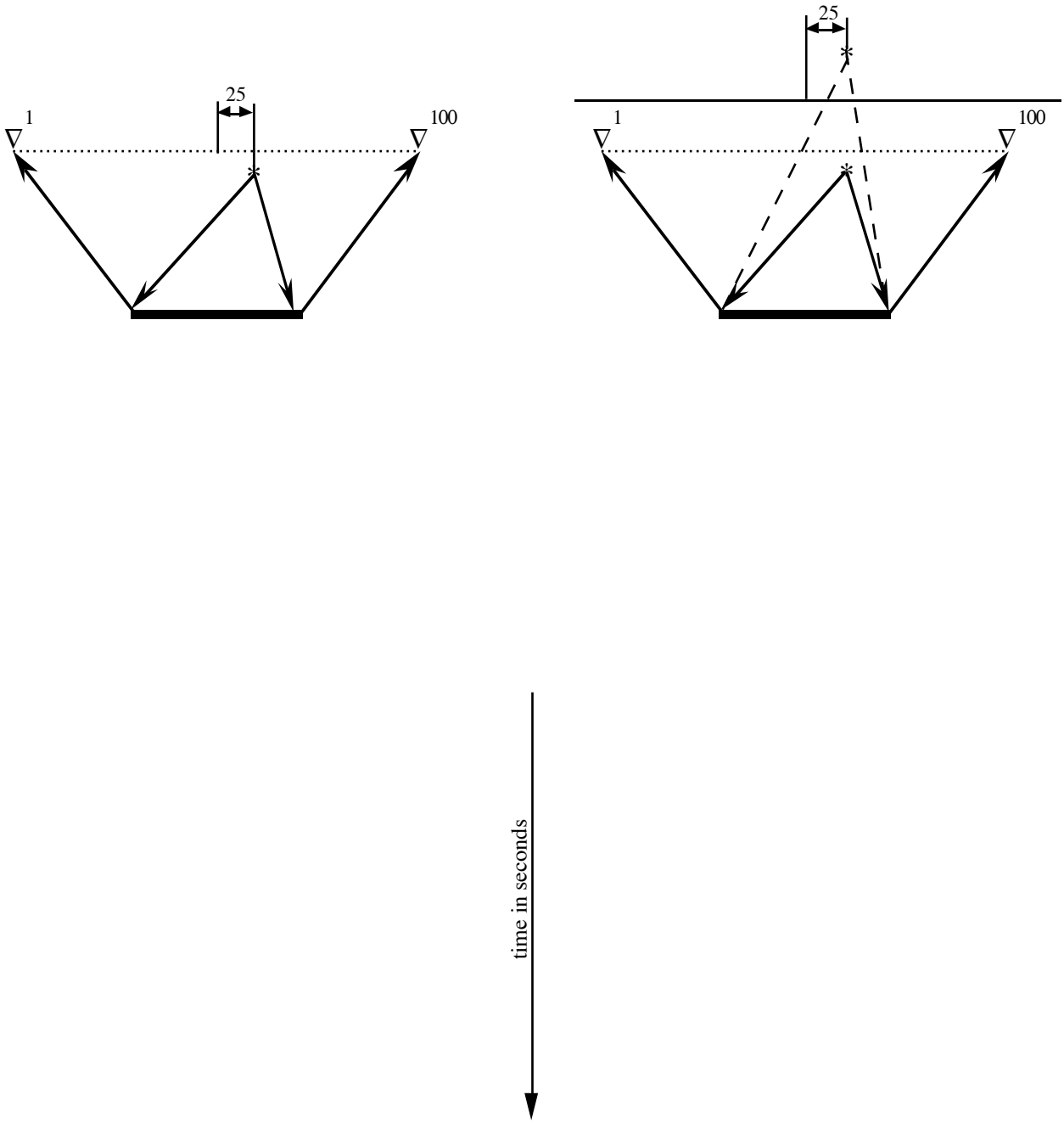

Figure 6.9 : Compliant strip in an unbounded medium (left picture) and in a bounded medium (right picture) with the source position 25 metres away from the center of the strip. The scaling is done per trace.

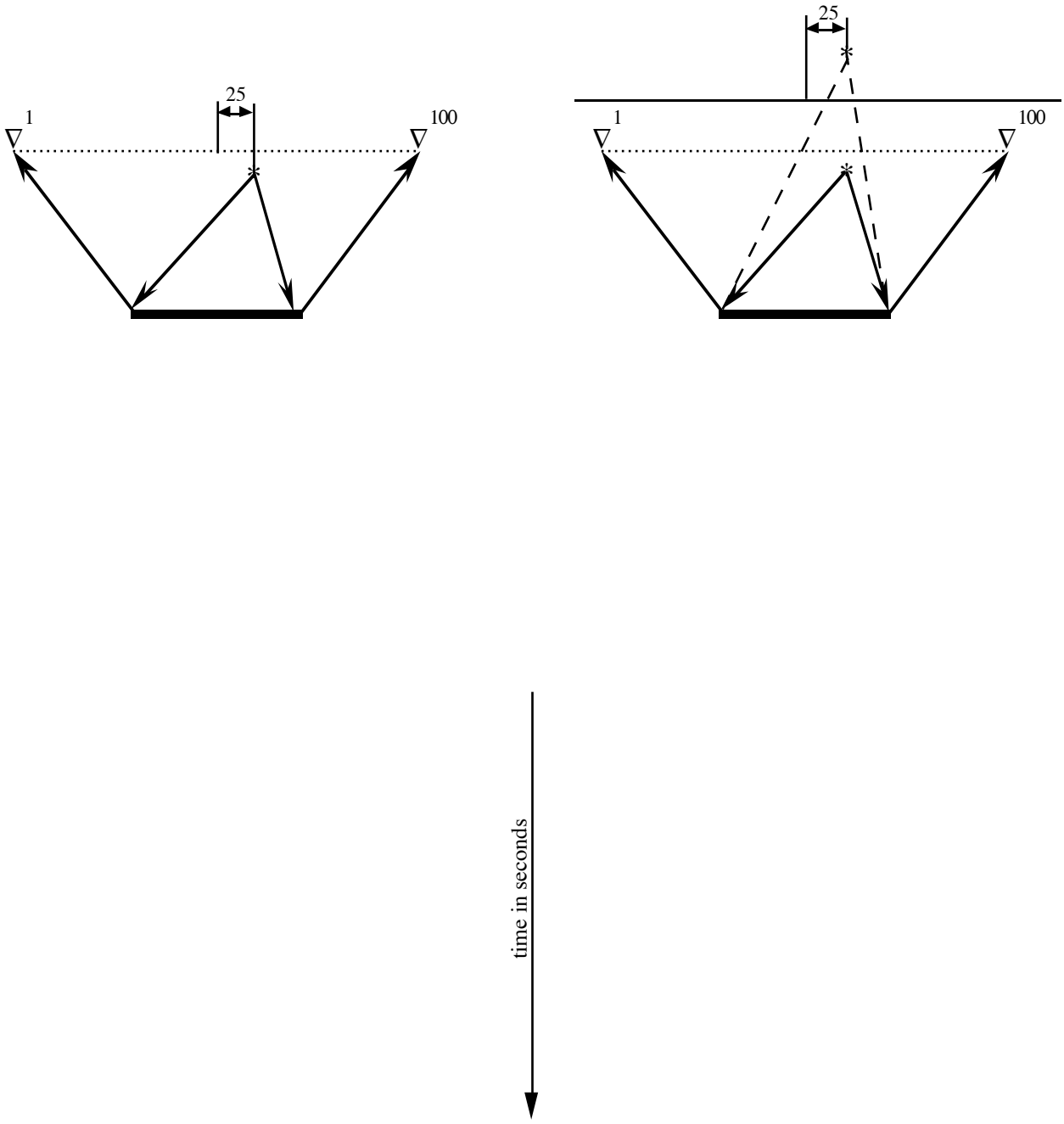

Figure 6.10 : Rigid strip in an unbounded medium (left picture) and in a bounded medium (right picture) with the source position 25 metres away from the center of the strip. The scaling is done per trace.

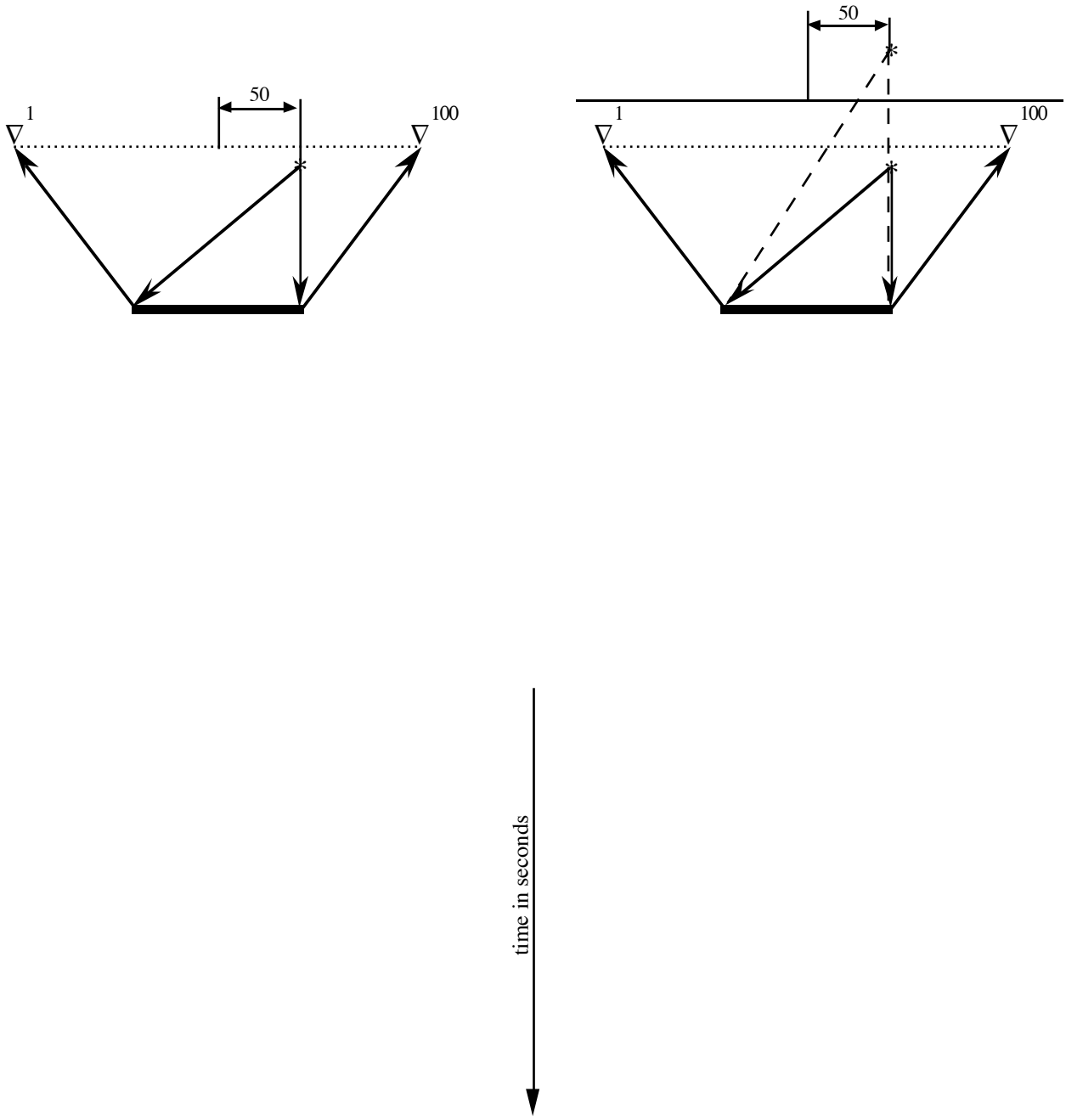

Figure 6.11 : Compliant strip in an unbounded medium (left picture) and in a bounded medium (right picture) with the source position 50 metres away from the center of the strip. The scaling is to the maximum value of the shotgather

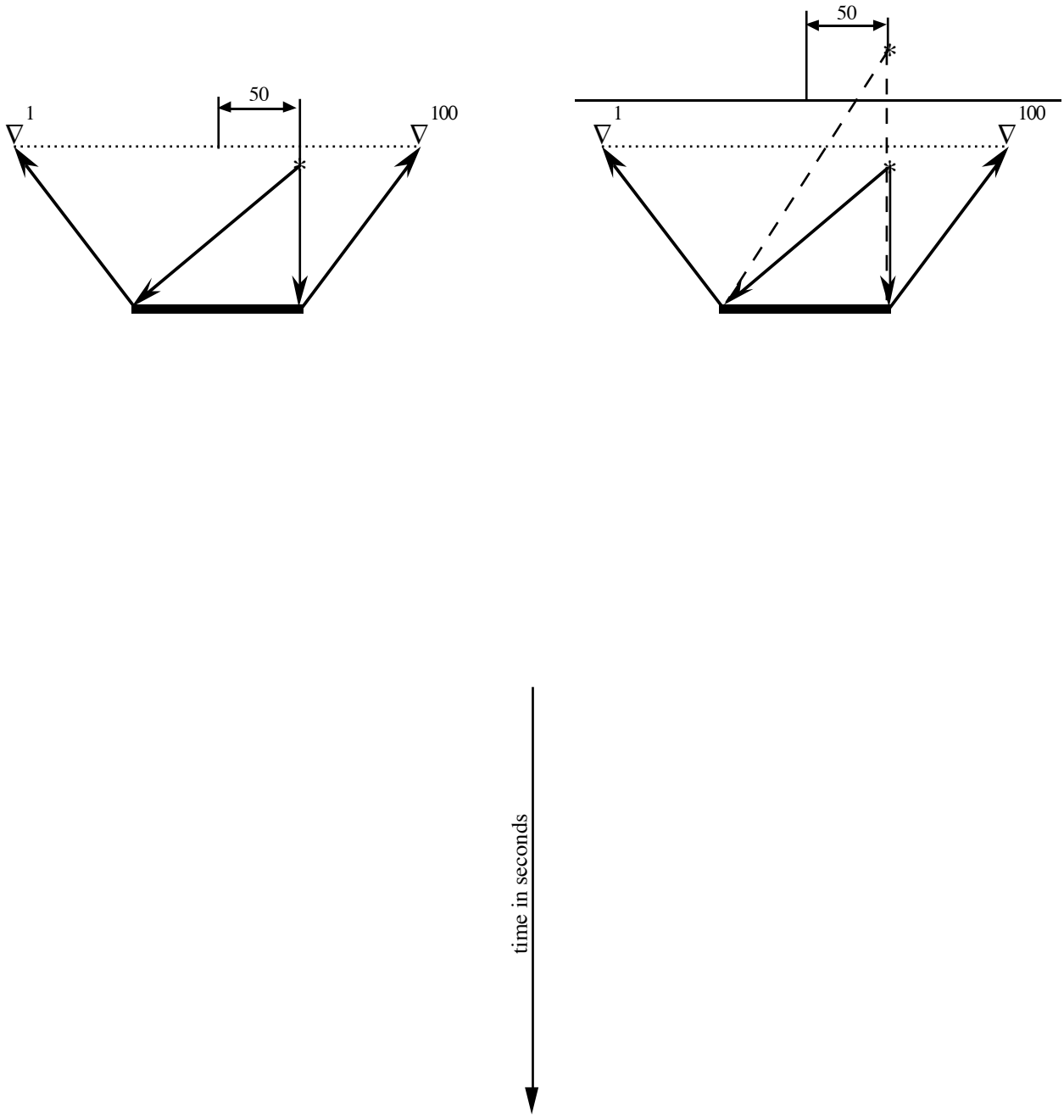

Figure 6.12 : Rigid strip in an unbounded medium (left picture) and in a bounded medium (right picture) with the source position 50 metres away from the center of the strip. The scaling is to the maximum value of the shotgather.

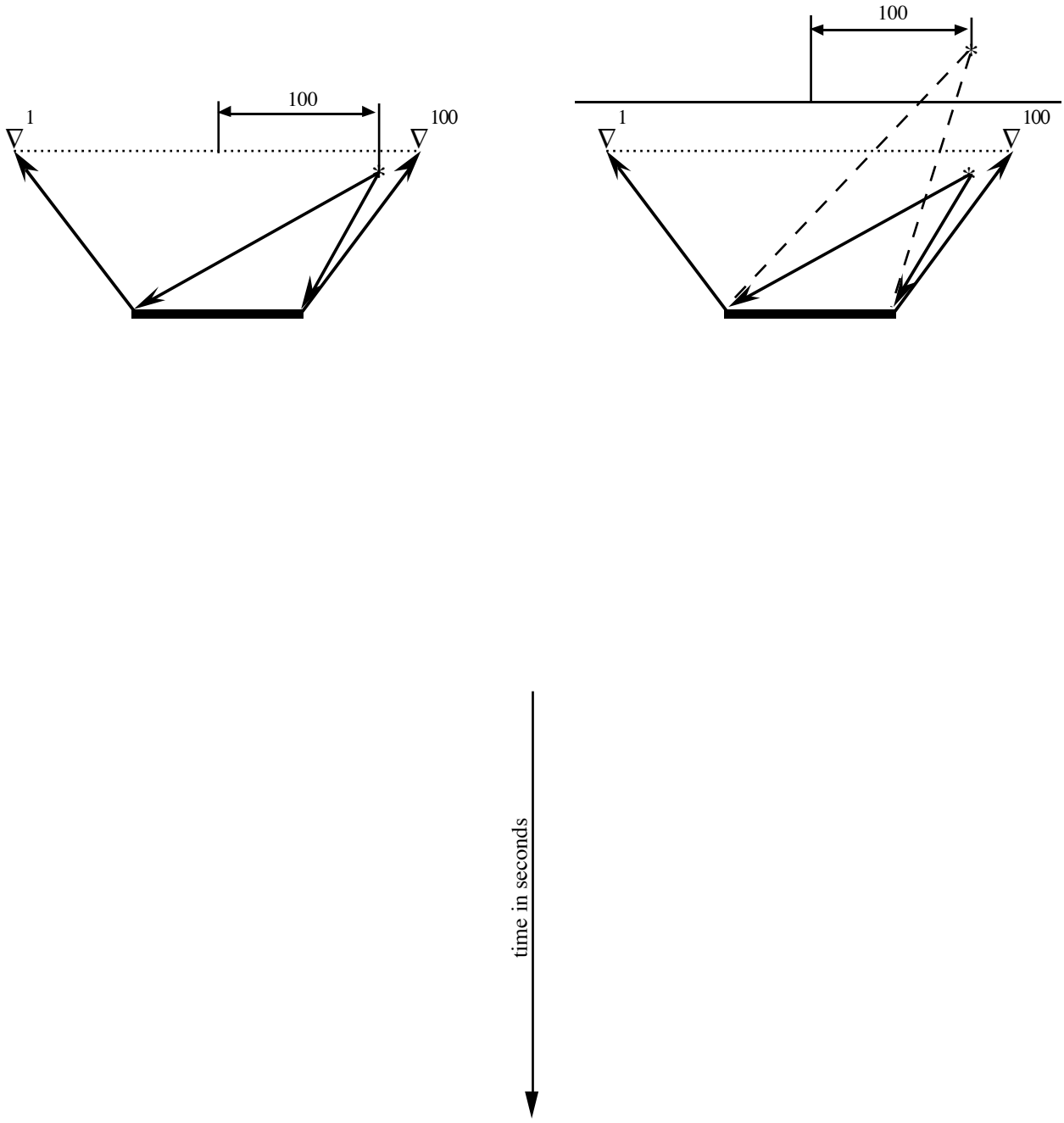

Figure 6.13 : Compliant strip in an unbounded medium (left picture) and in a bounded medium (right picture) with the source position 100 metres away from the center of the strip. The scaling is to the maximum value of the shotgather

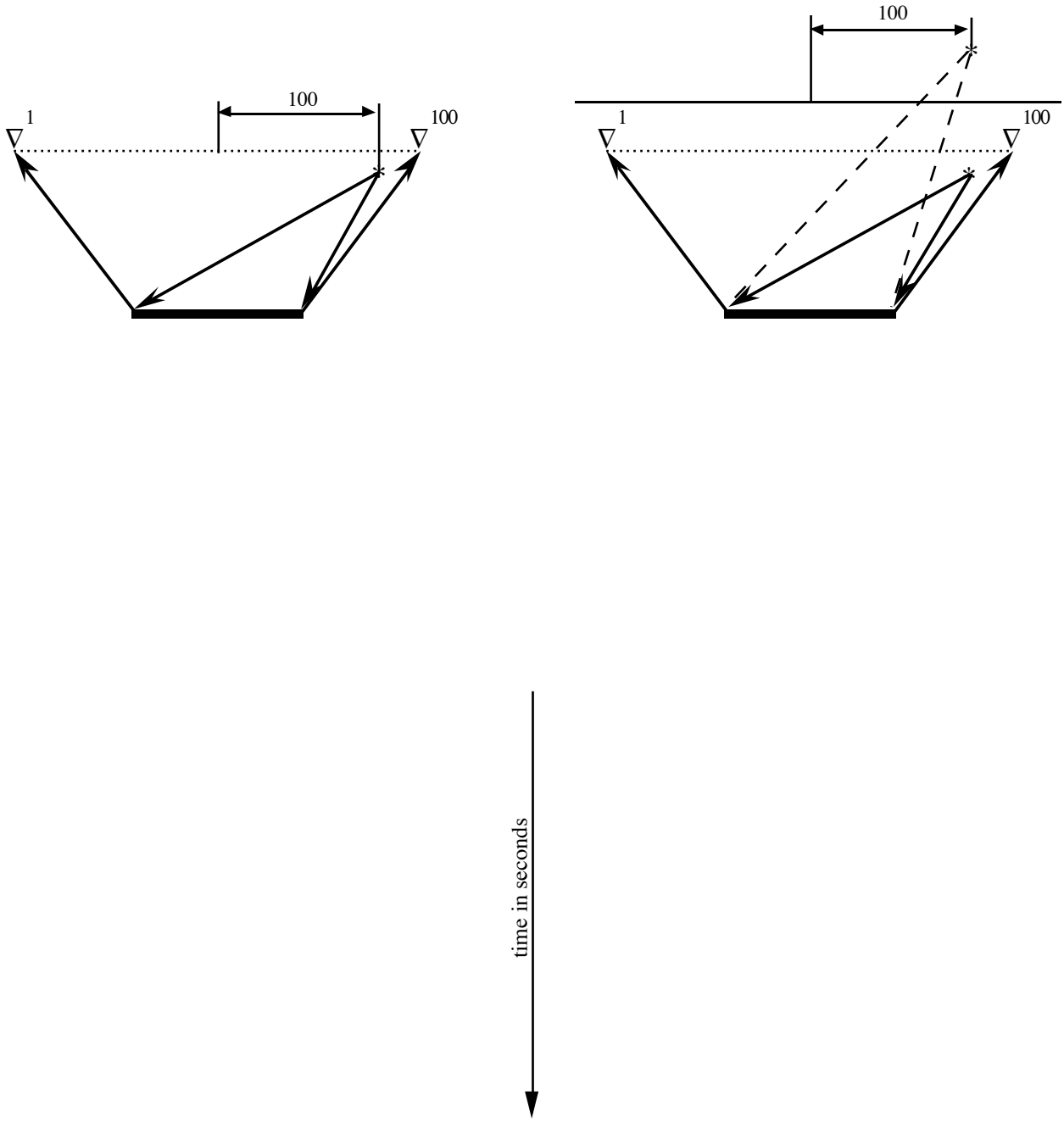

Figure 6.14 : Rigid strip in an unbounded medium (left picture) and in a bounded medium (right picture) with the source position 100 metres away from the center of the strip. The scaling is to the maximum value of the shotgather.

The pictures show clearly the effects of the influence of the halfspace; the multiples and the ghost. They also show the end points of the strip, which are appear as diffraction curves. These diffraction curves are most clearly present in the pictures which are scaled per trace (Figure 6.5,Figure 6.6,Figure 6.9 and Figure 6.10). In the other pictures the diffraction curves of the end points can, with a little effort, also be recognized.

For the rigid strip the end points really serve as point diffracters and can be considered as line sources radiating in the medium. For a compliant strip the end points do not have such a strong effect (which can be seen by comparing the compliant figure with its rigid counterpart). This observation can be explained by the fact that the compliant strip moves along with the incident field. The rigid strip does not move with the incident field and therefore diffracts most of the energy.

6.2 RELIABILITY OF THE RESULTS

Testing the data set is important because it serves as a reference set for the surface multiple removal program, which is at this moment in development. The reliability of the implemented scattering theory, described in the other chapters, can be tested on several aspects of the scattering problem.

Arrival times and the 'shape' of the picture can be used to see of the 'overall' solution is correct. These and related aspect are threaded in the first paragraph of this section. In the second paragraph the numerical Green's function is compared with the analytical Green's function. In the third paragraph the solution of an infinite long compliant strip is compared with the analytical result which is given by the Green's function. The considered aspects in these three paragraph's are necessary for the results to be proper, but they are not sufficient. Nevertheless they may be convincing enough for the reader to have at least a little confidence in the results.

6.2.1 Arrival times and point diffractors

All the pictures in this paragraph are calculated with a discrete time sampling of 2 ms and with 100 receiver positions split-spread positioned around the middle of the strip. The distance between the receivers is in all pictures 3 metres. The field on the strip is itteratively calculated on 99 points.

Figure 6.15 is the scattered pressure field of a rigid strip of 120 metres in an unbounded medium The source positions is 20 metres above the middle of the strip and the receivers are positioned 10 metres above the strip. In this picture the endpoints of the strip can clearly be seen as point diffractors, which is as expected. The symmetrical shape of the picture reflects the chosen symmetrical configuration. The arrival time of the first arrival is, 30 divided by the velocity of the medium, 0.021 ms. So for this simple picture it can be said that the arrival times and point diffractors are correct.

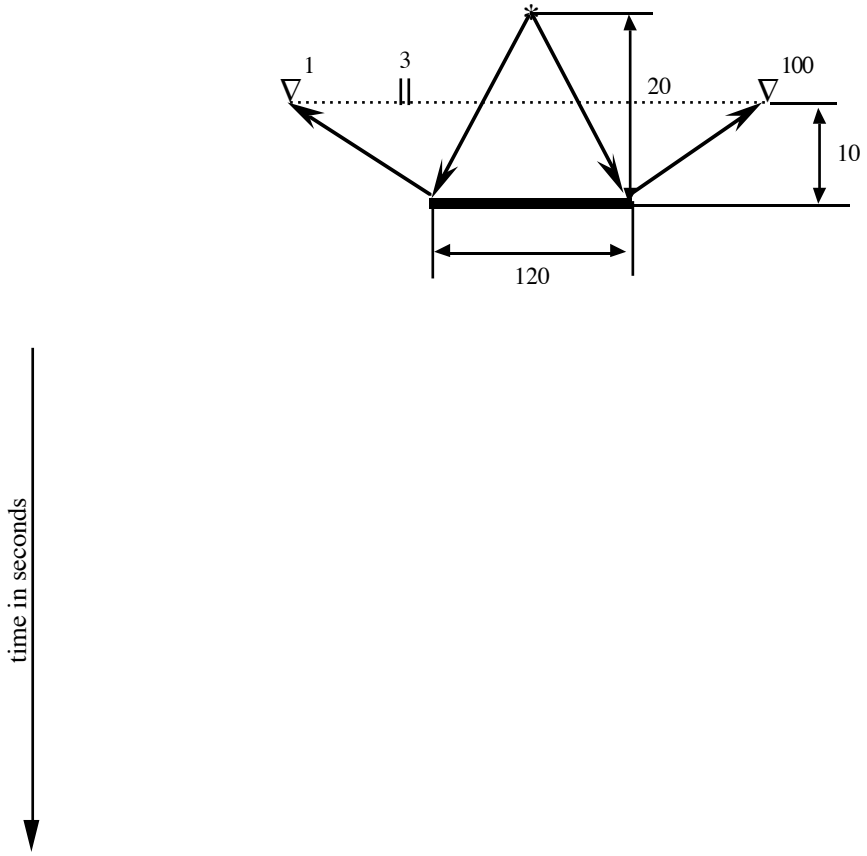

Figure 6.15 : Rigid strip in an unbounded medium with the source position 20 metres above the center of the strip. The scattered pressure field is scaled per trace.

The effects of the halfspace can be seen in the occurrence of multiples. To see this clearly the source, strip and receiver position are chosen close to the surface. In this way most of the energy is trapped between the surface and the strip. In Figure 6.16 the strip is positioned 10 metres below the surface and is 180 metres long. The source is positioned 5 metres above the middle of the strip and the receivers are 8 metres below the surface. The arrival times for the scattered field, the ghost and the multiples are shown in Table 6.1 for the receiver above the middle of the strip.

Arrival	Distance [m]	Time [ms]
First	7	5
ghost	17	12
Multiple 1	37	25
Multiple 2	57	39
Multiple 3	77	53
Multiple 4	97	67

Table 6.1 : The first six arrival times of Figure 6.16

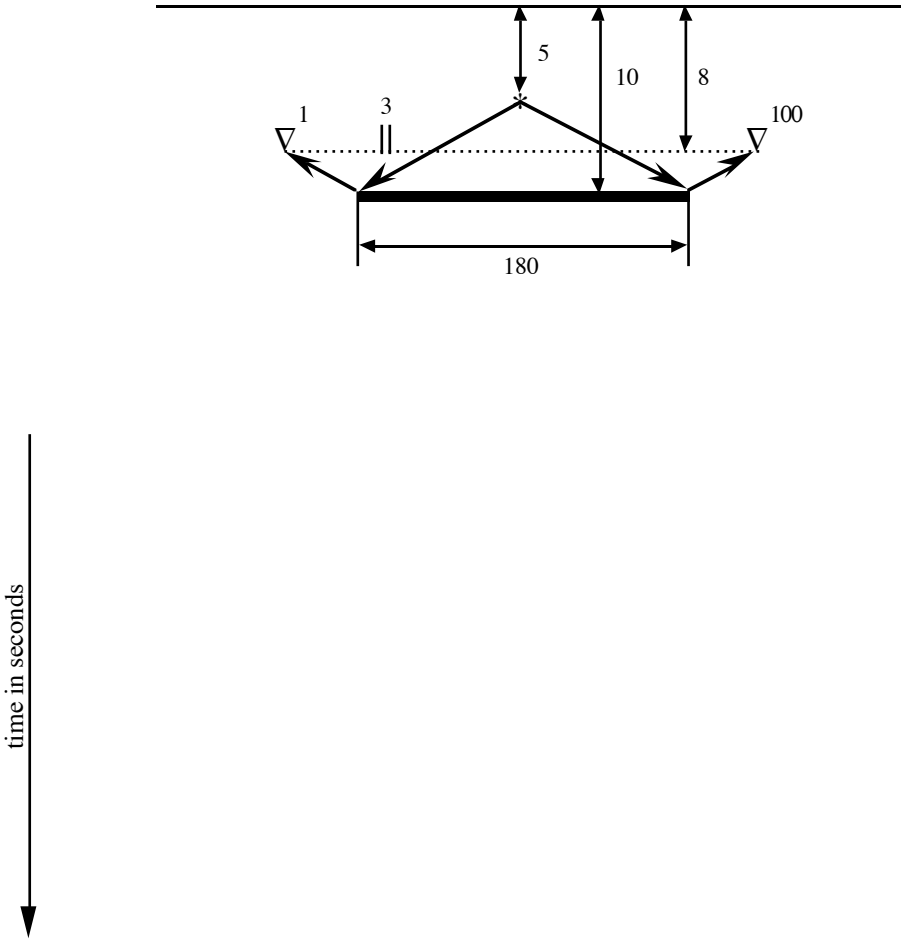

Figure 6.16 : Scattered pressure field for a rigid strip in a bounded medium with the source position 5 metres above the center of the strip, the strip 10 metres below the surface and the receivers 8 metres below the surface.The field is scaled per trace.

The last figure in this paragraph, Figure 6.17, is a configuration where the source is 250 metres away from the middle of the strip and 90 metres below the surface. The receivers are 100 metres below the surface and the strip, of length 120, 150 metres below the surface. In this strange looking picture the point diffractors and the ghost, which has switched polarity due to the reflection coefficient of -1 of the surface, can bee seen clearly.

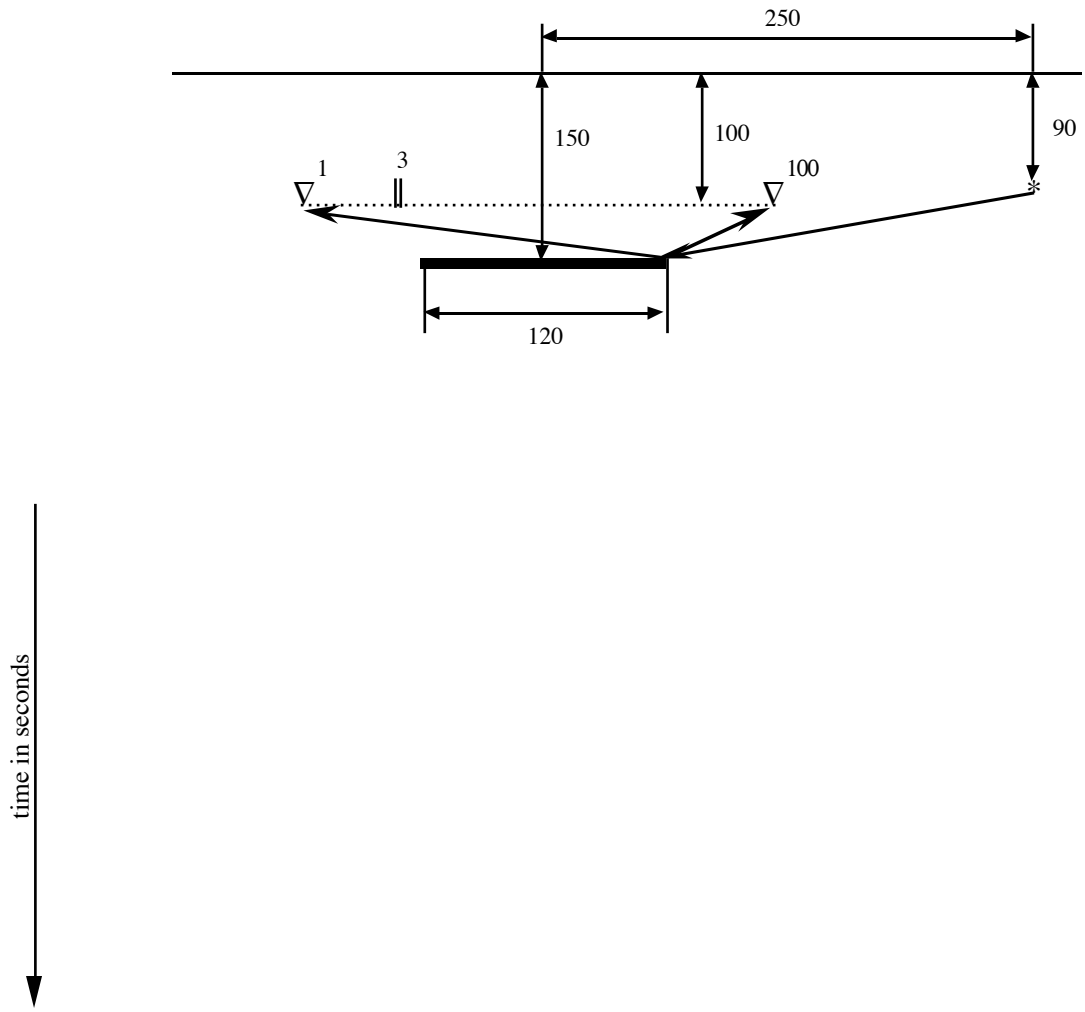

Figure 6.17 : Rigid strip in a bounded medium with the source position 90 metres below the surface and 250 metres away from the middle of the strip. The strip 150 metres below the surface and the receivers 100 metres below the surface. The scattered pressure field is scaled per trace.

6.2.2 The numerical Green's function

As described in the theoretical chapters; the Green's function is calculated in the wave number frequency domain where the wave number was made complex in order to avoid the pole / branch point,.in the expression of the Green's function, in the backtransform to time-space. It was necessary to know the Green's function in the wavenumber frequency domain in order to make use of the preconditioning operator in the itterative scheme. A.T. de Hoop has calculated the exact solution for the 2-dimensional Green's function.by using a Cagniard de Hoop contour in the backtransform from wavenumber frequency to space time domain (de Hoop, 1960). The result of this calculation is shown in equation (6.2-1)

$$u(x,y,t) = \frac{1}{2\pi}\int_{\frac{r}{v}}^{t} f(t-\tau)\left(\tau^2 - \frac{r^2}{v^2}\right)^{-\frac{1}{2}} d\tau \qquad \left(\frac{r}{v} < t < \infty\right)$$
$$= 0 \qquad \left(0 < t < \frac{r}{v}\right). \tag{6.2-1}$$

In equation (6.2-1) f(t) is the source function. If the source function is chosen to be the Delta function then the function u(x,y,t) is the Green's function in the time space domain. So

$$g(x,y,t) = \frac{1}{2\pi}\left(t^2 - \frac{r^2}{v^2}\right)^{-\frac{1}{2}} \tag{6.2-2}$$

is a representation for the Green's function in an unbounded medium. This Green's function is compared with the Green's function calculated numerically. The comparison is done for three different offsets. The numerically Green's function is calculated with a spatial interval of 0.5 metres, a complex part of 0.01, a time sampling of 1 ms and in the Fourier transformations 1024 points are calculated. The source position is 2.5 metres below the receivers and the horizontal offsets under consideration are 0, 25 and 50 metres. Figure 6.18 shows a comparison between the analytically Green's function and the numerical Green's function for zero offset. Figure 6.19 shows both the Green's functions convolved with the wavelet of Figure 6.2 .Figure 6.20 and Figure 6.21 show the Green's function with an offset of 25 metres and Figure 6.22 and Figure 6.23 with an offset of 50 metres. Figure 6.24 shows the Green's function with a vertical offset of 2 and 25 metres and Figure 6.25 shows the Green's function with a vertical offset of 50 and 100 metres.

Figure 6.18 : above; the analytical Green's function with offset 0
below; the numerical Green's function with offset 0

Figure 6.19 : above; the analytical Green's function with offset 0 convolved with a wavelet
below; the numerical Green's function with offset 0 convolved with a wavelet

Figure 6.20 : above; the analytical Green's function with offset 25
below; the numerical Green's function with offset 25

Figure 6.21 : above; the analytical Green's function with offset 25 convolved with a wavelet
below; the numerical Green's function with offset 25 convolved with a wavelet

Figure 6.22 : above; the analytical Green's function with offset 50
below; the numerical Green's function with offset 50

Figure 6.23 : above; the analytical Green's function with offset 50 convolved with a wavelet
below; the numerical Green's function with offset 50 convolved with a wavelet

Figure 6.24 : above; the analytical Green's function with a vertical distance of 2 metres
below; the numerical Green's function with a vertical distance of 25 metres

Figure 6.25 : above; the analytical Green's function with a vertical distance of 50 metres
below; the numerical Green's function with a vertical distance of 100 metres

Comparing the analytical Green's function and the numerical Green's function it can be seen that the shape of the numerical Green's function remains for all offsets the same while the analytical one becomes less steeper at larger offsets. This difference can be explained by the fact that the numerical Green's function is calculated with only a complex wavenumber, the contour existing of a line above the real axis. This is wrong because the contour should be a different Cagniard de Hoop contour for every different wavenumber. Despite of this the numerical results are not so bad that they are useless. Physically the difference means that the numerical Green's function damps out quicker than the analytical one.

In order to be complete the numerical Green's function in the bounded medium is given in the next three figures. The same offsets as in the previous pictures are used. Figure 6.26 shows the Green's function and the Green's function convolved with the wavelet, with zero offset , Figure 6.27 with an offset of 25 metres and Figure 6.28 with an offset of 50 metres. In these pictures it can be seen that in a marine configuration the ghost arrives quickly after the first arrival. The numerical Green's function has for further offsets a higher noise content.This noise is high frequent and dissapears when the Green's function is convolved with the wavelet.

Figure 6.26 : above; the numerical Green's function with offset 0
below; the numerical Green's function with offset 0 convolved with a wavelet

Figure 6.27 : above; the numerical Green's function with offset 25
below; the numerical Green's function with offset 25 convolved with a wavelet

Figure 6.28 : above; the numerical Green's function with offset 50
below; the numerical Green's function with offset 50 convolved with a wavelet

6.2.3 The infinite compliant strip

By taking the lenght of the compliant strip infinite long the resulting field must be equal to the Green's function in the halfspace. Making the strip infinite long means in the computer that the number of samples on the strip is equal to the number of samples in the Fourier transform. Because of the periodicity of the discrete Fourier transform is in this case the strip infinitely long. In calculating the scattered field the number of iteration steps must be one, because the scattered field is now obtained by direct deconvolution. Direct deconvolution was not possible in the case where the number of samples on the strip was not equal to the number of samples in the Fourier transform because outside the strip interval the field is in that case not known.

So a first check for the numerical procedure was that the number of iteration steps is one in the case of an infinite long strip. This was indeed the case. A further check on the program was to compare the result of the infinite long strip with the Green's function in a halfspace. The result for the infinite compliant strip is shown in Figure 6.29 in this figure both the direct field and the totally reflected field are present. In Figure 6.30 the Green's function in the halfspace is shown (which is the direct field plus the ghost). Omitting the direct field in the resulting pictures gives in the case of the infinite strip the totally reflected field and for the Green's function only the ghost. In Figures 6.31 and 6.32 the comparision between these two results can be made.

By comparing the resulting pictures it can be concluded that the arrival times are identical, which was aspected because in both cases the configuration was chosen the same. Only the amplitude for the infinite compliant strip case is slightly less (in the order of 1%) than the amplitude for the Green's function. This could be explained by the fact that for the infinite strip the resulting field *on* the strip is obtained by direct deconvolution in the itterative procedure. This field *on* the strip is lineair interpolated for the receiver positions and then in the wavenumber domain multiplied with the Green's function in order to obtain the resulting field at the receivers. For the Green's function the results is obtained by direct calculation in the wavenumber frequency domain and no interpolation is needed.

Figure 6.29 : The infinite long compliant strip (totally reflected field plus direct field)

Figure 6.30 *:* The Green's function in a halfspace (ghost plus direct field)

Figure 6.31 : The infinite long compliant strip (only totally reflected field)

Figure 6.32 *:* The Green's function in a halfspace (only ghost)

References

Abramowitz, M. and Stegun, I.A., 1970, - *Handbook of mathematical functions*, Dover Publications Inc., New York.

Berg van den, P.M. , 1989, - *Iterative schemes based on minimization of a uniform error criterion*, notes, Department of Electrical Engineering, TU Delft.

Bracewell, R.N., 1978, - *The Fourier transform and it's applications,* MacGraw-Hill Book Company, New York.

Fokkema, J.T. and Berg, van den, P.M., 1990, - *Removal of surface related wave phenomena: the marine case*, submitted for publication, TU Delft.

Greenberg, M.D., 1971, - *Application of Green's functions in science and engineering*, Prentice-Hall Inc., New Jersey.

Hoop de, A.T., 1988, - *Radiation and scattering of acoustic waves in fluids,* Lecture notes A76, Department of Electrical Engineering, TU Delft.

Hoop de, A.T., 1960, - *A modification of Cagniard's method for solving seismic pulse problems*, Applied Scientific Research, Section B Vol. **8**, 349-356.

Morse, P.M. and Feshbach H., 1953, - *Methods of theoretical physics,* Part 1, MacGraw-Hill Book Company, New York.

Morse, P.M. and Ingard, K.U., 1968, - *Theoretical acoustics*, MacGraw-Hill Book Company, New York.

Ottes, W., 1987, - *Calculation of the acoustic wavefield emitted by a point source of volume injection in a cylindrical configuration,* M. Sc. Thesis, Department of Mining and Petroleum Engineering, TU Delft.

Skudrzyk, E., 1971, - *The foundation of acoustics,* Springer Verlag, Wien.

Spiegel, M.R., 1964, - *Complex variables*, MacGraw-Hill Book Company, New York.

Tan, T.H., 1975, - *Diffraction theory for time-harmonic elastic waves,*
Ph. D. Thesis, Faculty of Electromagnetic Research, TU Delft.

Appendix A

ERRORS IN THE DFT

Changing a continuous integral to a discrete summation,which is done in a DFT, an error is made. The error of the trapezoidal rule can be calculated and is given by

$$\int_a^b F(x)\,dx = \Delta x\left[\frac{F_0}{2} + \frac{F_N}{2} + \sum_{n=1}^{N-1} F_n\right] - \frac{1}{12}\Delta x^3 \sum_{n=1}^{N-1} F_n'' + \tilde{O}\left(\Delta x^4\right) \tag{A-1}$$

Comparing equation (A-1) with equation (5.3-15), the DFT, the error made in the DFT can be expressed.
The DFT of a signal gives

$$\tilde{X}(k) = \Delta x \sum_{m=\frac{-N}{2}}^{\frac{+N}{2}-1} X_m \exp\left(-jnm\Delta xk\right) \tag{A-2}$$

The trapezoidal rule of the integral of the Fourier transform gives

$$\tilde{X}(k) = \Delta x \sum_{m=\frac{-N}{2}}^{\frac{+N}{2}-1} X_m \exp\left(-jnm\Delta xk\right) - \frac{\Delta x}{2}\left(X_{\frac{-N}{2}} + X_{\frac{N}{2}-1}\right) + \text{ERROR} \tag{A-3}$$

Comparing equation (A-2) with equation (A-3) there are two kinds of error appearing, one at the end and beginning of the sample points and one due to the linear interpolation of the trapezoidal rule. If X is a bounded function in space then the error in the wavenumber domain must contain the aliased spectrum.

In order to investigate only the aliased spectrum, the summations are running from minus infinity to infinity. The error at the endpoints is then vanishing. Analogous to the discrete wavenumber function (equation (5.3-8)) the discrete space function can be derived

$$X_m = \int_{\frac{-1}{2\Delta x}}^{\frac{1}{2\Delta x}} \sum_{m=-\infty}^{+\infty} \widetilde{X}\left(k + \frac{m}{\Delta x}\right) \exp(jm\Delta x k)\, dk \tag{A-4}$$

in which

$$\widetilde{X}^a(k) = \sum_{m=-\infty}^{+\infty} \widetilde{X}\left(k + \frac{m}{\Delta x}\right) \quad \text{periodic function} \tag{A-5}$$

The periodic function in the wavenumber domain can be expanded in a Fourier series. The Fourier series coefficients of a periodic function are given by

$$\widetilde{X}^a(k) = \sum_{m=-\infty}^{+\infty} a_m \exp(-jm\Delta x k) \tag{A-6}$$

$$a_m = \Delta x \int_{\frac{-1}{2\Delta x}}^{\frac{1}{2\Delta x}} \widetilde{X}^a(k) \exp(jm\Delta x k)\, dk \tag{A-7}$$

Equation (A-7) is equal to equation (A-4), where the summation formula of Poisson is used
The summation formula of Poisson is given by

$$\sum_{m=-\infty}^{+\infty} \widetilde{X}\left(\frac{m}{\Delta x}\right) = \Delta x \sum_{m=-\infty}^{+\infty} \widetilde{X}_m \tag{A-8}$$

so equation (A-6) becomes

$$\widetilde{X}^a(k) = \Delta x \sum_{m=-\infty}^{+\infty} X_m \exp(-jm\Delta x k) \tag{A-9}$$

The integral of the continuous Fourier transform is the exact expression (equation (5.3-1)). The summation of equation (A-9) is the expression which is given by the DFT .The difference between these equations is the error which represents the aliased spectrum. So the error is given by equation (A-9) minus equation (5.3-1)

$$\text{error} = \widetilde{X}^{a}(k) - \widetilde{X}(k) \tag{A-10}$$

The error can be approximated by using a Taylor expansion around the origin.

$$\text{ERROR} = \sum_{n=0}^{+\infty} \frac{k^n}{n!} \frac{\partial^n}{\partial k^n} \left[\widetilde{X}^{a}(k) - \widetilde{X}(k) \right] \tag{A-11}$$

$$\frac{\partial^n}{\partial k^n} \widetilde{X}^{a}(k) = \left(-j\Delta x\right)^n \Delta x \sum_{m=-\infty}^{+\infty} X_m \exp\left(-jm\Delta x k\right) \tag{A-12}$$

In equation (5.3-1) the integration variable is changed to $\tau = x\ \Delta x$

$$\frac{\partial^n}{\partial k^n} \widetilde{X}(k) = \left(-j\Delta x\right)^n \Delta x \int_{-\infty}^{\infty} (\tau)^n X(\Delta x \tau) \exp\left(-jk\Delta x \tau\right) d\tau \tag{A-13}$$

Combining equation (A-12) and equation (A-13) gives

$$\text{ERROR} = \sum_{n=0}^{+\infty} \frac{k^n}{n!} \left(-j\Delta x\right)^n \Delta x \left[\sum_{m=-\infty}^{+\infty} X_m \exp\left(-jm\Delta x k\right) - \int_{-\infty}^{\infty} (\tau)^n X(\Delta x \tau) \exp\left(-jk\Delta x \tau\right) d\tau \right] \tag{A-14}$$

Assuming that $\left|\Delta x k\right| \le \frac{2\pi}{2}$ (which is the anti-aliasing condition), the maximum value of the summation in equation (A-14) can be written as

$$\sum_{n=0}^{+\infty} \frac{-j\pi}{n!}^n = \exp(-\pi) \sum_{n=0}^{+\infty} -j^n \tag{A-15}$$

The summation is not vanishing for big n so there is always a remaining error if the difference between the brackets is not equal to zero.

Assuming that $\left|\Delta x k\right| > \frac{2\pi}{2} = \alpha$ the summation reduces to

$$\exp(-\alpha)\sum_{n=0}^{+\infty} -j^{n} \tag{A-16}$$

From these results it can be seen that there is always a difference (the aliased spectrum) between the exact Fourier transform and the DFT.

Appendix B

THE INPUT PARAMETERS

B.1 The input parameters and computation time

The data set which is used to make the first set of figures in Chapter 6, is calculated with the following parameters:

the FFT discretization number;	1024	
the strip partition number;	99	
the discretization step in time	0.002	[s]
the error criterion for the conjugate gradient scheme	1E-6	
the acoustic wave speed	1457	[ms^{-1}]

With this data set the CPU computation time is about seven minutes. Increasing the FFT-number increases the computation time at most. With an FFT number of 256 the computation time is less than a minute. Reducing the number of samples on the strip also reduces the computation time, but not as fast as the FFT number does. The error criterion for the conjugate gradient scheme must be small enough to get a strong scattered field at the edge points of the strip. The error criterion given in this data set is good enough to get the field on the strip right for most situations. A smaller error criterion means that more iterations are needed to arrive at the desired precision; it takes therefore more computation time. The acoustic wave speed is the wavespeed in seawater.

All files have a filename which indicates the problem which has been calculated. All files have the configuration shown in Figure 6.1. The number in the filename is used to indicate the x1-position of the source.

The filenames have the following meaning;

comp means a compliant strip in an unbounded medium,
rigd means a rigid strip in an unbounded medium,
haco means a compliant strip in a halfspace,
hari means a rigid strip in a halfspace.

With these filenames every name can be understood as a scattering problem; for example hari75.d states that the problem of a rigid strip in a halfspace is calculated with the configuration of Figure 6.1 and with the x1-position of the source 75 metres away from the middle of the strip.

The field calculated is for all files the scattered pressure field. The first sample is the sample which is the value of the scattered field at time is zero.

For the program which implements the theory of multiple removal a different data set was needed; 255 different shotgathers were to be calculated with the receivers split-spread around the source.The shotpositions are chosen split-spread around the middle of the strip. The original program was slightly changed and all shotgathers could be calculated at one run. In Figure B.1 the configuration for this data set is shown. The distance between the receivers is chosen at 3.125 metres this choice is an important one because there are some restrictions on the input parameters which are explaned below.

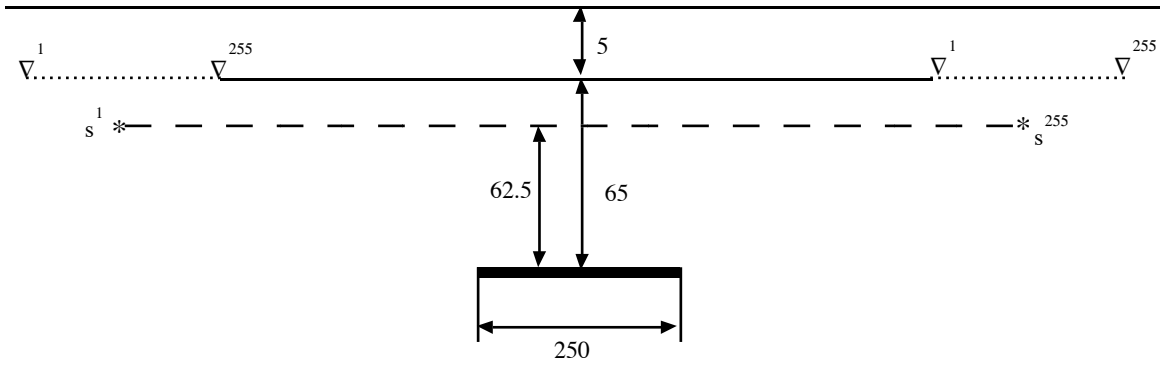

Figure B.1 : the configuration of the dataset needed for the multiple removal program

B.2 Restrictions on the input parameters

- restrictions due to aliasing in the time / frequency domain

In the discrete time domain the discrete frequency step is chosen as follows

$$\Delta f = \frac{1}{\Delta t\, N} \qquad \text{(B-1)}$$

And the Nyguist frequency is given by

$$f^{Nyq} = \frac{1}{2\Delta t} \qquad \text{(B-2)}$$

- restrictions due to aliasing in the spatial / wavenumber domain

$$\Delta k_1 = \frac{2\pi}{\Delta x\, N} \qquad \text{(B-3)}$$

In the k_1 - ω domain the pole at the wavenumber k must be excluded properly. The maximum wavenumber is given by the wavenumber at the Nyquist frequency.

$$k^{Max} = \frac{2\pi f^{Nyq}}{c} \tag{B-4}$$

Substituting the expression for the Nyquist frequency gives

$$k^{Max} = \frac{\pi}{\Delta t\, c} \tag{B-5}$$

The Nyquist frequency in the k_1 - ω domain must in order to exclude the pole properly at least be as great as the maximum wavenumber

$$k_1^{Nyq} \geq k^{Max} \tag{B-6}$$

Substituting the maximum wavenumber

$$k_1^{Nyq} \geq \frac{\pi}{\Delta t\, c} \tag{B-7}$$

The Nyquist number is given by

$$k_1^{Nyq} = \frac{\pi}{\Delta x} \tag{B-8}$$

Substituting this in equation (B-7) gives a restriction on the discretization step in space

$$\frac{\pi}{\Delta x} \geq \frac{\pi}{\Delta t\, c} \tag{B-9}$$

or

$$\Delta x \leq \Delta t\, c \tag{B-10}$$

- restriction due to the finite lenght of the receiver array

In giving the receiver positions care must be taken that the receiver positions are not outside the interval which is calculated. The program gives no error message and the results which are obtained look good, but when the first arrival times are checked the error can be detected.

Appendix C

THE PROGRAM

The program which calculates the scattered field by a strip is written in FORTRAN 77. The name of the program is scatter, the name of the input file is input.prm. This input file is given in Figure C.1.

Figure C.1 : input file of program scatter

The output file for the configuration,of the input file of Figure A.1, is given in figure A.2.

Figure C.2 : the configuration output file

Given the strip width and the wavenumber, the number of integration points are chosen such that numerical discretization errors are less than the errors made in the resulting approximating of the field values at the strip. As soon as the number of iterations grows larger, the danger of a loss of significant figures turns up. For this reason, all computations have been carried out in double precision.

In the program all possible problems, which can be solved with the same program structure, are build in in the program (this could be done with a little extra effort). So not only the scattered pressure field can be calculated, but also the total field and the particle velocity field can be calculated. This can be useful for other applications. If the strip lenght is taken to be zero only the direct field is calculated.

Given a valid input set the program calculates for every discrete frequency the scattered field on the strip. The calculation of the scattered field on the strip is done by solving the integral equation by the preconditioning conjugate gradient scheme described in Chapter 4. This usually converges within a few iterations. If after 200 iterations the scheme has still not converged, the program stops. Probably, in this case, a wrong input value has been given. After the iteration is completed the field on the strip is known, for the frequency under consideration. This field is used to calculate the scattered field at the receiver positions. The frequency discretization steps are chosen such that the maximum frequency calculated is the Nyquist frequency. The frequency data are multiplied by the spectrum of a wavelet (given from the input file).

After the field is calculated for every frequency value, a Fourier transform is used to calculate the field in the time domain. In this Fourier backtransform the zero frequency is set at zero, which is equal to setting the time baseline, and for the value at the Nyquist frequency the imaginary part is set to zero, which is the best thing to do because this is all the information known for the Nyquist frequency. The time signal is multiplied with an inverse exponential taper to compensate for the use of complex frequencies. Finally this time signal is written to the data output file. This is done for only positive time samples, the mathematical negative time samples are calculated but they can not be used in the final result.

The most critical parameter in the program is the space discretization step. For a discretization step bigger than five the discrete wavenumber becomes to small to include the branch point completely. The data still looks fine for small offsets, but for larger offsets the signal disappears in the noise due to the incomplete calculation of the branch point.

The program has been written on a network which uses a Convex C1 and the Unix operating system, version 8.1.